AD-A134 183 OPTICAL EXCITATION OF TRAPPING STATES IN FE DOPED INP (U) NAVAL ACADEMY ANNAPOLIS MD J GIESSNER 20 JUN 83 USNA-TSPR-124 1/2

UNCLASSIFIED F/G 20/12 NL

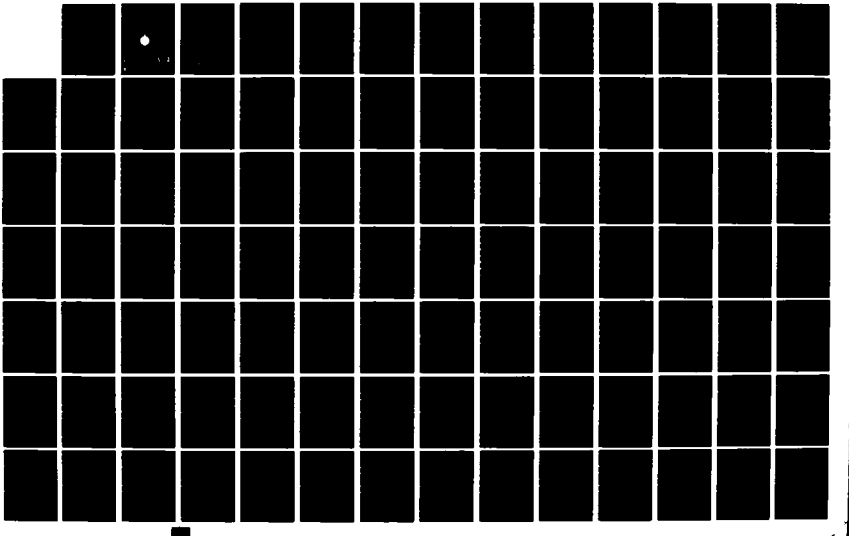

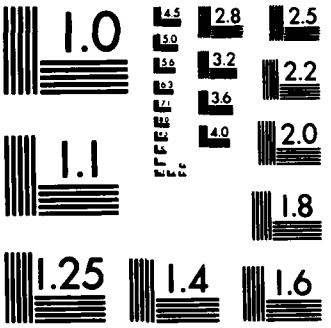

A134 183

23

DTIC
ELECTE
OCT 31 1983
S D
B

88 10 28 054

U.S.N.A. - Trident Scholar project report; no. 124 (1983)

"Optical Excitation of Trapping States in Fe Doped InP"

A Trident Scholar Project Report

by

Midshipman 1/C Jack Giessner 1983

U. S. Naval Academy

Annapolis, Maryland

R. N. Shelby

Advisor: Professor R. N. Shelby, Physics Dept.

Accepted for Trident Scholar Committee

Charles F. Rowell

Chairman

June 20, 1983

Date

ABSTRACT

The knowledge that defect states affect the performance and speed of semiconductors is well known. Defect and trappping states are categorized according to their sex (hole or electron trap),energy in the gap and capture cross sections. The Deep Level Transient Spectroscopy (DLTS) technique that is useful for electrical pulsing, becomes increasingly profitable using optical pulsing. The optical pulsing was accomplished using a simple, but efficient, infrared light emitting diode (LED). The LED had the fortunate property that with decreasing temperature, the average energy output of the LED stayed about equal to the bandgap for the III-V semiconductor InP. Because of these ~~fortuitous~~ findings, ~~I concentrated~~ on Fe-doped InP using LED excitation. These particular samples are being studied by NAval Research Labs(NRL) in connection with lasing that results from Fe transitions. ~~I set up models~~ for both the p+n junction and Fe transitions to help explain experimental results obtained. ~~A~~ coupled state that could be related to Fe+3 to Fe+2 hole emission was found to have an energy of .24ev on the n-side of the p+n junction, and an energy of .24ev on the p+ side of the metal-p+ rectifying junction(a result proposed in the capacitance-junction model). Another energy related to the Fe+2 to Fe+3 electron emission was found in agreement with the model (E=.807ev). Trap states related to defects inherent in the growth of InP were also found. Many of the states seen by authors recently could be explained by the energy data in these experiments.

Acknowledgements

I'd like to thank the people who pushed me so hard to work on this project. These people are the friends in my company. They encouraged work down in the labs at all hours of the night. I, also, would like to thank Dr. Magno at NRL for providing me with InP samples and a ton of questions to think about.

Finally, I'd like to thank Dr. Robert Shelby for his eager and aggressive approach in working with me. His ability to question the obvious with "Don't forget that..." has taught me an invaluable lesson in experimental analysis. I am grateful for all the time and effort he has put in to the project.

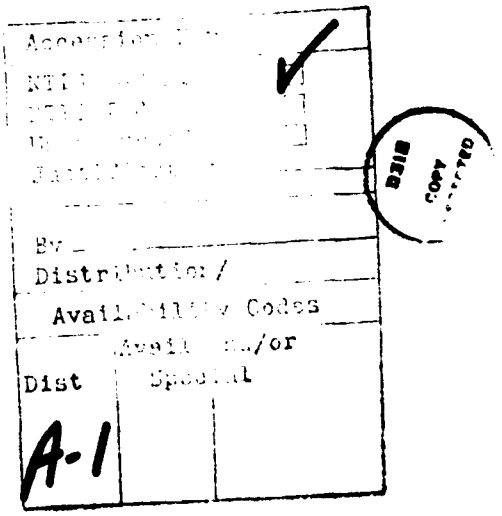

Contents

Introduction

The purpose of this paper is to expound the knowledge learned throughout the year regarding the techniques of optical excitation and the optical trapping states in a particular sample; namely Fe-doped InP.

The technique is very important in the optical case, because today the major emphasis in research is the ability to excite states through unique methods that will yield the most fruitful or at least the most desired conditions. The LED was one of the first devices tested and although some work was done with the lightpipe, the crux of the work centered on the LED. The reason for this is that the LED was unique for a certain semiconductor under study:InP. After I found this special property of the LED, I began experimental work on one of the hottest and controversial areas in InP: Fe doping in the bulk.

Why is Fe-doped InP so important today? The first reason is simply the nature of III-V compounds. Because of their high electron mobility, this group is often regarded as the next generation of "super fast-switching" semiconductors. Impurities or defect states that thermally emit holes or electrons may hinder or change the properties of the semiconductor. That is why the nature and interaction of these states are so important to understanding specific device fabrications. Specifically, with regard to the sample under study, InP has superior properties that make it a fine microwave device in amplifiers and

oscillators. The Fe in the bulk of InP is being studied, because of lasing that has been seen between the Fe+2 and the (Fe+2)* - excited - state.

Analysis, therefore, is essential in finding some of the key parameters of Fe. These include:energy position,energy transitions, saturation states, capture cross sections and stability. After these basic questions are answered, detailed work can begin on these specially doped samples. The paper is broken up into four sections:theory of pn junctions,emission and LED's; the DLTS system and technique; actual data for trap states; possible models to describe junction behavior and Fe transitions in the gap.

Background Theory

The basic theories used in the experiments can be divided into four parts: basic theories arising from general semiconductor equations, capacitance theories from junction characteristics, generation and recombination equations for electron and hole trapping states, and chacteristic data interpretation of the high output infrared LED. Since the LED was actually in the system, it is essential that one knows the response of the LED at the critical temperatures. Making assumptions about the intensity and pulse width of the optical signals can not be done with confidence, until spectral analysis is completed.

Semiconductor Theory

Section II-1

Given the band diagram below for a simple semiconductor, the important region becomes the region around the valence and conduction bands.

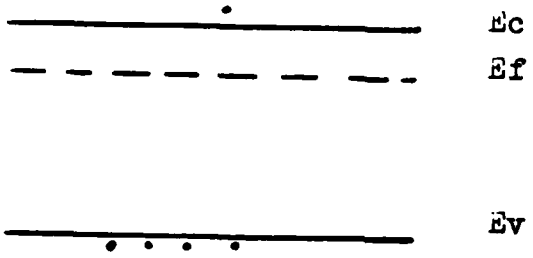

Fig II-1

Using simple thermal physics, one obtains:

$$n = \int_{E_c}^{E_{top}} N(E)F(E)dE \qquad \text{II-1}$$

$$p = \int_{E_v}^{E_{vb}} N(E)F(E)dE \qquad \text{II-2}$$

Where N(E) is the density of states, F(E) is the Fermi-Dirac distribution function and n and p are the number of occupied electron and hole levels respectively. Using calculus and equation manipulation one can determine a set of fundamental semiconductor equations that will be used throughout the experiments:

$$n = N_c EXP\left(-\frac{Ef-Ev}{kt}\right) \qquad \text{II-3}$$

$$p = N_v EXP\left(-\frac{Ec-Ef}{kt}\right) \qquad \text{II-4}$$

$$N_v = 2\left(\frac{2\pi kmo}{h^2}\right)^{1.5} \left(\frac{mh^*}{mo}\right)^{1.5} T^{1.5} \qquad \text{II-5}$$

$$N_c = 2\left(\frac{2\pi kmo}{h^2}\right)^{1.5} \left(\frac{mn^*}{mo}\right)^{1.5} T^{1.5} \qquad \text{II-6}$$

Where k and h are Boltzman's and Planck's contants respectively, m is the restass of the electron or hole and mh* and mn* are the effective masses of the holes or electrons being considered. The np product equation is a simple result from II-3 and II-4:

$$np = N_c N_v^{\cdot} \; EXP(-Eg/kt) \qquad \text{II-7}$$

Although the above equation is for intrinsic semiconductors, doped semiconductors are handled in the same way, with the Fermi energy(defined as that energy which, at absolute zero, is the highest energy level that is occupied - all other available states below the fermi energy are occupied) moving closer to the valence or conduction band dependent on whether the sample is a p or n type semiconductor. This is shown below.

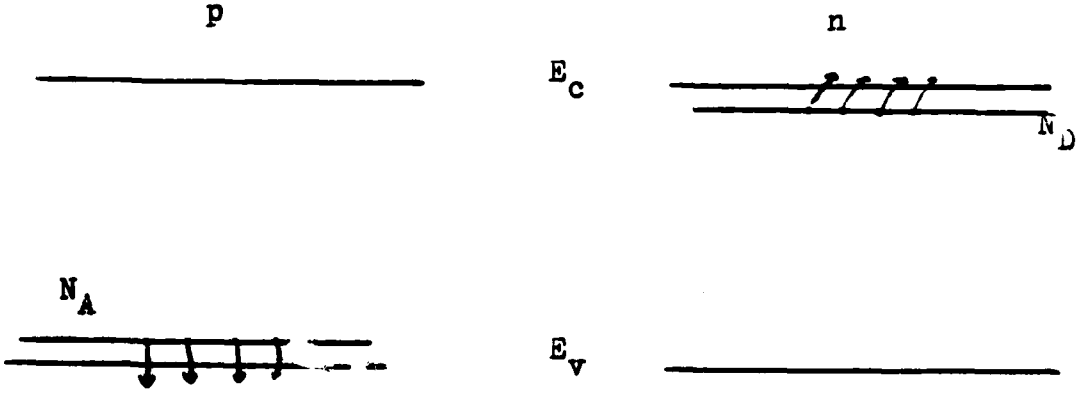

Fig II-2

The p+n Junction

Section II-2

If an impurity concentration changes abrupty from a certain type of region to another, the junction formed is called abrupt. As shown in Fig II-3.1, ions of this sort are highly dependent on the type of growth of the n and p layers. For now consider an abrupt but non one-sided junction. Later in the actual sample data, I will check the validity of these assumptions.

The p+n junction is used as our example. The important theoretical point to make is that to achieve charge conservation at equilibrium, donors must be stripped off the n side and congregate on the p side. This leaves ionized donors -ND + - on the n side. The same is true for the p side (Fig II-3.1). The region that is now devoid of any mobile chare carriers is called the depletion region or space-charge zone. The equations below summarize the theoretical basis of the depletion region(DR). Equations 8-10 represent definitions of charge conservation and Poisson's equation. Equations 11-12 are simply applied boudary conditions and direct substitution.

$$N_A x_p = N_D x_n \qquad \text{II-8}$$

$$V_{bi} = kt\ln\left(\frac{NAND}{ni^2}\right) \qquad \text{II-9}$$

$$-\nabla^2 = \frac{\partial \mathcal{E}}{\partial x} \qquad \text{II-10}$$

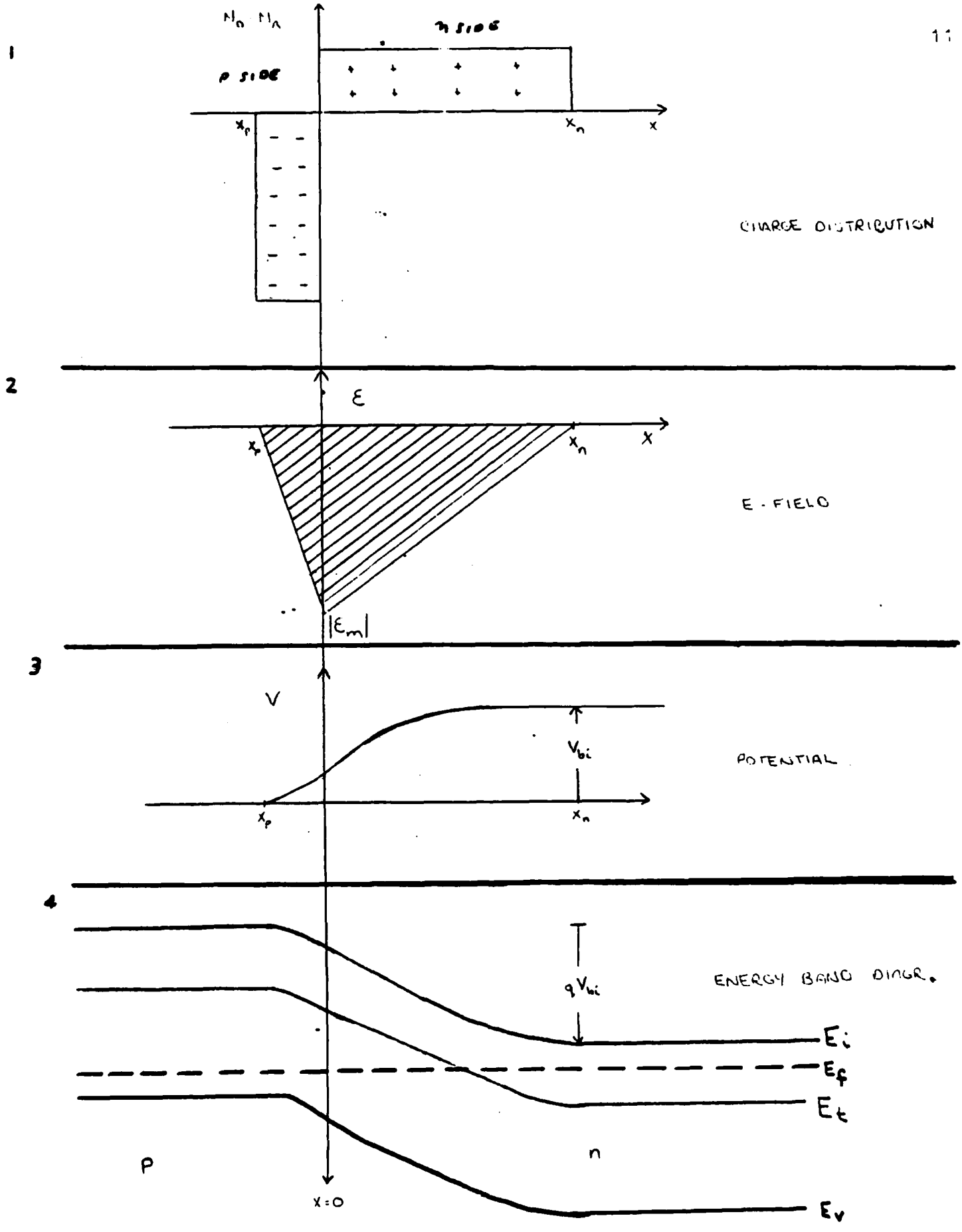

p+n JUNCTION - NO BIAS -

Fig II-3

$$V_{bi}=\tfrac{1}{2}\mathcal{E}_m W \qquad \text{II-11}$$

$$W=\sqrt{\frac{2\varepsilon_s}{q}\left(\frac{NA + ND}{ND\,NA}\right) V_{bi}} \qquad \text{II-12}$$

If one now assumes that the semiconductor is a one-sided junction of p+n, then NA>>ND. Also, in more general terms, Vbi may be replaced by any voltage applied. This is true because the width of the DR is dependent on the size of the barrier. Hence a forward bias (+ to p side) will tend to breakdown the barrier and inject high amounts of carriers across the DR. In this case equation 12 and common sense suggest the width of the region will be reduced and finally destroyed under high bias. On the other hand, increasing reverse bias increases barrier height and makes it tougher to cross the DR. This will cause the with of the space-charge layer to increase. Since the aim is to look at trapping states, a sizable depletion region and this quiescent reverse bias must go together. The general equation for the width of a p+n junction under the mentioned conditions is :

$$W=\sqrt{\frac{2\varepsilon_s}{q}(1/ND)(V_{bi}+V_r)} \qquad \text{II-13}$$

Since the capacitance per unit area $C'=\varepsilon/W$, the form for capacitance is below:

$$C'=\sqrt{\frac{q\varepsilon_s ND}{2(Vbi+Vr)}} \qquad \text{II-14}$$

This equation will be used constantly in analysis of the parameters of the sample and other possible models. Because properties of the sample are found through parameters such as Vbi and ND, one finds the 1/C^2 versus V plot very useful. Theoretically this plot should yield a straight line with the following equalities: slope=2/(qeND) and intercept=2Vbi/(qeND). With the effect the bias has on capacitance already explained, the next step is to see the effect that energy traps has on the capacitance.

Emission and Capacitive Theory

Section II-3

Before one tackles emission equations, it is a good idea to look at the capacitive transient which is the manifestation of the trap's emission of carriers. The concentration now will be on the simple capacitive transients from electrical pulsing initially studied by Lang, Miller et al.[1]. Later a model will be developed to help explain optically generated transients.

Using Fig II-4.1, the transient is a majority carrier trap(electrons on the n side of the p+n junction. The schematic shows a quiescent reverse bias followed by a pulse which is majority, meaning it carries electrons to the barrier. The pulse is less negative closing the gap of the depletion region. A less schematic and more revealing band diagram of FigII-5.2 shows what is going on. As majority carriers slip into the n region, trap 1 begins to fill. The bands begin to bend less approaching the picture of FigII-5.1, but mobile carriers can not stay in the depletion region (the electric field sweeps them out). The traps will only fill below the Fermi energy as the bands shift. The barrier to electron flow will likewise shift only enough to match the injected electrons (the suppplied bias).

But at the end of the pulse, the region is sudddenly forced back to its normal, large width. Some of the electrons, though, identified as the transition region,

Capacitance Transient Response

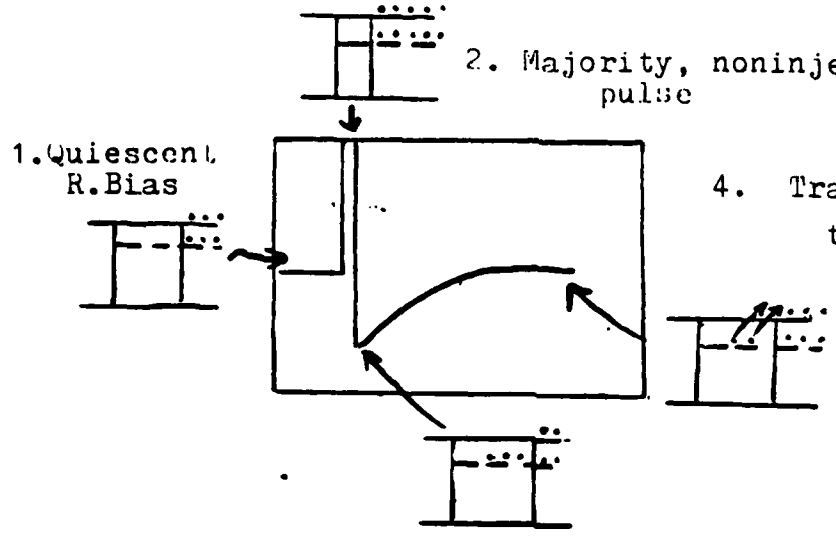

Majority Carrier

Fig II-4.1

---

2. Injection Pulse

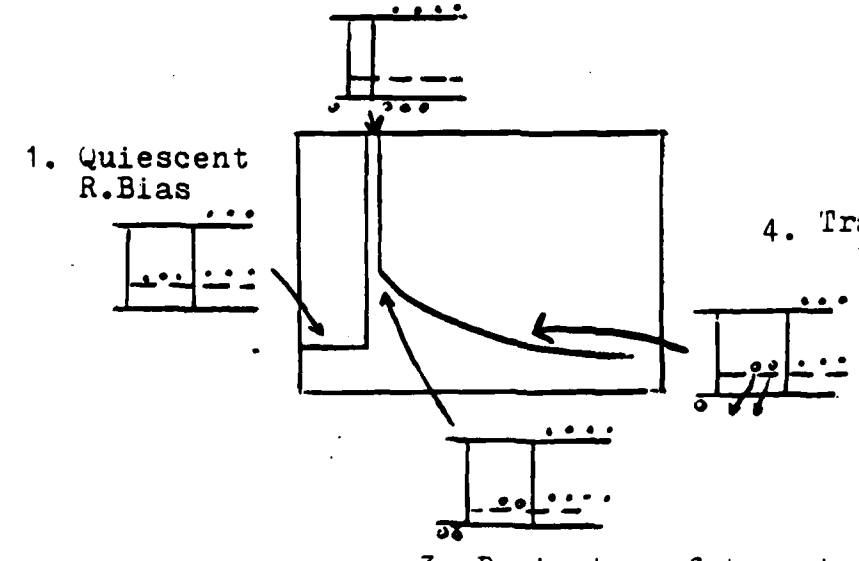

Fig II-4.2

Minority Carrier

*From D v Lange

Fig II-5.1

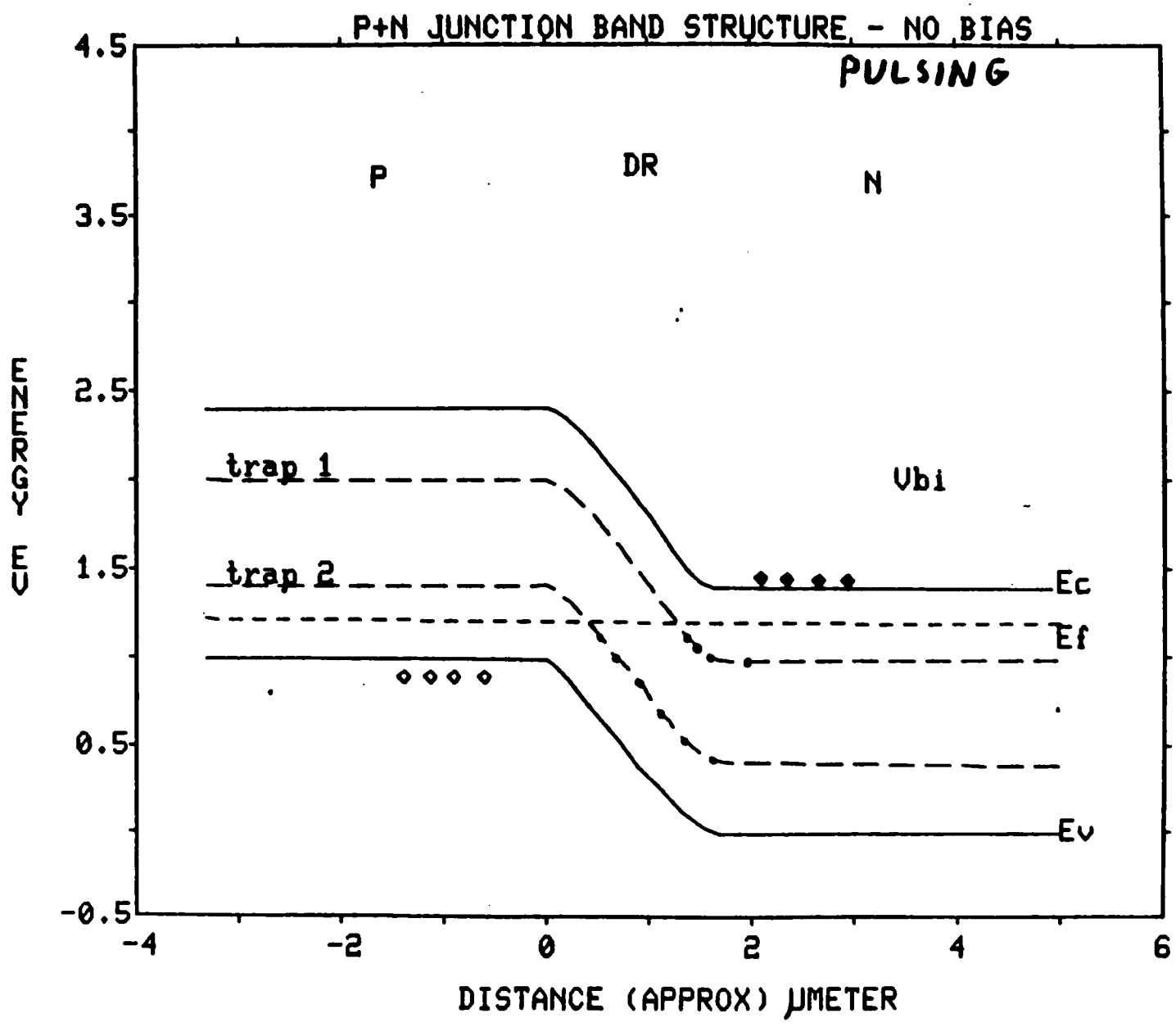
P+N JUNCTION BAND STRUCTURE - NO BIAS
PULSING
P
DR
N
trap 1
trap 2
Vbi
Ec
Ef
Ev
ENERGY EV
4.5
3.5
2.5
1.5
0.5
-0.5
-4
-2
0
2
4
6
DISTANCE (APPROX) μMETER

Fig II-5.2

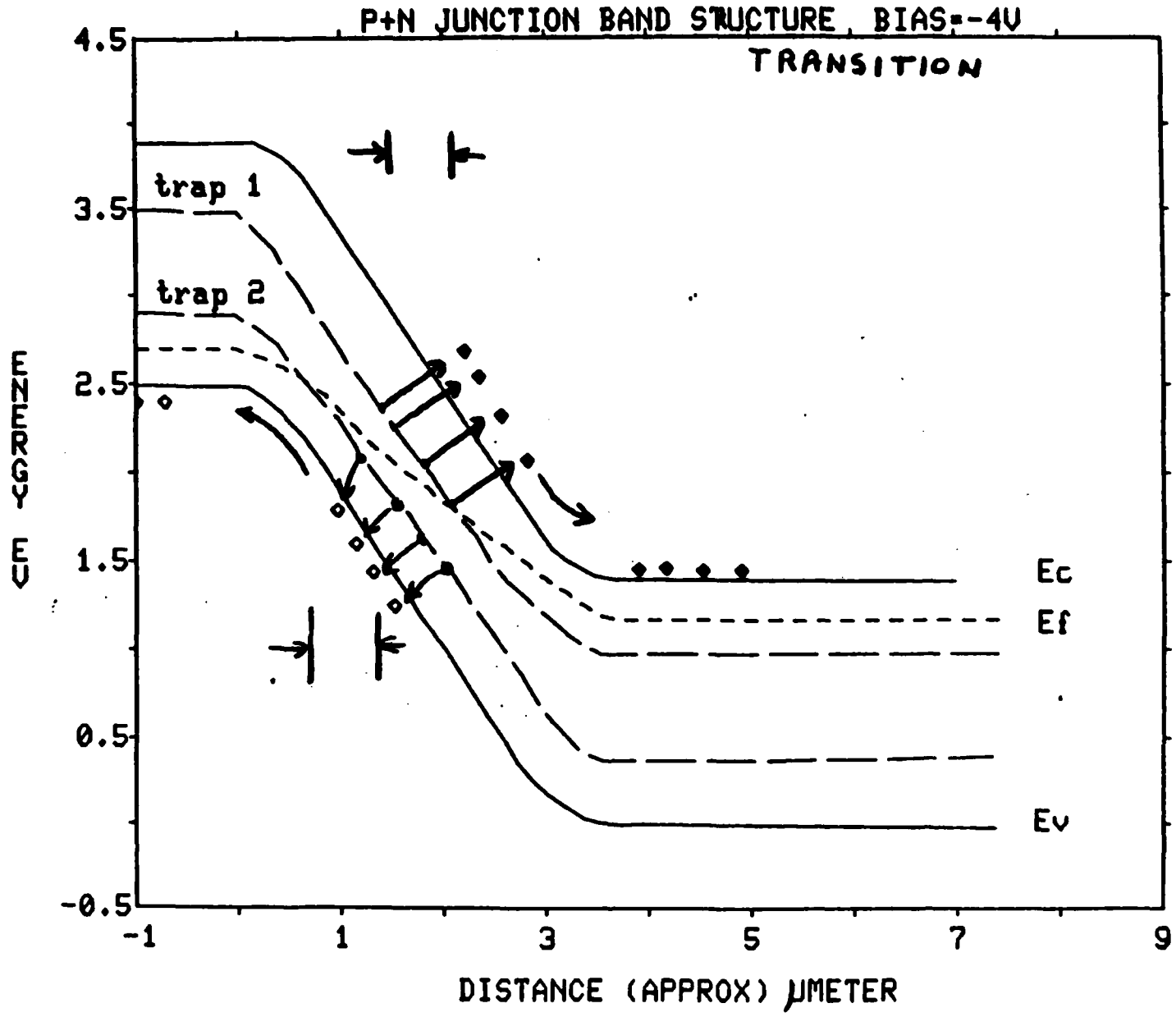
P+N JUNCTION BAND STRUCTURE, BIAS=-4V
TRANSITION
trap 1
trap 2
Ec
Ef
Ev
ENERGY eV
4.5
3.5
2.5
1.5
0.5
-0.5
-1
1
3
5
7
9
DISTANCE (APPROX) μMETER

Fig II-5.3

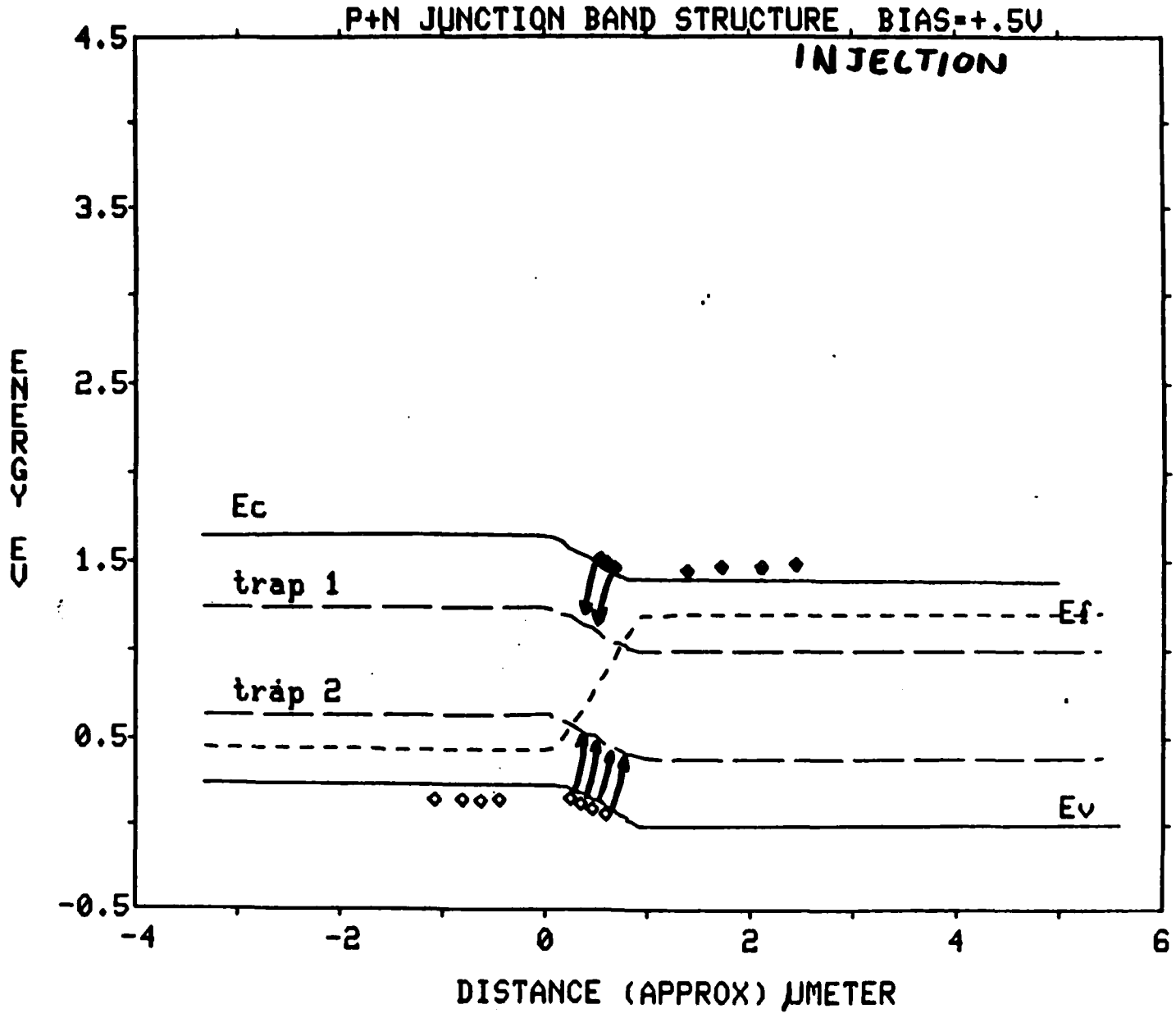
P+N JUNCTION BAND STRUCTURE, BIAS=+.5V
INJECTION
4.5
3.5
2.5
1.5
0.5
-0.5
ENERGY EV
Ec
trap 1
trap 2
Ef
Ev
-4
-2
0
2
4
6
DISTANCE (APPROX) μMETER

are now above the steeper Fermi level. And under normal conditions, they will thermally emit. The emission and capture processes are shown schematically and relative to the band gap. The decrease below the quiescent value immediately after the pulse can be explained by a first approximation to be a correction term to EqnII-14. This correction applies during the transient when the electrons that still remain trapped subtract off an amount from the net background doping ND. As the electrons emit to the conduction band and are subsequently pulled back to the + charged n side, the capacitance returns to its quiescent value ;

$$C' = \sqrt{\frac{2\varepsilon_s (ND-Nt)}{q(V_{bi}+V_r)}} \qquad \text{II-15}$$

It should be noted that this correction is only a first approximation which does not take into account the location or width of the transition region. This is done more completely by Lange et al.[2].

For the electrical injection of holes and electrons the barrier must be destroyed, implying the pulse must start at the Q level and extend past 0 bias forward. For this case consider trap 2, a hole trap, schematically in FigII-4.2 and and actually in FigII-5.3.

This case represents the minority trap generated by an electrical pulse and is a little more complex than the majority trap case. Initially, as has been put forth by DLTS theory, it is impossible to inject holes into the DR, because the electric

field will sweep them out if a barrier is present. If there is injection then the large DR at negative bias, becomes a very small region in pulsing forward. As the injection occurs, holes begin to fill trap 2. Dependent on the time of filling and the density of states in the trap is the ability to completely fill or saturate the trap. Traps will fill similar to majority traps except that a hole trap filling represents an emptying of an electrons from that trap. Therefore, traps will fill such that below the Fermi level they are filled with electrons (absent of holes) and above the Fermi level they are filled with holes. As the pulse is removed, the band structure returns to the normal reverse bias; any holes that are below the Fermi level are forced to thermally emit in a comparable transition region. The transient capacitance starts at a higher value than its quiescent value explainable as as a first correction to the capacitance equation of II-14. When the pulse is removed, there are extra holes in the depletion region which means that electrons that would normally be in the trap under seady state conditions are now adding to the doping on the n side. Equation II-16 shows the positive capacitance transient.

$$C' = \frac{2\,(N_D+N_t)}{q(V_{bi}+V_r)} \qquad \text{II-16}$$

As one might think, the position of the Fermi energy in the depleted region is a key factor in transition regions and probablities of occupation. Most literature discusses quasi-Fermi hole and electron levels, but not the actual bending of the energy. This is because the calculations are indeed

complex and must be developed from the basic equation. In my diagrams, I make crude assumptions related to the applied voltage and the crossing of a specific band. This was the only guideline to follow in this area, but it is one of the most important parts to any model proposed.

The emission theory is based on the Fermi probability that a certain level is occupied. This was the key to the transient capacitance arguments. The sketch below represents all possible emissions from a trap.

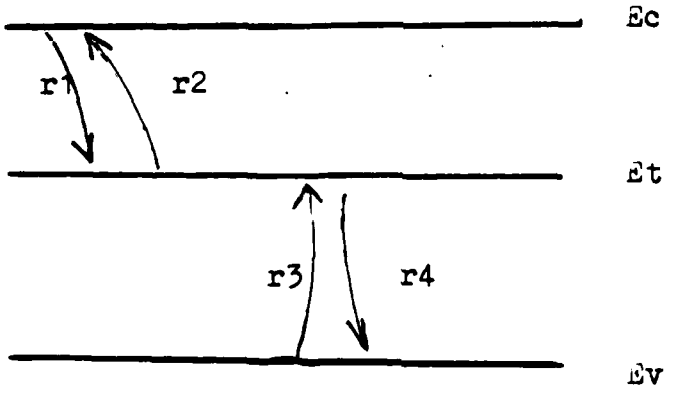

Looking at the r2 and r1 pair for electron emission and capture, one can find the rate of electron capture for the trap by noting trap properties. The rate must be proportional to the number of electrons available from the conduction band, the number of empty states in the trap and the probability that an electron near the trap will be captured. The values for the

first two are straightforward, but the capture probability is related to vthXσn where σn is the capture cross section and vth is thermal velocity. the product of those three factors is:

$$r1=n(Nt(1-f(Et)))v_{th}\sigma_n \qquad \text{II-17}$$

In this case, near equilibrium, the probability of occupation ,f(Et), is equal to fD - the Fermi statistic. This may not seem an important assumption, but in nonequilibrium conditions this is simply not true.

Similar reasoning for the rate of emission,r2, except that r2 is not dependent on n, because one can assume there are enough available states to pick up an emitting electron. Therefore, r2 depends only on the number of occupied trap sites and the emission rate probability defined as en. Eqn II-18 is the exp ression for r2.

$$r2=Nt(f(Et))e_n \qquad \text{II-18}$$

With the assumption that f(Et) is the Fermi probabilty, the general case for en can be found by setting r1=r2 in quasi-equilbrium. Solving for en one gets,

$$e_n=v_{th}\sigma_n N_c EXP(-\frac{Ec-Et}{kt}) \qquad \text{II-19}$$

Using the same analysis for hole traps, one obtains equation II-20:

$$e_p=v_{th}\sigma_n N_v EXP(-\frac{Et-Ev}{kt}) \qquad \text{II-20}$$

These equations for en and ep are general equations that can be used in nonequilibrium as long as the Fermi assumptions are made. For most cases being considered, II-19 and II-20 are applicable. Moreover, these two equations are the central equations governing all DLTS work and Arrhenius plotting. Recombination and generation within traps are the actual mechanisms of charge transfer and can be directly related to r1-r2=r3-r4.

LED Theory

Section II-4

Since the LED is in the system and affected by temperature, it is essential that its operating characteristics as a function of temperature are determined or known qualitatively so that particular assumptions can be made concerning its performance. Appendix A is the manufacturer's data on the high output infrared LED. Light produced from it is noncoherent at 880nm. Thus, a spectral analysis would be proper to determine bandwidths and maximums at a lower limit of liquid nitrogen (77 $^{\circ}$K) and an upper limit at room temperature(300°K). Three important characteristics must be obtained. 1. Temperature dependence on the number of photons being supplied (Intensity vs Temperature). 2 The wavelength of maximum intensity and relative bandwidth separation at the upper and lower temperature limits. 3. The ability of the optical pulse to follow the input current pulse supplied to the LED.

The first characteristic assumes that intensity scales directly with the current pulse height sent into the LED. We find that current is directly proportional to output intensity. Using the relative height of the capacitance signal, the intensity of light at a specific energy at room temperature was 2.0 times as small as the intensity at liquid nitrogen temperature. This was confirmed by using a spectrometer at a characteristic wavelength at the two temperatures. This means

that the number of photons supplied doubles even though the input current is kept the same.

The second, and most important characteristic, is the peak energy as a function of temperature. Fig II-6 shows intensity as a function of wavelength at 77°K and 300°K. The data summary indicates E-peak-(300°K)=1.354ev and E-peak- (77°K)=1.449ev. Thus, in temperature sweeping of the system one must keep in mind that the peak energy of the photons being emitted from the LED gets larger by .095ev. The broadness of the peaks - full width at half maximum varies from 1.354ev + or - .045ev at 300°K; 1.449ev + or - .055ev at 77°K.

The third parameter is the ability of the optical pulse to follow the electrical input; that is, is the pulse width supplied to the LED equal to the optical pulse of light that illuminates the sample? For a good range of 1 to 500 microseconds, the range of widths involved in the runs, the rise and fall time off the pulse was about .15 microseconds. So there is confidence that the pulser width is equal to the light pulse width.

Another item of concern is the ability of the LED to follow the sweeping temperatures of the system. To maintain consistency, one must assume that the LED is at the same temperature as the sample. If the system heats or cools too rapidly then the LED may be at a different temperature than the recorded temperature. At "fast" sweeping rates (greater than 3.0° C per min), the LED do not follow the system temperature. This was determined indirectly using a transient capacitance response signal that comes out of a lock-in amplifier (to be discussed).

Holding all else constant, the heating and cooling rates were varied. Using rates that had known system and temperaure response, such that one could assume that the system itself was at the recorded temperature of the electrode, one could find the maximumrate for which the response signal matched previous signals without much variation. This cooling or heating rate was about 1 to 1.2 °C/min. This became the standard that was used for all optical excitation. Although the physical presence of the LED may pose some electrical differences in the capacitance transients, a first approximation indicates that it probably effects the DC level of our signal and not a time dependent effect that needs to be considered.

In concluding this summary on the LED data, the changing factors as a function of temperature effect the ability of certain states to be occupied. This is true because the number of photons and their energy do change in temperature variations. The data collected here helps sort out the possible transitions at a specific temperature, energy and intensity.

Fig II-6

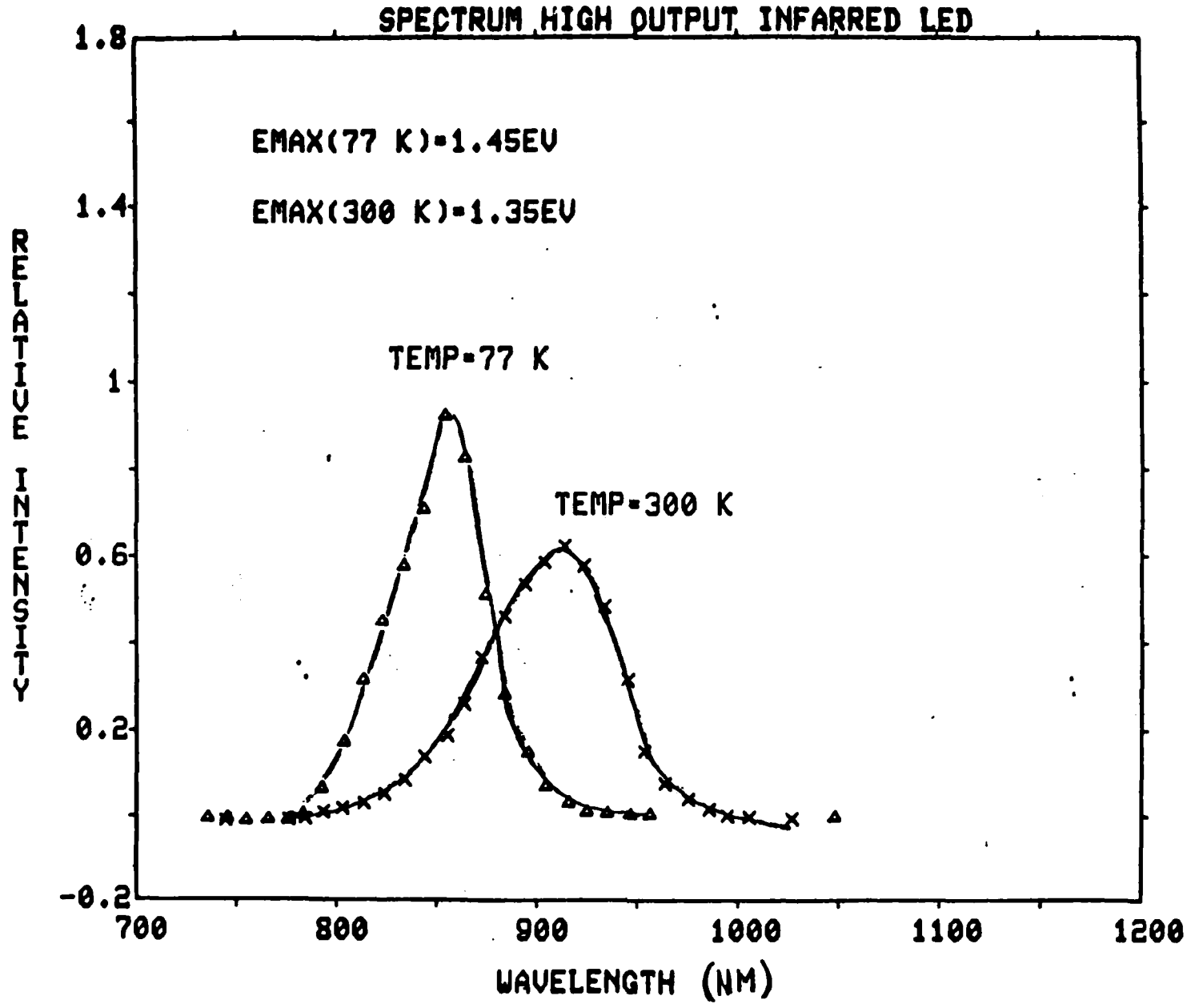
SPECTRUM HIGH OUTPUT INFARRED LED
EMAX(77 K)=1.45EV
EMAX(300 K)=1.35EV
TEMP=77 K
TEMP=300 K
RELATIVE INTENSITY
1.8
1.4
1
0.6
0.2
-0.2
700
800
900
1000
1100
1200
WAVELENGTH (NM)

The Technique

Section III-1

The technique of capacitance transient spectroscopy developed by Lange was examined from a theoretical point of view in section II-3. The emission and capture theories led to Eqns. II-19 and II-20 which describe emission rates. The capacitance transient was also examined in terms of theoretical hole and electron emissions. What Lange did was to come up with an experimental technique that could link the two aspects of emission theory. There are actually several different setups available for the study. The system at U.S.N.A. utilizes a lock-in amplifier that was put into a working system by a previous Trident Scholar Stephen Spehn[3].

The lock-in technique uses a test sine wave at a specific frequency that is multiplied by the analog signal from the capacitance transient. The system will "lock on" a specific frequency when the emission rate of the emitting electrons is equal to the set rate of the lock-on at some given temperature. The lock-in rate is related to the frequency by a factor; that factor can be calculated by using fourier anaysis on the signal.

Let figure III-1 represent a sample input pulse and transient response. The end of the input electric or optical pulse is called T1 (all times stated are referenced to t=o at the begining of the test sine wave). T2 is called the gating time. Because of some large signals, it is necessary to block off some

Fig III-1

Capacitance Parameters

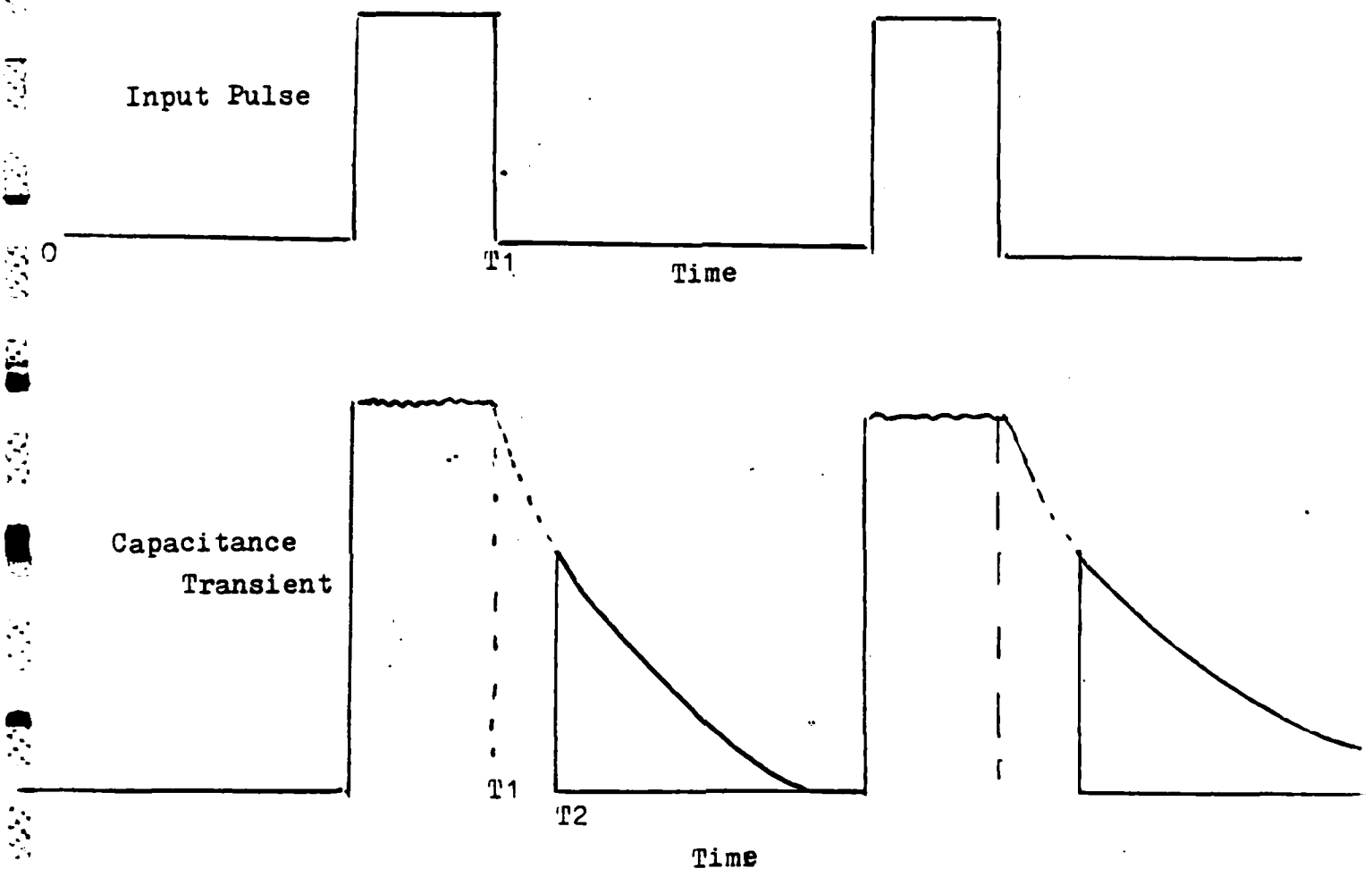

small fraction of the signal that will not cause any change in the output of the lock-in. T2 represents the time that the transient response begins to be sent into the lock-in. It is important to note that the physics that governs the situation is the time between the actual start of the transient and the measured start of the capacitance transient (T2-T1).

With parameters of the system defined (T1,T2,f,ϕ-the phase angle of the sine wave), one can determine the lock-in response.

The first assumption in the analysis is that indeed the emission rates are exponential. Using emission theory, this seems like a solid assumption. If one lets e=r so one does not confuse the exponential with the emission rate, the signal is:

$$S(t)=\ddot{C}'e(-rt) \qquad t:\{0,T2\} \qquad \text{III-1}$$

$$C'e(-rt) \qquad t:[T2,T]$$

Here, $C'=Coe(-r(T2-T1))$, $T=1/f$. Plugging in for Co and taking the first harmonic of the fourier series, yields III-2.

$$S(t)=ao/2 + a1\cos(2\pi ft) + b1\sin(2\pi ft) \qquad \text{III-2}$$

One arrives at the lock-in output through the simple weighting of the phase angle set into the system.

$$LO=2/\pi\,(a1\sin\phi + b1\cos\phi) \qquad ;ao=0 \qquad \text{III-3}$$

One can use this weighting, since all the lock-in is really doing with its reference signal is extracting the fourier component and displaying it as a DC signal. Thus, the constants are found by using the fourier defintion. Equations III-4,5,6 are the constant defined a0,a1,b1.

$$a_0 = 2/T \int_0^{T2} S(t)dt \qquad \text{III-4}$$

$$a_1 = 2/T \int_0^{T2} S(t)\cos(wt)dt \qquad \text{III-5}$$

$$b_1 = 2/T \int_0^{T2} S(t)\sin(wt)dt \qquad \text{III-6}$$

In following through on the integrals it turns out that the zeroeth harmonic is independent of time. This inputting DC level will be destroyed with a signal tuned amplifier. Therefore, the contributions to the lock-in come from a1 and b1. The final lock-in output, although tedious to simplify, is straightforward. The final formula is long, but easily programmed into the computer. The formula is noted below for completeness.

$$L(T) = 2/\pi \left(\frac{S0}{\pi}\sin(2\pi fT2) + \frac{2S1}{T1}\frac{1}{R^2 + (2\pi f)^2}\left(-Re^{-RT} - e^{-RT2}\right.\right.$$
$$\left.(2\pi f)\sin(2\pi fT2) - R\cos(2\pi fT2)\right) + \frac{2S1}{T(R^2 + (2\pi f)^2)}\left(\right.$$
$$\left.-2\pi f e^{-RT} + e^{-RT2}(R\sin(2\pi fT2) + 2\pi f\cos(2\pi fT2))\right) +$$
$$\frac{So}{\pi}(1-\cos(2\pi fT2)). \qquad \text{III-7}$$

The input variables supplied on any given set of experimental data include ϕ, T1, T2, f. To determine the point where r(or e) is locked unto f, one finds the maximum lock-in output. One way to do this is to take the derivative of the lock-in and set it equal to zero. Another way using the advantages of the computer uses stepping intervals, until one reaches the lock-in maximum. This is the general procedure I used. The four variables were inputed and an associated emission

rate was the computer output. The limits of e approximately equal to 2.35f as T approached infinity were consistent with Lange,Spehn and other previous works [4,5].

With the ability to find the emission rate, e, it becomes quite easy to get data for certain traps. Using the emission equation in general form,

$$e=AT^2EXP(-\Delta E/kT)$$

and taking the ln of both sides, we obtain

$$\ln(\frac{T^2}{e})= -\ln A + \Delta E/kt$$

$$y=mx + b ,$$

with m= E/k and x=1/T.

Plots such as the one above are called arrhenius plots and should plot as straight lines. The process requires a sweeping temperature system. At a specific temperature, unique in nature, a corresponding e is found as the peak in the DLTS signal (a maximum lock-in response). Note that in the context above T represents temperature and not the period as it did in the fourier work. With a set of points, one can generate a line whose slope is proportional to the trap energy and whose intercept is proportional to the capture cross section.

Equipment

Section III-2

The system is set up so that optical DLTS runs and electical runs can be accomplished with little change. The electrical pulsing system is similar to the original system used by Spehn[6] and is shown in Figure III-2. The diagram traces the system from the trigger to the output recorder. A trigger pulse supplied by the lock-in for proper phase control, signals the pulser at the proper time. The delay mechanism in the pulser set T1. A transformer sends the positive pulse through the sample which is already in a stable reverse bias situation; causing the transient response as expected. The capacitance is measured by a Boonton capacitance meter whose analog output signal goes into a gating mechanism. This piece of equipment sets T2 and enters it as input to PARC-113 preamp. The preamp is equipped with low and high frequency rolloffs and the preamp may be supplemented with an attenuator in the circuit to suppress unwanted noise.

The output of the preamp is then put into the HR-8 PAR lock-in amplifier. Frequency adjust, phase control, sensitivity to the capacitance signal and averaging time constant are all controlled directly on the front panel of the lock-in. The time constant selects the time span for which the lock-in averages the capacitance transients. The output of the lock-in goes to the y-axis analog voltage plotter. The x-axis is an analog signal related to a voltage across a piece of platinum that scales with temperature directly.

Fig III-2

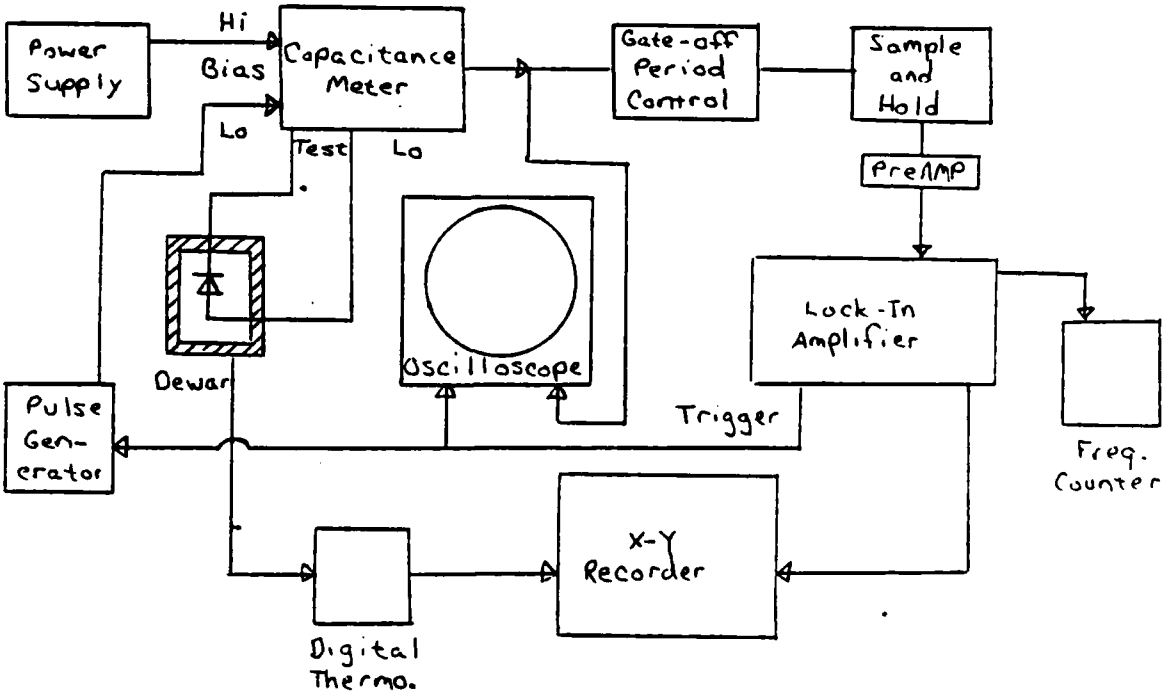

Lock-In Amplifier DLTS Apparatus

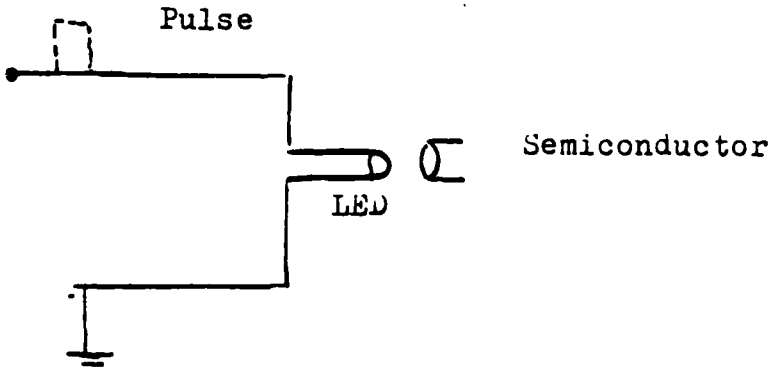

LED Excitation

Fig III-3

The plotter is then designed to show the DLTS signal as a function of temperature. It is important to note that in the lock-in technique it is not essential to have a constant sweep rate, because the lock-in is sampling continuously. The sweep rate, for obvious reasons should not be comparable the time constant. If that is the case, then error could be introduced due to the ambiguity in the actual temperature of the system.

For the optical DLTS runs, the setup is similar with a few distinctions (FigIII-3). The transformer for electrical pulsing is not used. A separate terminal on the dewar that holds the sample is used as the lead to the LED. The LED is located in the dewar and physically rests about 1cm from the sample header. The pulser provides a pulse of electricity to the LED. The LED has been discussed previously, concerning the temperature effects in the system.

A combined LED and electrical excitation experiment involves using two pulsers and the transformer. All three types of excitation, electrical, optical and their combination were carried out.

InP Available Data

Section IV-1

The sample being studied is InP, P+n electron diffused, with Fe doped in the bulk. The sample was obtained through NRL in Washington. Hall effect measurements conducted by the group at NRL yielded the net background doping in the sample to be 1.3E15 cm(-3) and the doping on iron to be about 1.5E15 cm(-3). The p side is very heavily doped around 1E18 cm(-3). The significance of the high doping in Fe, makes it an interesting sample in which to study Fe transitions and defect traps. Here is a table of some inherent properties of InP.

Table IV-1

Eg=1.35 (T=300°K)

Eg=1.41 (T=0°K)

u-h=150 cm^2/Vsec (300°K)

u-e=5000 cm^2/Vsec (300°K)

me=.067mo

mh=.6mo

er=10

There are some interesting characteristics worth noting. The preciseness of the energy gap is not good. Some sources quote a lower limit on the bandgap at room temperature to be about 1.27ev [6], while others including Sze use about 1.35ev [7]. At absolute zero the difference is not that bad (1.40ev to 1.43ev). These differences should be noted, because the energy of a trap as was set forth in emission theory is closely related to the

bandgap. One must be careful concerning this discrepancy when making statements noting trap energies.

The most fruitful observation concerns the change of bandgap with temperature of InP. If one compares that data to the spectra data of the high output infarred, LED, it appears as if they match each other. In other words, The highest intensity photons have energy that is equal to bandgap light regardless of temperature. This temperature independence of the average energy supplied to semiconductor, is a resourceful piece of information. states are mobilities and effective masses. The electron mobility is much greater than the hole mobility. Also, the hole effective mass is 10X greater than the electron effective mass. With all the data grouped as it is, one can simplify the capacitive and emission equations. Using Eqns II-19 and II-20, the hole and electron emission rates are:

$$e=\sigma v_{th} N_c EXP(-\Delta E/kT) \qquad \text{IV-1}$$

$$e_p=(2.09 \times 10^{25} \sigma_p) T^2 EXP(-\Delta E/kT) \qquad \text{IV-2}$$

$$e_n=(2.51 \times 10^{24} \sigma_n) T^2 EXP(-\Delta E/kT) \qquad \text{IV-3}$$

Thus, the prefactor A , defined previously as A=exp(-yintercept),can be used to solve for the capture cross section.

$$\sigma\text{-}h=A/2.09E25 \qquad \text{IV-4}$$

$$\sigma\text{-}e=A/2.51E24 \qquad \text{IV-5}$$

A value for the capacitance at 0 bias can be calculated from the Hall effect data, using a reasonable value of Vbi=1V. The value, using Eqn II-12 turns out to be,

$$Co=55.8pF$$

A huge descrepancy between theoretical and the measured value of about 2.41pF suggest some problems in the simple p+n junction. These problems will be considered in the capacitance modeling in section V. Now that I have discussed the sample and its inherent properties, I must now discuss the DLTS system to discover what specific effect a certain parameter has on the electronic properties of the sample.

System Characteristics

Section IV-2

Parameters that change the physics of the situation in the depletion region are called controlling parameters, while system parameters that merely facilitate in the sensing or the resolving of states are called secondary parameters. Emphasis will be placed on explaining the controlling parameters. The reason this is done is to look straight at those things that affect the physics of the semiconductor not the experimental technique.

Reverse Bias

The reverse bias controls the height of the barrier between the p and n sides of the junction. Previous equations showed that the reverse bias controls the width of the depletion region. Thus, a signal that disappears by reducing reverse bias, keeping all else constant, would indicate a trap state that is indeed in the depletion region off the metallurgical junction. A signal that remains unchanged at low reverse biases, could be considered close to the junction. These places for traps considers only transition regions and is therefore, not a very precise parameter. So, reverse bias itself, does not offer a decisive testing parameter. But in combination with other parameters,

such as pulse width or height, it becomes a better testing parameter.

Pulse Height

Electrically, the pulse height indicates the change off the quiescent bias toward or above 0 bias. The height, then, controls the transient change in voltage and also, the transient barrier height. As has been discussed, a pulse that still is negative in bias, can not inject holes into the trap region. According to trap theory, one does not expect to see a hole trap in this region, without the ability to make holes available for capture - injection. Depletion region edge effects where holes are sitting on the valence band of the p side of the junction could make some holes available. As to that trap's ability to thermally emit holes which can be observed as a minority trap is uncertain.

Optically, since the barrier height is pinned by the reverse bias, one can not change the barrier height through optical excitation, but it can change the DR width dependent on filling or emptying of carriers in the trap The pulse height is actually the current amplitude being supplied to the LED. Since the direct proportion between the current and intensity has been firmly established, one can control the number of photons per volume incident on sample. Control of this parameter yields the

control of the electron-hole pairs created. Although one may not expect 100% transfer of one photon to one hole-electron pair, the relative changes in these numbers by controlling the intensity are the key factors.

Pulse Width

Electrically, this represents the time the sample is at non-steady state conditions. In the semiconductor it controls the time of filling of particular traps. According to work done previously[8], the traps fill exponentially to a saturation value that is equal to the allowed density of states, Nto.

$$Nt = Nto(1-\exp(-et)) \quad \text{IV-6}$$

In equation IV-6 "e" is the emission rate derived in earlier equations. This could apply to the filling of hole or electron traps. Varying the pulse width and observing the DLTS peak actually yields data that is proportional to the trap concentration (considering that the DLTS peak represents the change in capacitance effected by extra holes or electrons according to II-15 and II-16). The technique in theory represents a simple approach for finding the trap concentration. Two key experimental problems will make the finding of the trap concentration close to impossible. The first is the inability to find the place where the pulse height is actually equal to zero. This is called a baseline problem and in all the tests that were

performed this has been the problem. Although the first problem might not allow for precise trap measurements, the second problem is more serious. Lange developed for small changes in capacitance a simple approximation for the trap concentration:

$$Nt=2(ND-NA)(\text{delta } C/C) \qquad IV-7$$

As one can see referring back to Fig II-4, that the key assumption in this approximation was that the change in capacitance was small compared to the initial pulsed capacitance value. This implies that if the trap concentration is comparable to the doping concentration, then the equation above is invalid. If iron was seen in the gap, then its large trap concentration would negate all the approximate transient equations. As to the validity of the emission equations and subsequent use of Arrhenius plots, theory behind hole and electron emission does vary with ultra-high trap concentrations, but not enough that would invalidate those equations.

Secondary Parameters

The secondary parameters are important, because they determine the ability to see a certain trap and the ability to enhance or smooth over a peak. T2-T1 determines the offset time. This could be essential if there was a specific part of the transient one wanted to gate off. The other parameters such as preamp gain settings, sensitivity settings, time constant settings, and

attenuation settings allow for control, clarity, sharpness and definition of trap peaks.

Electrical Runs

Section IV-3

The InP sample, Fe in the bulk(pad-7), was first tested using electrical excitation. Over 100 runs were done with this particular pad. Two traps become dominant in all of the runs: a hole trap labeled H2 and an electron trap E1. The total data summary is included in the beginning of the optical section, but I include the energies here for convenience:

$E_c - E_1 = .499ev \quad \sigma_n = 3.5E-15$

$H_2 - E_v = .691ev \quad \sigma_n = 2.4E-14$

A representative curve is shown in Figure IV-1 with a frequency of 50hz, PW=100usec,bias -6 to +4 and T2-T1=200usec. The value for Co with pad-7 was 2.4pF which is much lower than the predicted value.

In the figure there appears to be a coupling of the two peaks. The transient itself showed this inseparability (The wave eductor channel outputs:Fig IV-2.1 and Fig IV-2.2. As the temperature decreases, the minority trap melds into a huge majority trap (positive transient into a negative transient).

The change in capacitance, the central item of concern for the trap concentration approximation, is actually smaller than the change in capacitance due to the voltage pulse. For a standard run pulsing -8V to 0 V at room temperature, the changes in capacitance were: pulse capacitance change-

0.03 pF, the majority trap - .1pF, the minority trap - .02pF.

Fig IV-1

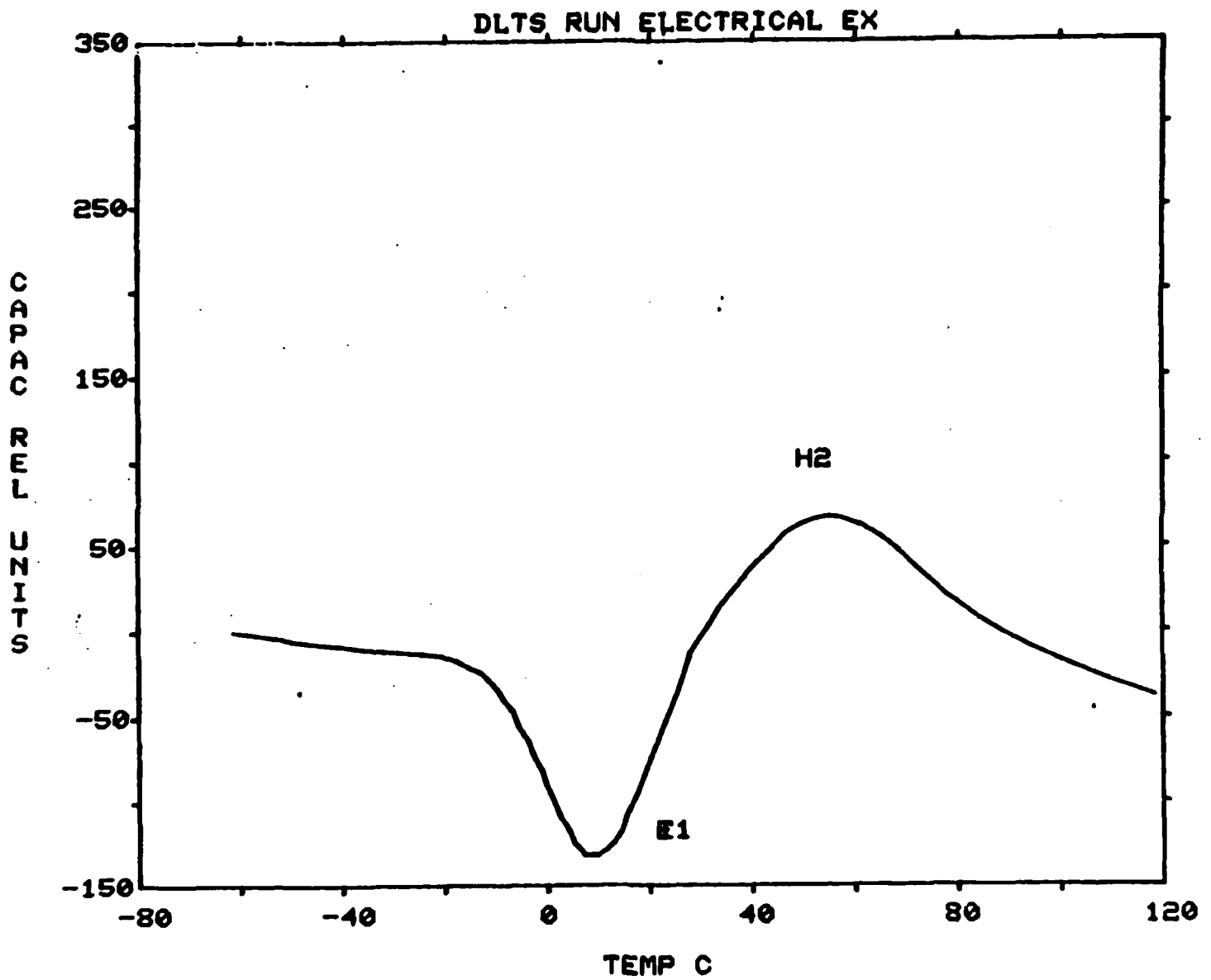
DLTS RUN ELECTRICAL EX
350
250
150
50
-50
-150
CAPAC REL UNITS
H2
E1
-80
-40
0
40
80
120
TEMP C

Fig IV-2.1

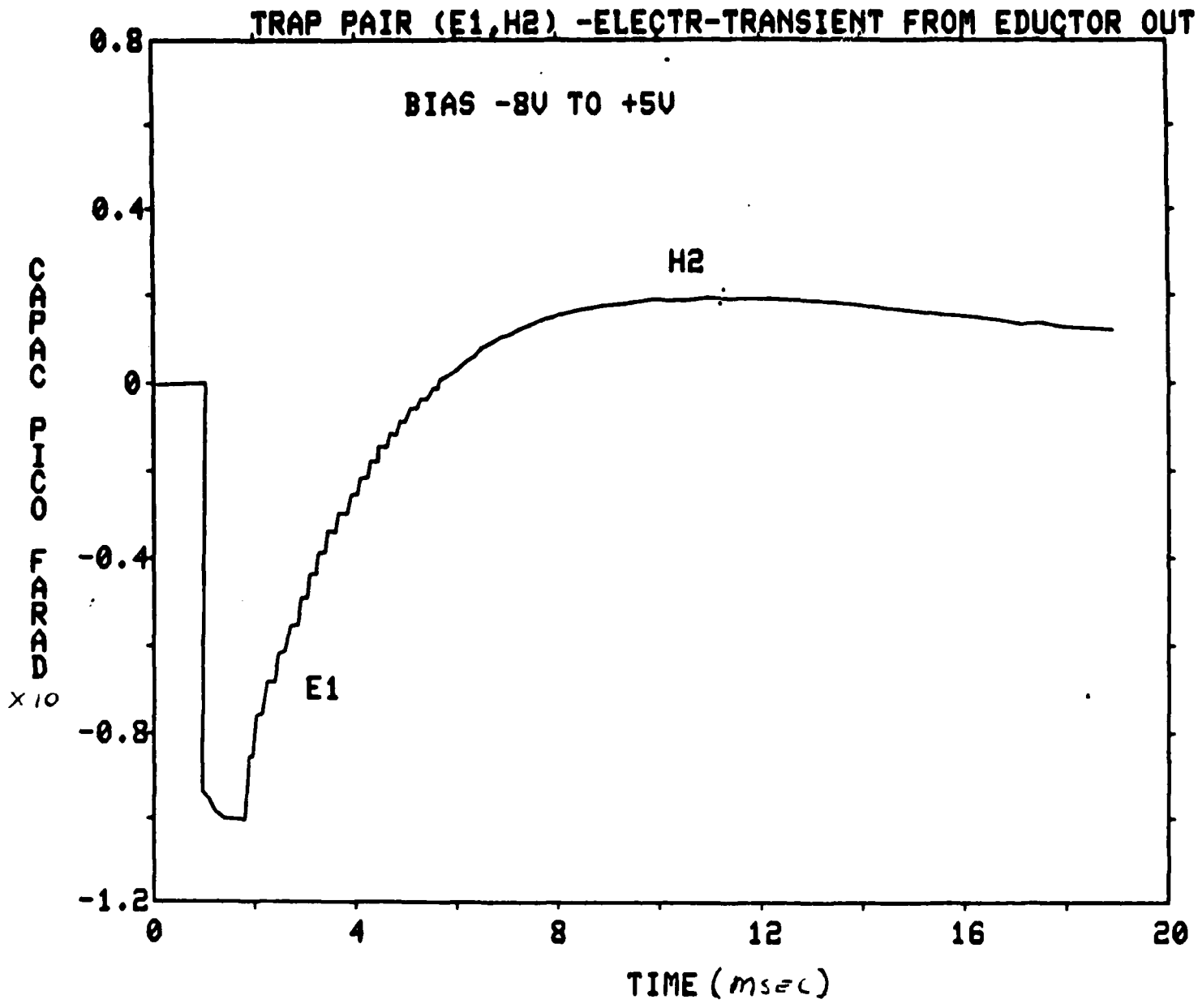
TRAP PAIR (E1,H2) -ELECTR-TRANSIENT FROM EDUCTOR OUT
BIAS -8V TO +5V
H2
E1
CAPAC PICO FARAD
X 10
0.8
0.4
0
-0.4
-0.8
-1.2
0
4
8
12
16
20
TIME (msec)

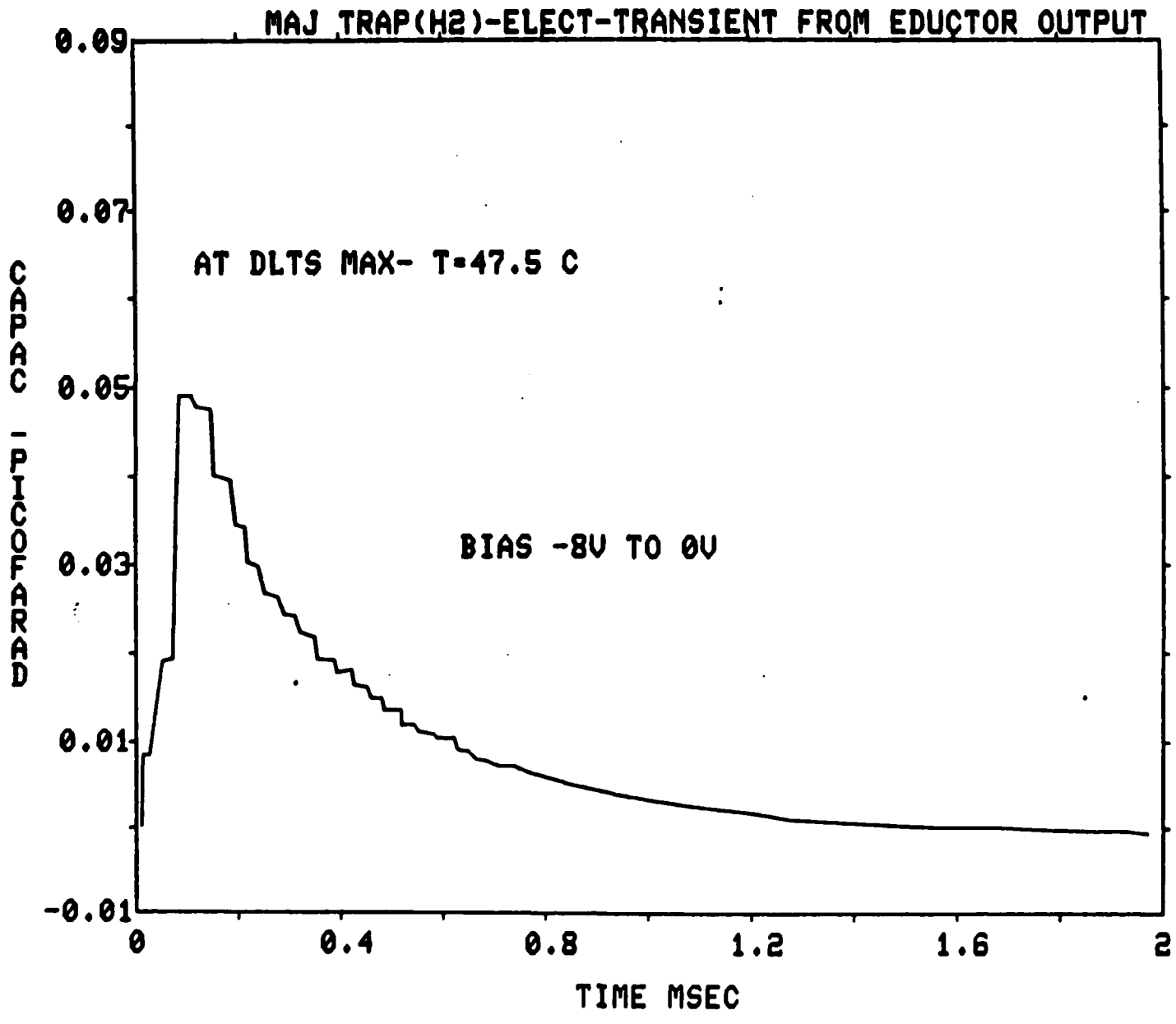
MAJ TRAP(H2)-ELECT-TRANSIENT FROM EDUCTOR OUTPUT
AT DLTS MAX- T=47.5 C
BIAS -8V TO 0V
CAPAC - PICOFARAD
0.09
0.07
0.05
0.03
0.01
-0.01
0
0.4
0.8
1.2
1.6
2
TIME MSEC

The interesting combination was further analyzed by controlling the parameter of pulse height. Using a standard of -8V and a standard emission rate of about 56 sec(-1), I found what appeared to be a minority carrier trap when I was not injecting. In the DLTS theory that is not possible. Figure IV-3 represents three of these runs with the conditions stated. One of the problems that seems evident in IV-3 is the shift in peak along the temperature axis with a constant emission rate. This should not happen since the trap is uniquely determined by e and T. If the shift in peak does not come from a theoretical basis then it comes from a "pulling" of the majority trap by the growing appearance of the minority trap (the stronger the pulse forward the stronger the pull). This pushing and pulling of the peak location can effect the temperature recorded at a specific frequency. The effect is not small! It ranges from -15 $^{\bullet}$C at little pulses (-8 to -6V) to +3 $^{\bullet}$C at injecting pulses. With that in mind, the two traps that can't seem to be separated leads to enormous uncertainty in the calculations of E1 and H2. The values given earlier are close to a point where both are present with a modest injection forward of +2V. This was done in hope to give middle-of-the-road values for the energy. Nevertheless, that coupling produces energies that are not precise; this must be kept in mind when considering the Fe transition model.

Stemming from this coupling, data was collected concerning the pulse height and the relative heights (change in trap concentrations) of the majority and minority traps. The values of DLTS peak height are referenced to the largest peak each trap

Fig IV-3

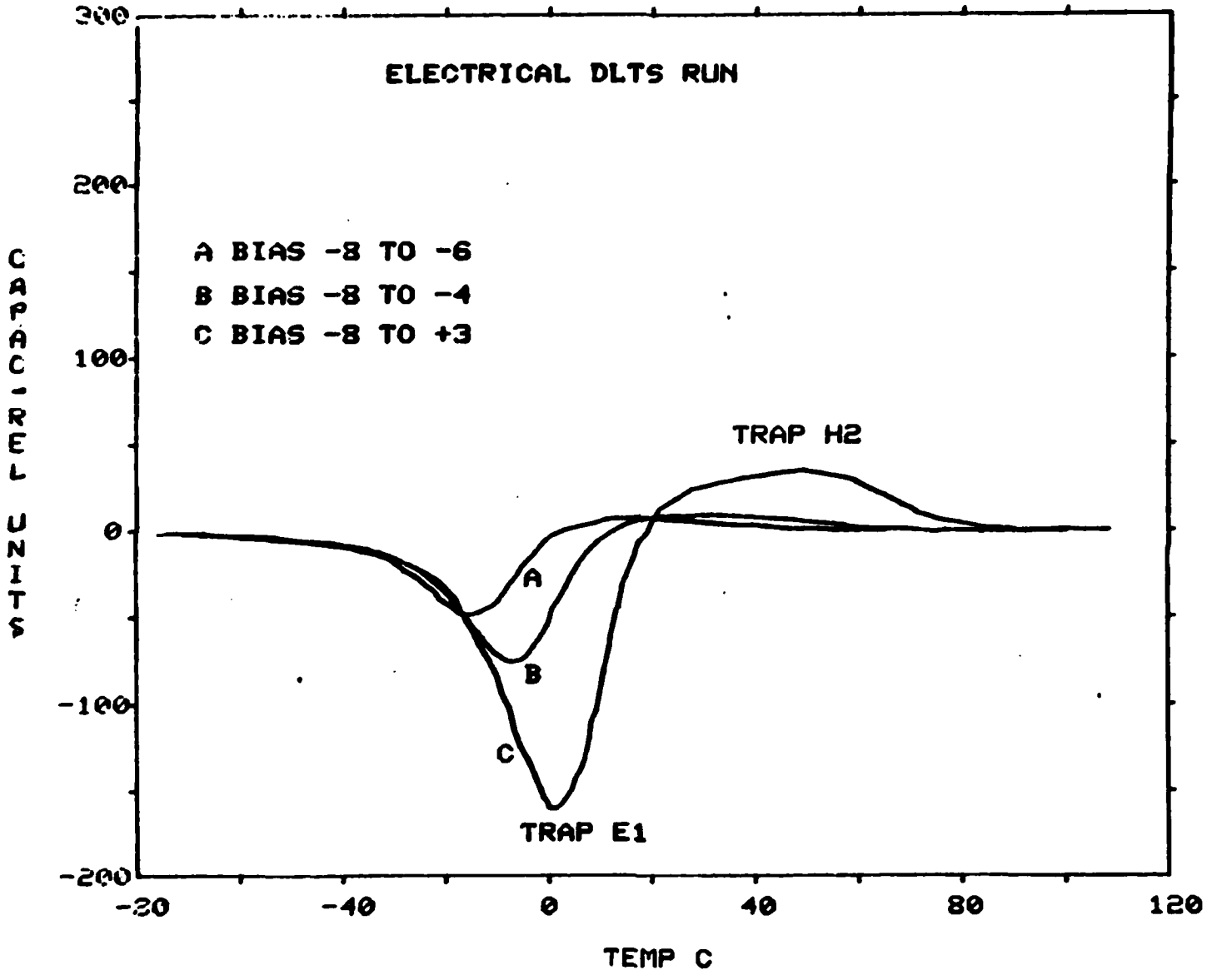
ELECTRICAL DLTS RUN
A BIAS -8 TO -6
B BIAS -8 TO -4
C BIAS -8 TO +3
TRAP H2
TRAP E1
A
B
C
CAPAC-REL UNITS
TEMP C
200
100
0
-100
-200
-20
-40
0
40
80
120

had. In this case it turned out to be the high injection to+3 for both traps. Also plotted in FigIV-4 is the ratio of the capacitance change for the majority trap at a certain bias to that of the minority trap for the same bias. Since it is not possible to calculate the trap concentration, one looks at at the comparison or ratio of the two traps. The data shows that within the limits of error the trap concentration H2 divided by the trap concentration E1 is approximately constant in the forward bias region and constant (but a different constant than in the forward region) in the reverse bias region. These results will help develop the model in section V.

The electrical DLTS was limited in its ability to observe high and low saturation states, because the transformer setup simply could not handle pulse widths much greater than 100usec and much less than 10usec without a large amount of distortion. This was one of the major regions for going to the LED excitation. It was clear that all the possibilities that were inherent in the excitation by light should be investigated.

Fig. 4-4

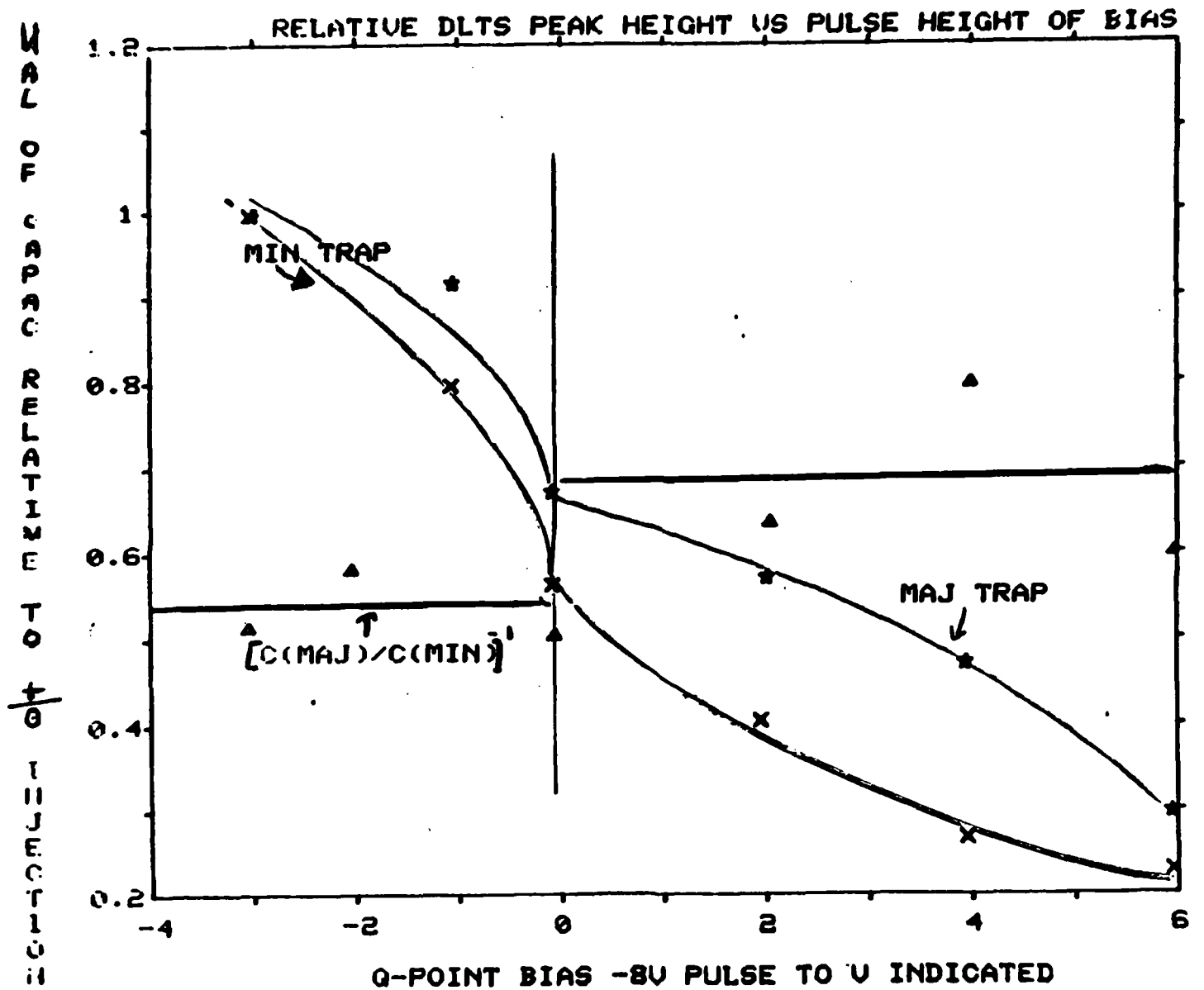
RELATIVE DLTS PEAK HEIGHT VS PULSE HEIGHT OF BIAS
VAL OF CAPAC RELATIVE TO +Q INJECTION
1.2
1
0.8
0.6
0.4
0.2
-4
-2
0
2
4
6
MIN TRAP
MAJ TRAP
[C(MAJ)/C(MIN)]'
Q-POINT BIAS -8V PULSE TO V INDICATED

Optical Runs

Section IV-4

Although an electric peak was detected at low temperatures (-150 C), the interest in low temperatures peaks did not become important until the LED was used. What was found was an abundance of traps. Table IV-1 illustrates all the peaks found in InP (Fe in bulk) and their energies.

Table IV-1 Calculated Energies

Trap	σ cm^2	E (ev)	PW (usec)	PH(Amp or V)	Type
H4	4.0E-12	.807	500	.4A	OP
H1 *	3.8E-16	.198	300	.6A	OP
H3B2	7.1E-16	.427	10-50	.8A	OP
H3B1	9.4E-10	.602	10-50	.8A	OP
H3A	1.5E-15	.316	10-50	.8A	OP
E1 #	3.5E-15	.499	100	+8V	EL
H2 #	2.4E-14	.691	100	+8V	EL
H3C	3.1E-11	.794	500	.4A	OP
E2	4.1E-11	.238	300	.6A	OP
H3(comp)	2.2E-15	.321	100	.6A	OP

\# Approximate value

* a combined peak with approx. H11= .24ev,H12=.15ev

The sample that was used was not the same sample that was used for the electrical excitation, because of contact problems. A different pad was used off the same grown semiconductor. I found

six measured hole traps and one measured electron trap. One hole trap that was not able to be measured was at about -130 C; one electron trap that was not able to be measured was located around -115 C. FigIV-6 is an ODLTS plot of all the traps designated. This run was done at a bias of -6V, a pulse width of 500usec and a current going into the LED of 0.4 Amps.

Note the gain downshift when the temperature decreases below -115 C. This means relative to the other peaks on the graph, the traps H1 and E2 are ten times larger than they appear. My analysis of all the peaks will be done on a peak to peak basis rather than on a parameter basis, because there are so many peaks. It will also help in devising an appropriate model for Fe transitions.

Basically, there are three peak regions. The first is another coupled state region containing the peaks E2 and H1. These peaks dominate the spectrum at moderate to large pulse widths 100-300usec. The next region is the peak 3 region containing H3A, H3B1 and H3B2. The region is lumped together at high pulse widths and distinct at low pulse widths 1-50usec. The peaks in this region are in the -40 to -140 C temperature range. The third region contains two peaks H4 and H3C. These peaks are prominent at very high pulse widths of 300-500usec. H3C has been dubbed "the spike" because of the thinness of the peak at that temperature. According to the emission equations and DLTS response this could not be a DLTS peak representing exponential emission of holes. But assuming a slightly non-exponential

Fig IV-5

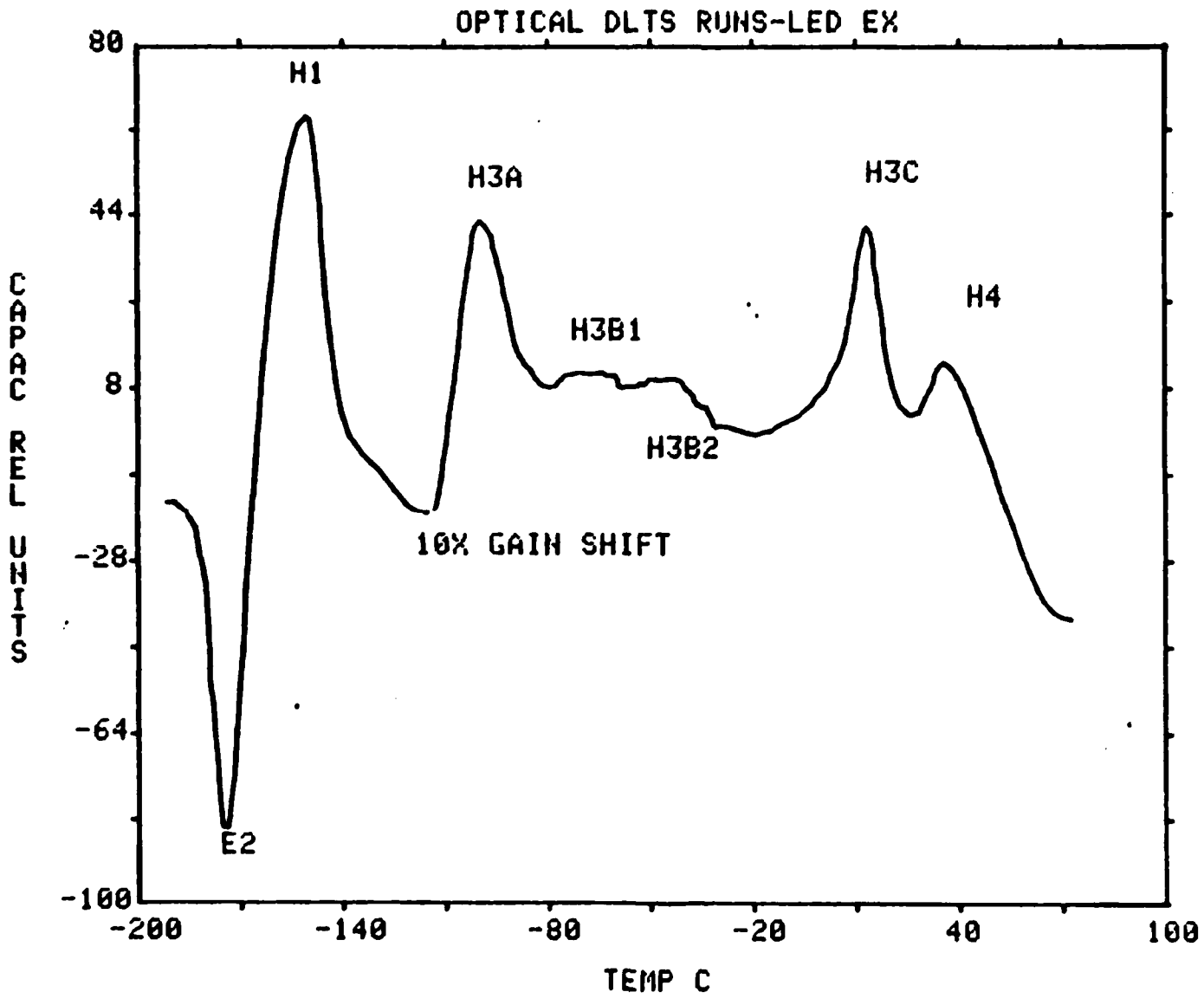
OPTICAL DLTS RUNS-LED EX
80
44
8
-28
-64
-100
CAPAC REL UNITS
H1
H3A
H3C
H4
H3B1
H3B2
10X GAIN SHIFT
E2
-200
-140
-80
-20
40
100
TEMP C

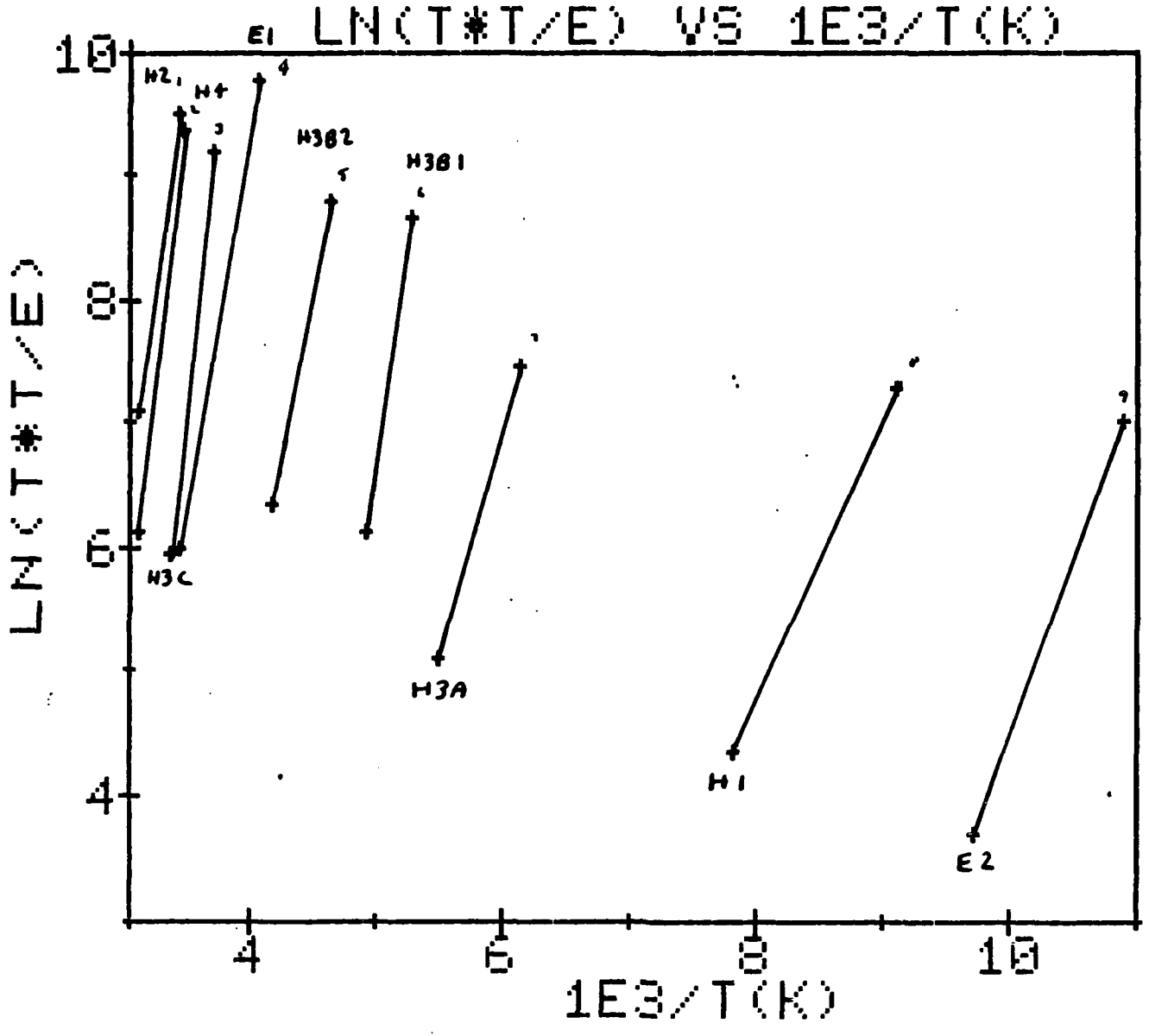
LN(T*T/E) VS 1E3/T(K)
E1
H2
H4
H3B2
H3B1
H3C
H3A
H1
E2
LN(T*T/E)
1E3/T(K)
10
8
6
4
4
6
8
10

emission to be exponential is probably the best approximation one can make.

Region A

The electron hole traps located here resemble the trap with electrical pulsing which were at room temperature. The melding of the hole trap to the electron trap follows - with regard to shape - almost identically to the "sex" change in the electrical case shown in FigIV-2. The relative transient heights, however, were the same for the two optically excited traps. This is manifested in the two DLTS peaks having the same height. The peaks remained inseparable. The two peaks stayed present, and at the same magnitude, no matter how drastically the parameters changed. This included long gating, high and low current pulses and large and tiny pulse widths. The ratio of capacitance change of the minority to the majority trap remained constant throughout all changes in pulse width. And this constant remained at "1". The wave eductor output for the transients is shown in FigIV-7. Note the symmetries in the transients at both peak temperatures.

Figure IV-8 shows a representative set of peaks at various frequencies. This data enabled the energy and cross section to be calculated via the the equations already set forth. Note the hump on the high temperature side of hole trap H1. That trap was

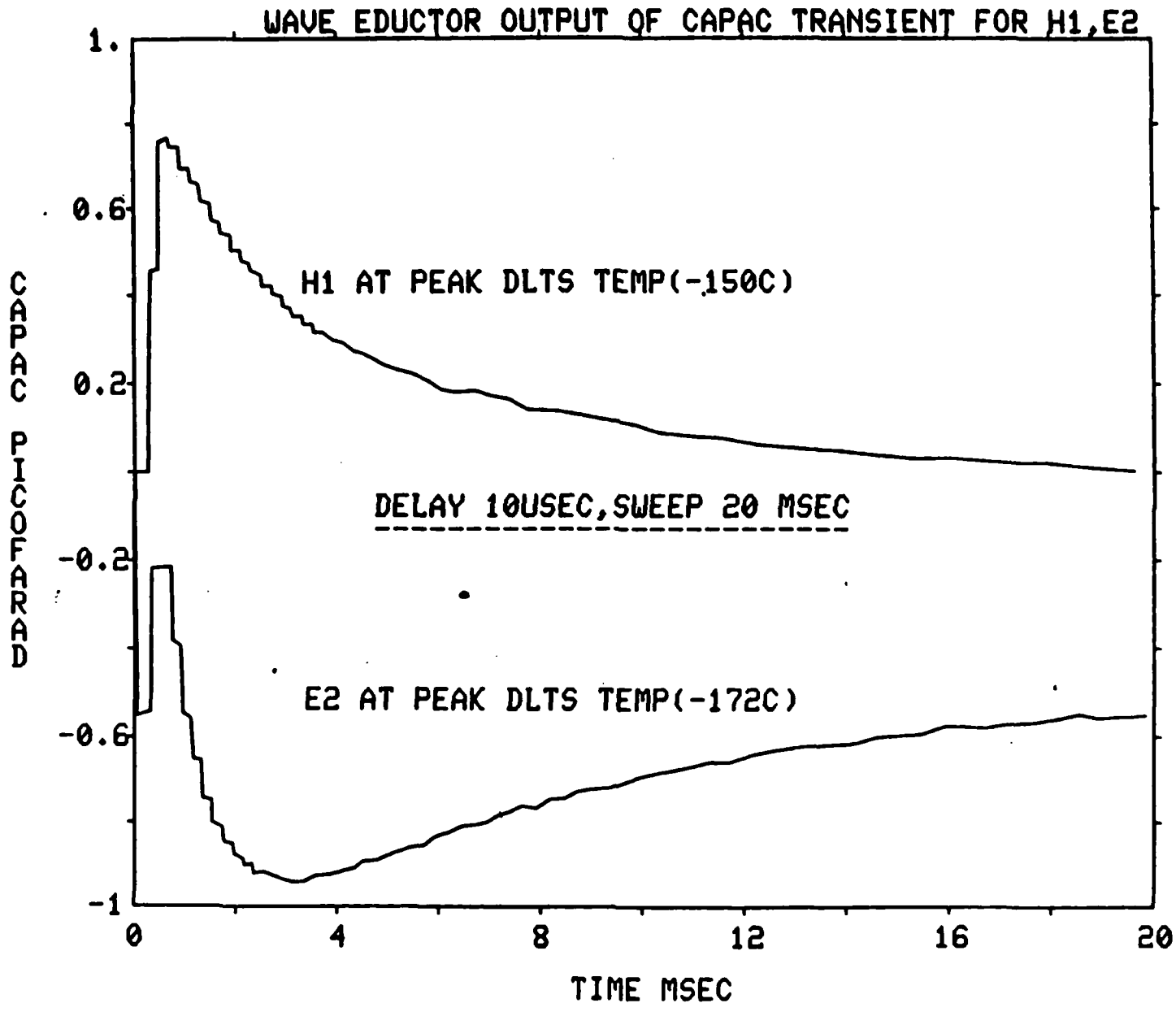
WAVE EDUCTOR OUTPUT OF CAPAC TRANSIENT FOR H1,E2
1.
0.6
0.2
-0.2
-0.6
-1
CAPAC PICOFARAD
H1 AT PEAK DLTS TEMP(-150C)
DELAY 10USEC,SWEEP 20 MSEC
E2 AT PEAK DLTS TEMP(-172C)
0
4
8
12
16
20
TIME MSEC

Fig IV-8

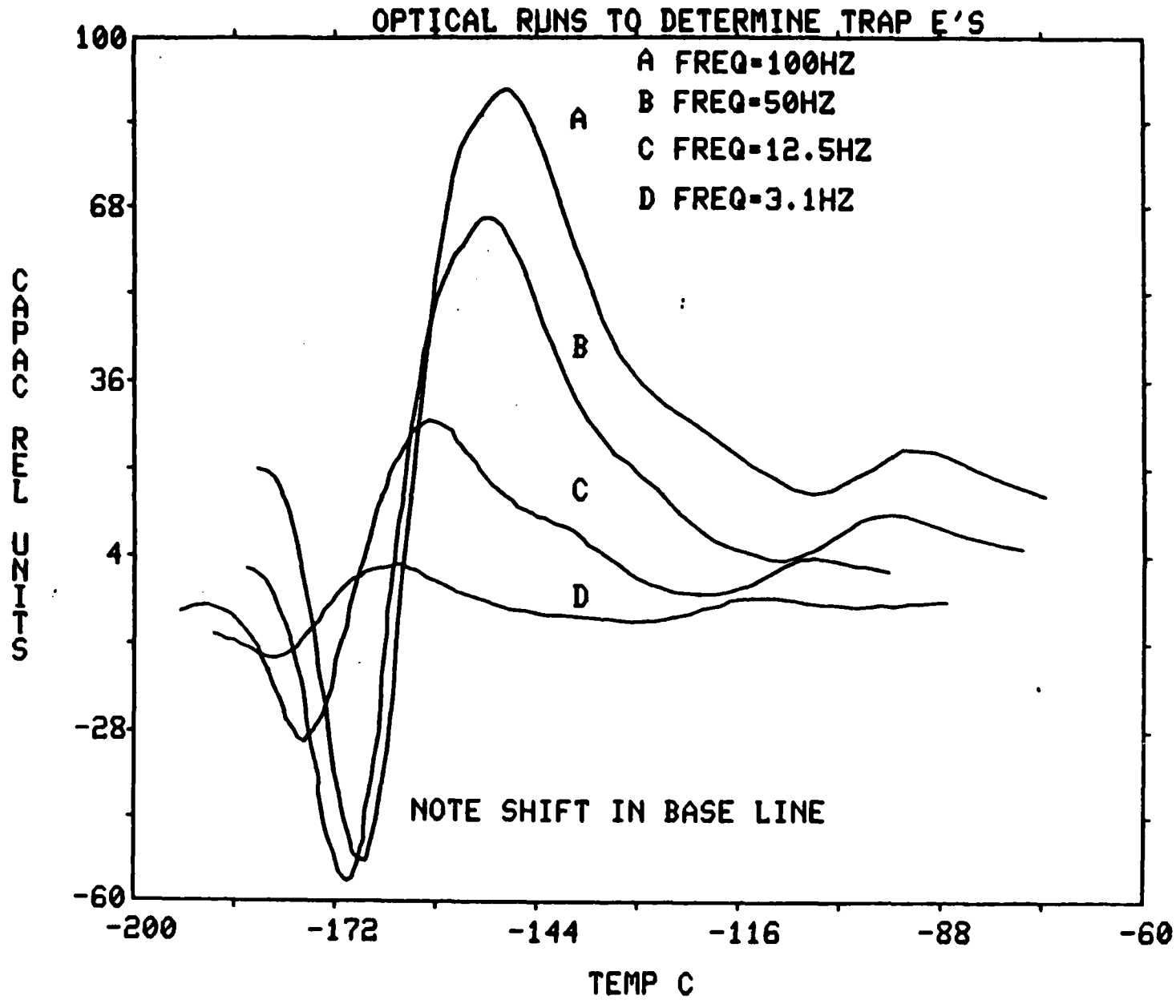
OPTICAL RUNS TO DETERMINE TRAP E'S
A FREQ=100HZ
B FREQ=50HZ
C FREQ=12.5HZ
D FREQ=3.1HZ
A
B
C
D
NOTE SHIFT IN BASE LINE
CAPAC REL UNITS
100
68
36
4
-28
-60
-200
-172
-144
-116
-88
-60
TEMP C

originally designated H11, because it could not be isolated from trap H1. H11 like H1 seemed to disappear at low pulse widths.

With the system set up nicely for the isolation of of peaks H1 and E2, I looked at the important plot of delta C vs the pulse width. Using a first approximation, and indeed it is very crude, the assumption will be made that the change in capacitance is directly proportional to to the trap concentration. It is not the proportionality that is the approximation, but rather the direct proportionality that is the assumption. Because the transients are comparable to quiescent and pulsed values, the equation cited for a direct trap concentration calculation is no good. But qualitatively, Figure IV-9 shows the trap concentration (in terms of the DLTS peak) as a function of pulse width. Looking at FigureIV-10, the saturation curve leads us to believe that the traps located at the low temperatures are far from being saturated at 300usec. If the trap was saturated, one might expect to see no change in peak height with increasing pulse width. A rough extrapolation of FigIV-10 finds saturation occurring at about 700-1000usec.

Along with the extremely important results above, high frequency runs at 150-200Hz yielded the splitting of peak H1 into two smaller peaks. H11 was seen before, but the high frequency enabled a peak to be seen instead of a simple hump. Using a purely mathematical approximation, the peaks were located about .04ev to either side of H1; that is H12=.158ev and H11=.238ev.

The final set of runs for this region concerned removing the bias and observing the peak height and shape. For H1 and E2

Fig IV-9

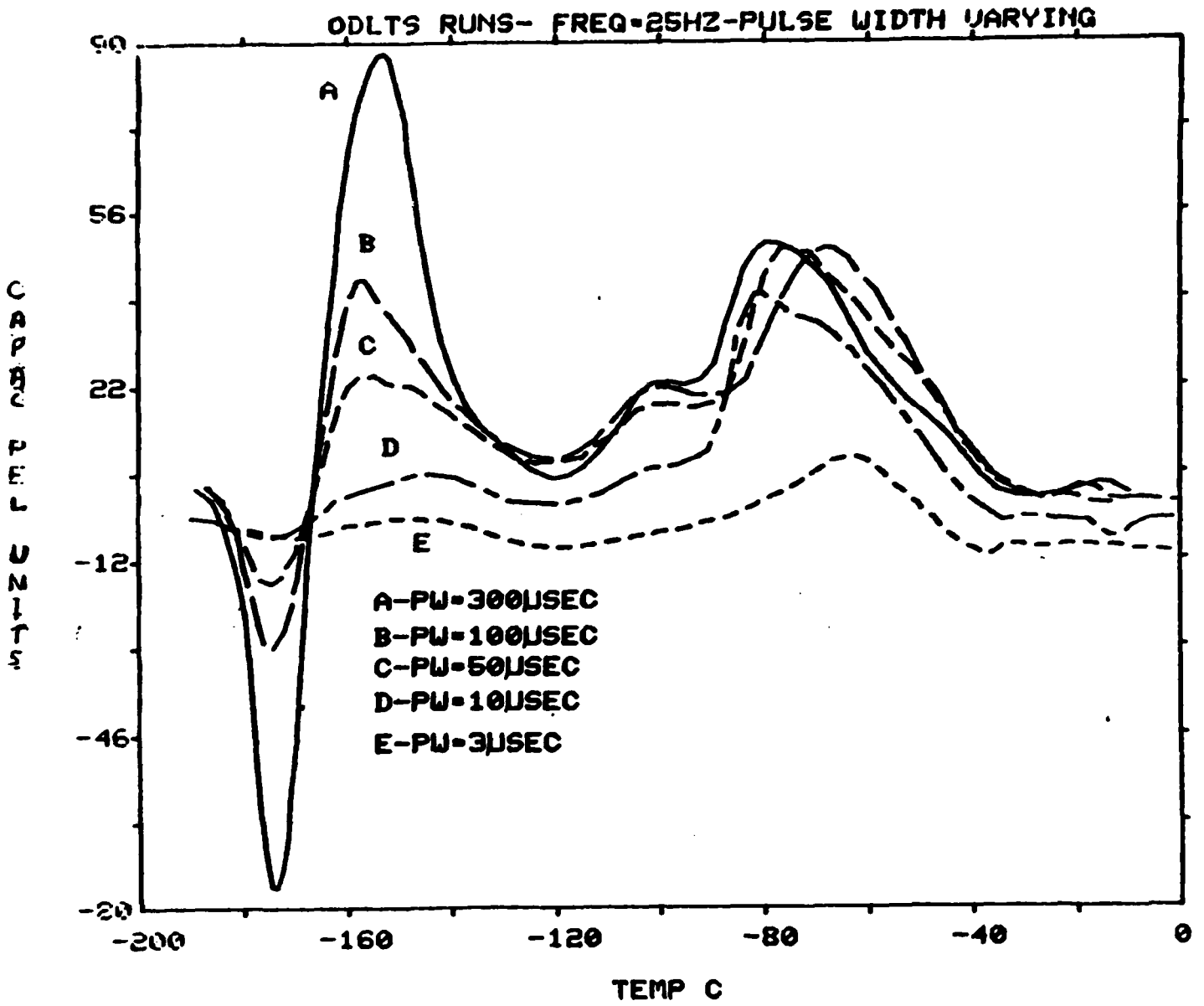
ODLTS RUNS- FREQ=25HZ-PULSE WIDTH VARYING
90
56
22
-12
-46
-20
CAPAC PEL UNITS
A
B
C
D
E
A-PW=300USEC
B-PW=100USEC
C-PW=50USEC
D-PW=10USEC
E-PW=3USEC
-200
-160
-120
-80
-40
0
TEMP C

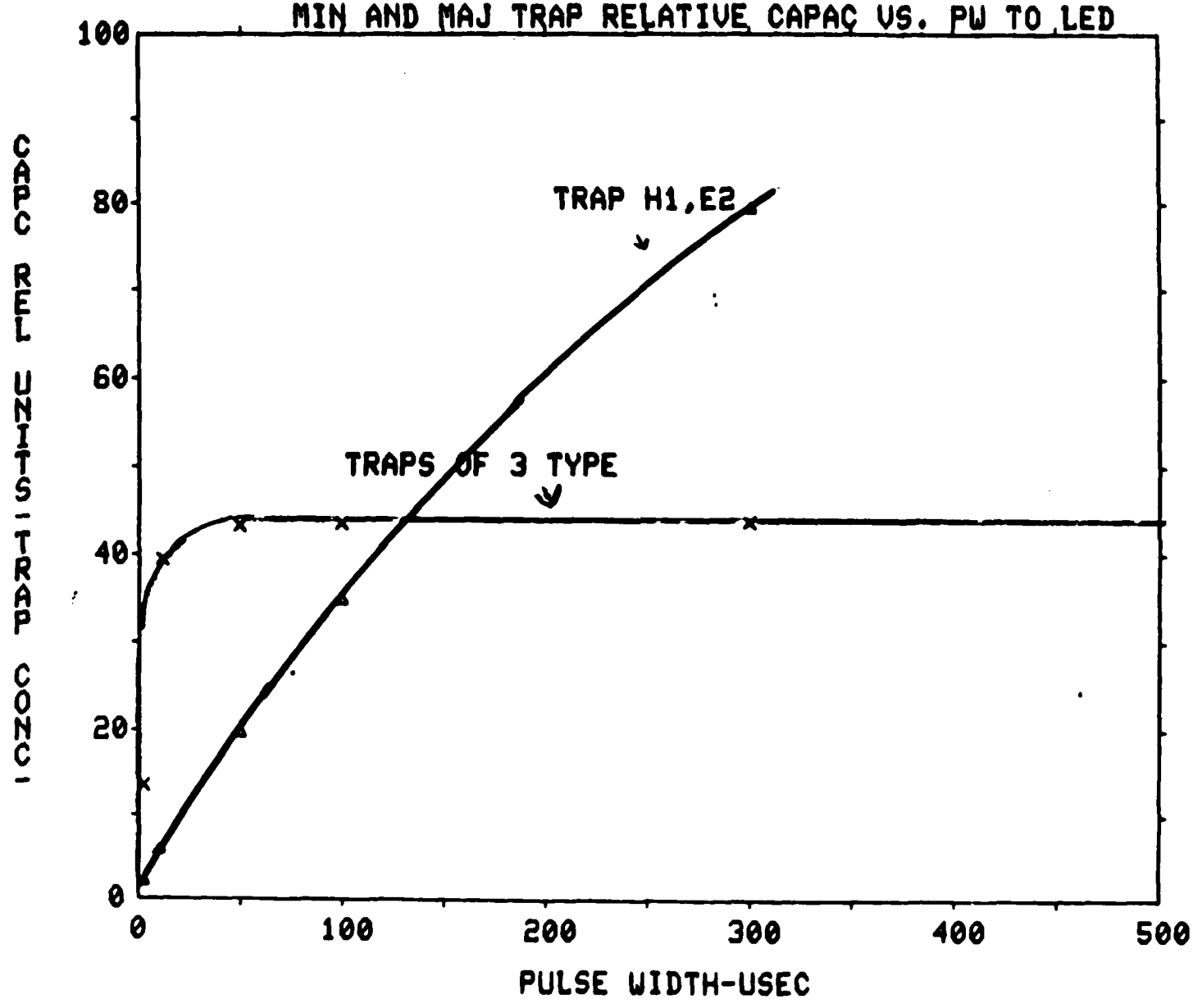
MIN AND MAJ TRAP RELATIVE CAPAC VS. PW TO LED
CAPC REL UNITS-TRAP CONC-
100
80
60
40
20
0
TRAP H1,E2
TRAPS OF 3 TYPE
0
100
200
300
400
500
PULSE WIDTH-USEC

there was no change at all when the light pulse was applied to zero bias condition. This suggests that the transition region is near the junction or that with light excitation the capacitance is not changing as much as the capacitance meter output says it is.

Region B

The next region of study is the group of peaks at mid-range temperatures. The three peaks were able to be clarified and and sharpened by controlling the pulse width. At high saturation widths, the entire B series is indistinguishable, but the lowering of the pulse width sorts things out. Referring back to FigIV-10, one notes the saturation in capacitance begins at about 40-50usec. This is one order of magnitude faster than H1 and E2. At about 10usec the peaks (3A, 3B1, 3B2) are all visible.

Using the systems secondary parameters together with changing pulse widths, the approximate saturation times can be found. Peak 3A is prominent at about 50usec, but fades away quickly at lower PWs. As 3A fades, 3B1 begins to dominate and peak at about 10usec. At the ultra-low PWs, both above-mentioned peaks fade as 3B2 dominates. This occurs at about 2usec. These traps were disentangled and each was analyzed in its prominent parameter settings so that energies and cross sections could accurately be determined.

The test of removing the bias was also conducted in this region and the peaks were still present, in general, although some were reduced slightly in size. One problem that came up was the apparent changes in the trap of the InP sample. Early results showed the group three peaks much smaller than the region peaks (by about a factor of ten) at low temperatures. But three weeks later, with the controllable and secondary parameters constant, the peaks seemed to get larger (about the same size as the region one traps). This seems to suggest some factor inherent in the growth or simply some defect in the InP sample rather than a trap related to Fe transitions.

Region C

The high temperature region was enhanced by the application of the longest optical pulses used in all the experiments (500-600usec). Although H3C was visible at 100usec, H4 did not become visible until a PW=400usec was used. These peaks were tough to look at , because they are located at temperatures that cause the contacts on the pad to become loose. Both peaks, even the spike, had superb exponential fits(see Appendix). The reverse bias test that showed no significant change in the peak height or shapes in the other two regions, had profound changes in this region. Figure IV-11 shows the two peaks with and without bias. Both traps disappear, but they seem to ride on

Fig IV-11

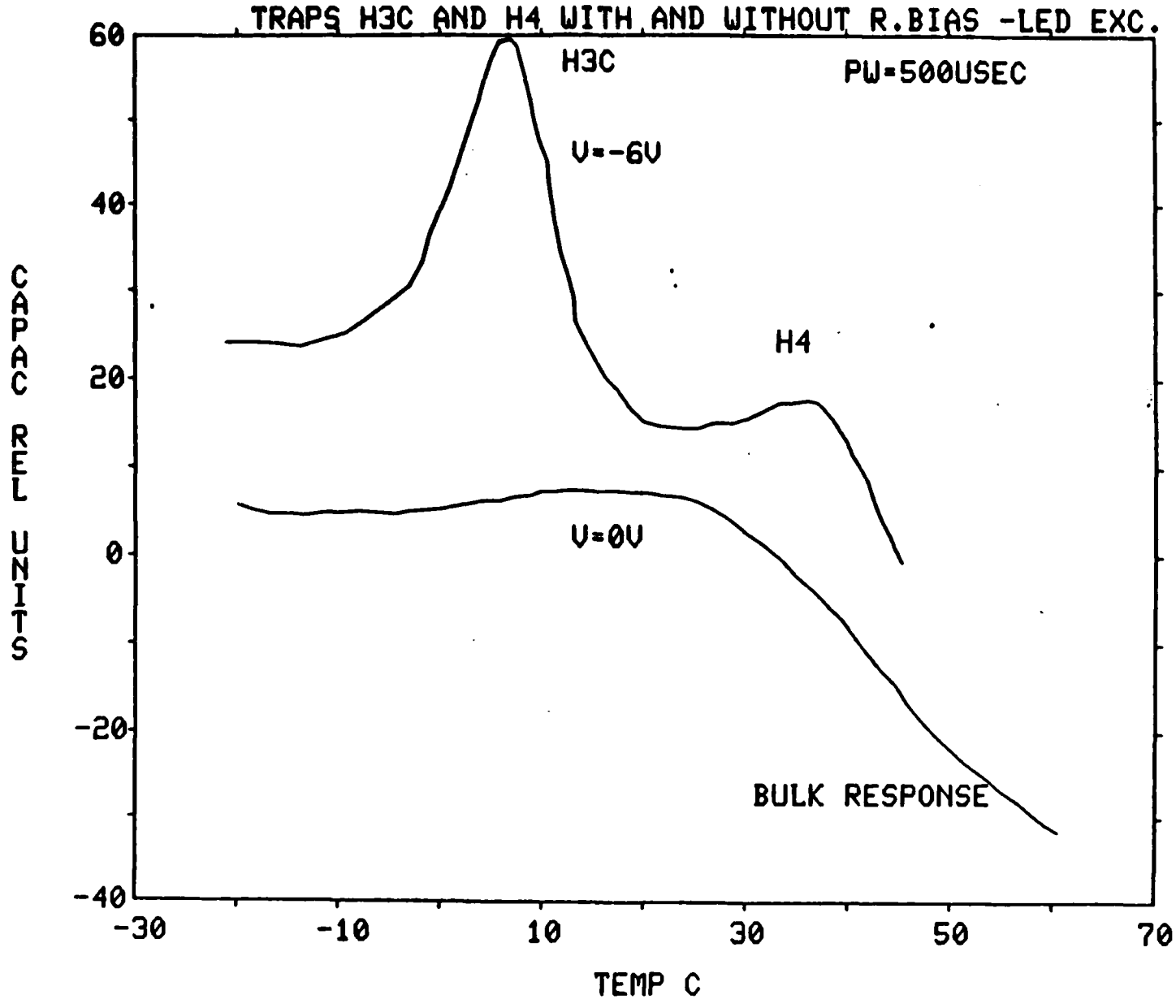
TRAPS H3C AND H4 WITH AND WITHOUT R.BIAS -LED EXC.
H3C
PW=500USEC
V=-6V
H4
V=0V
BULK RESPONSE
CAPAC REL UNITS
60
40
20
0
-20
-40
-30
-10
10
30
50
70
TEMP C

some background transient signal that is present even if there is no peak present. This bulk effect seems to take the form of a minority DLTS signal suggesting extra electrons in the n region.

In this section much information has been put forth concerning each of the traps. For conciseness I include TableIV-2. This includes a summary of the properties discussed here.

Table IV-2 Trap Characteristics

Peak	Traits
H1,H2	
	1.Saturation at 700-900μsec
	2.Cmaj/Cmin=1 under pulses(delta C)
	3.Nt(E2)=Nt(H1)
	4.Nt(E2),Nt(H1) not function of R.Bias
H1	Splits into H11 and H12
	H11=.15ev
	H12=.24ev
Group 3	
H3A	1.Saturation at 40usec
	2.Weak function of R.Bias
H3B1	1.Saturates at about 15μsec
	2.Weak function of R.Bias
H3B2	1.Saturates at 1μsec
	2. Weak function of R. Bias
H4,H3C	
	1.Saturation at 600+μsec

2. Trap filling strong function R.Bias

H3C Non-exponential decaying trap

LED Creation of e-h Pairs

Section V-1

Combined experiments with optical and electrical excitation are completely dominated by the light. Experiments where the electrical pulse extended past the end of the optical pulse by about 100usec can not compensate for the injected holes by the light. If one would want to know if the LED can actually excite a number of hole -electron pairs comparable to the doping or greater, a sample calculation could be done. For a sample calculations , I used the standard LED parameters (1mW at 20mA, half-power angle =24 deg) and some common operating conditions (PW=200usec, I=.4A, depth of penetration into layer=2um, distance to sample=.5cm).

In the first case, the 100% conversion from photon to pair is used. This result yielded : n(e-h)=1.5E18 cm(-3). This is a significant number of pairs and compared to the background doping, only about 1% conversion would be needed to equal that doping.

1/C^2 and Capacitance Model

Section V-2

One of the looming problems in the experiments is the small change in capacitance with applied voltage. The CvsV plots suggest a depletion of about 35um at 0 V and 36.5um at -10V. This yields an active range of about 1.4um. The light on the other hand could activate at -6V regions from 0 to 22um and n out to 36um. This would coincide with the strength relationship between the optical and electrical signals, but Hall effect measurments yielding over 50pF are simply to far from what was observed. The difference between the measurements arise because one is not measuring a simple capacitor, but a combination of capacitors and resistors.

Through many I-V-T and C-V-T experiments, it became apparent that the simple one capacitor model was no good. The factors that one must consider are: 1. Reverse leakage current at the junctions. 2. A series resistance for a conducting junction that may change with temperature. 3. A depletion region between the metal and the p+ contact. I-V curves at room temperature are shown in V-1.1 and V-1.2.

The possibility that the assumed ohmic contact (p+ on metal) could be a depleting contact, can have the strongest effect on our capacitance measurements. The problem could be compounded if one sees the possibilty that under certain conditions, namely any injecting type, that a trap thought to be exclusive to the n-type material, may actually be carriers of the opposite sex in the

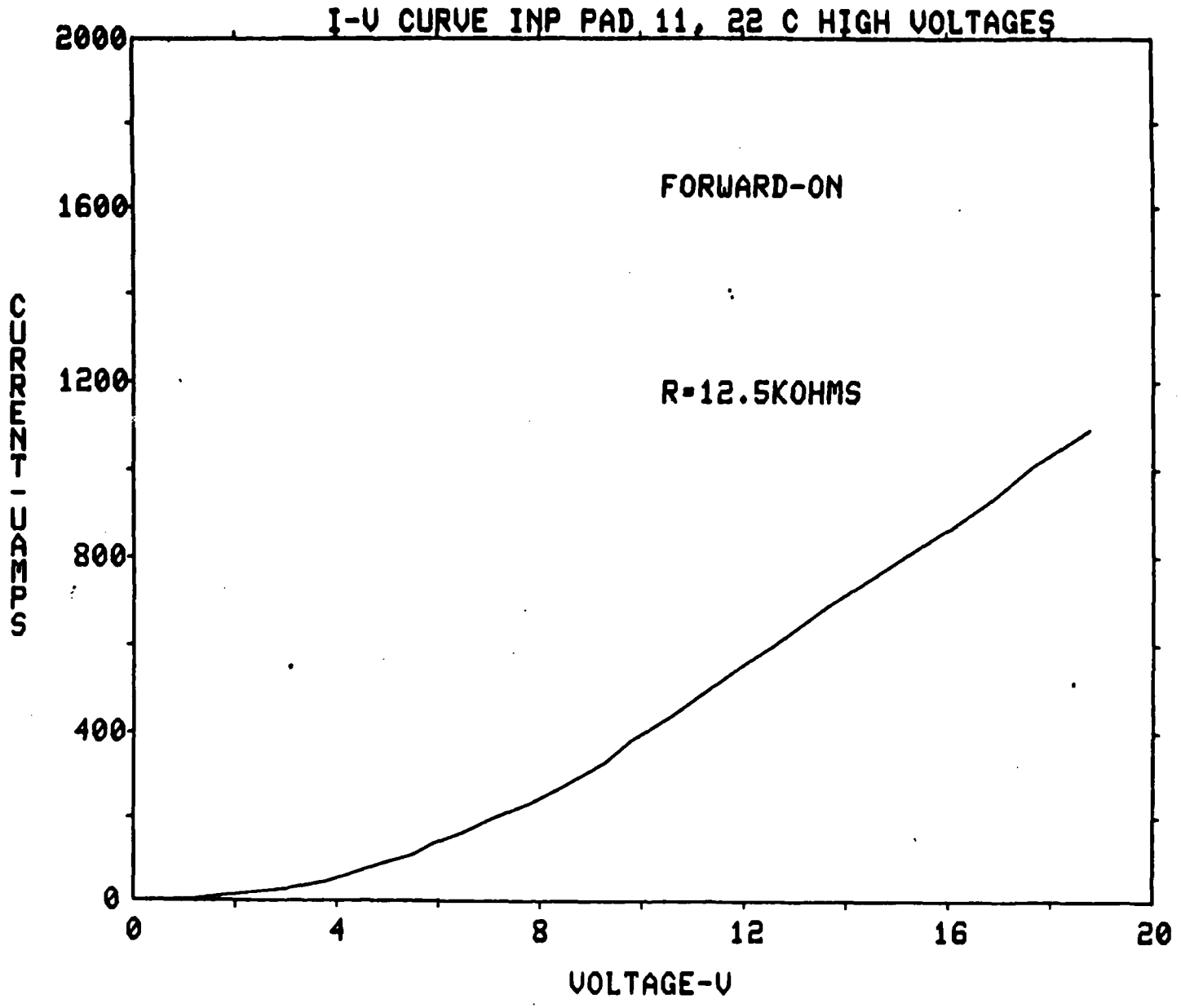
I-V CURVE INP PAD 11, 22 C HIGH VOLTAGES
FORWARD-ON
R=12.5KOHMS
CURRENT-UAMPS
2000
1600
1200
800
400
0
0
4
8
12
16
20
VOLTAGE-V

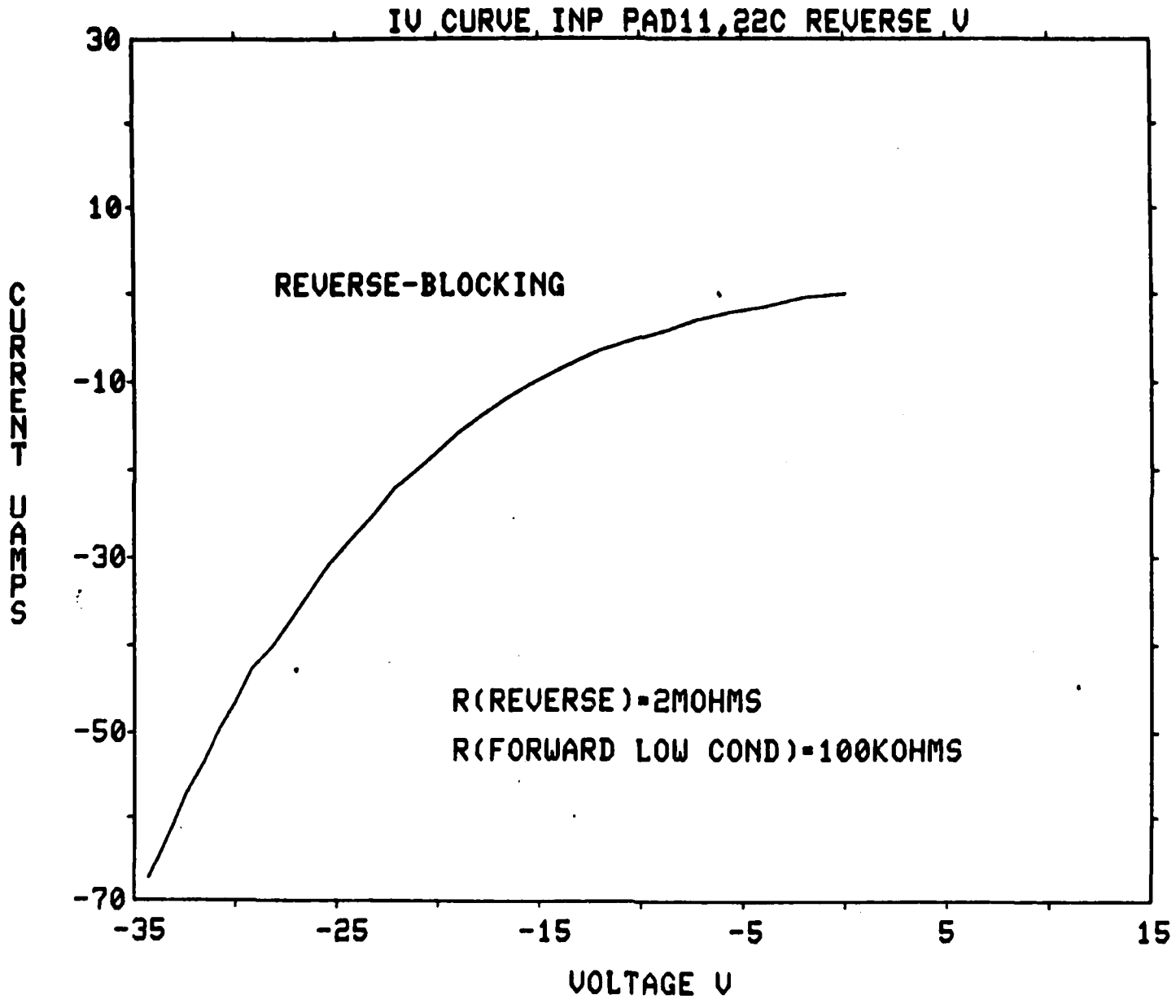
IV CURVE INP PAD11,22C REVERSE V
30
10
-10
-30
-50
-70
CURRENT UAMPS
REVERSE-BLOCKING
R(REVERSE)=2MOHMS
R(FORWARD LOW COND)=100KOHMS
-35
-25
-15
-5
5
15
VOLTAGE V

p+-metal depletion region (if it can be excited from equilibrium).

A model that I propose is the best model of many models, but it still can not explain all the discrepencies with certain parts of the I-V-T curves or some of the assumptions it must make. The model has its merits in that it can account for the huge differences in the C-V plots and thus, it can account for the doping observed.

The model is diagrammed in Figure V-2, where Cx is the actual capacitance of the p+n junction, Rs is a series resistance that will be considered to be negligible in this model, Co which is the fairly constant value for the junction capacitance of the p+-metal contact and the value of RL which is the reverse leakage current for the junction. Using electrical engineering principles, one can find impedances related to the network:

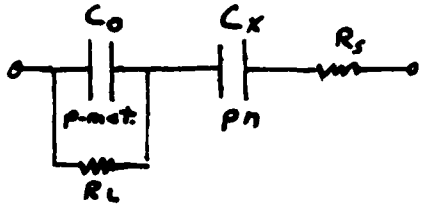

V-1

$$Z=(1/R_L + 1/(i\omega C_o))^{-1} + 1/(i\omega C_x) \qquad \text{V-2}$$

Using the conjugate multipliers and inverting for simplification, one can obtain the real and imaginary parts:

$$\mathrm{Re}(1/Z) = \frac{\omega^2 C_x(C_o + C_x)R_L - \omega^2 C_o C_x R_L}{1 + (\omega(C_x + C_o)R_L)^2} \qquad \text{V-3}$$

$$Im(1/Z)=C_x\left[\frac{1+\omega^2C_o(C_x+C_o)R_L^2}{1+(\omega(C_x+C_o)R_L)^2}\right] \qquad V\text{-}4$$

For the output of the Boonton a standard capacitance Cs is internal to the meter and a resonant circuit is obtained so that one may determine the unknown value (which is actually the output voltage) of capacitance in the bridge. The voltage that is registered as capacitance is Vcm. Therefore,

$$Vcm=REAL(Vout) \qquad V\text{-}5$$

$$Vcm=REAL(Vin/Z)(1/iwCs) \qquad V\text{-}6$$

$$Vout=Vin(iwCx)(1/iwCs)=VinCx/Cs \qquad V\text{-}7$$

Thus, the capacitance measured is directly proportional to Vout with Cm=Cx(1/Z'). In this case Z' is simply the bracketed terms in V-4. Using some possible values, one can test this model. Assuming the data for the sample obtained through the Hall effect measurements are correct, then using NB=1.3E15 cm(-3) and NA=1E18 cm(-3) are our doping concentrations.

For 1/C^2 vs V plots, the slope m can yield the background doping through the old equation II-14 concerning capacitance. This implies that ,

$$NB=2/[(A^2)(\varepsilon q m)]$$

A is the effective area of the pad determined to be 30 by 30 mils or A=5.81E-3 cm(-2). Therefore, for this InP sample the background doping can be found to be:

Units

NB=4.18E11/m ;m{V/pF^2}; NB{cm^3}.

In order to select a value for RL, one consults the many I-V curves such as Fig V-1 at room temperature. After averaging the leakage resistance, the model parameters can now be set up:

Cx=Cxo(1/(1+V)) ; Vbi=1V

RL=1.2Mohms

w=2πX(1Mhz)

Cxo=55.8pF

This data is straightforward, but the value for Co is not. Using hindsight, I note that with the data given, to yield the model self-consistent the value for the heavily doped p+ side the capacitance must be 1.5pF. But using the Hall effect data that was supplied and the area of the pad that was given,one would expect a capacitance of about 100X larger or 150 pF. Some explanations for this descrepancy could be: 1. the actual interacting area on the p+ layer is only 1/100 of the actual area. 2. An oxide layer forms creating a metal oxide semiconductor contact. In that case, one would have all the data necessary to calculate the oxide thickness that must be present. Using C=εA/W, the oxide layer would have to be on the order of 2um. This is a very large layer that would have to be formed. 3. Finally, it could be a combination of both situations. With the model intact, I used the computer to develop different parameter changes and see how the model compares to the results obtained. Figure V-3 and V-4 show two of the many (a sampling is supplied in the Appendix) theoretical models as compared to the actual data respectively.

The doping and slight bending of the actual data are explained reasonably well by this model. This model does have its problems away from room temperatures, because of the possibility to include Rs and a variable p+-metal capacitance. I will discuss the I-V at varying temperatures briefly, since a complete model would have to include this temperature dependence.

1/C*C VS. BIAS(V)

Theoretical Model

RUN DATE-THEORET MODEL IN P FE IN BULK
RUN DATA - RL=1M CXO=55.8PF CO=1.7PF

INPUT DATA

V-BIAS	C(PF)	1/C*C
0	1.65	.3673
1	1.6302	.37628
2	1.6153	.38326
3	1.60293	.38919
4	1.5922	.39446
5	1.5826	.39926
6	1.5739	.40368
7	1.56588	.40783
8	1.55842	.41174
9	1.55142	.41547
10	1.54483	.41902

SLOPE=4.9751995E-03
INTERCEPT=.372173236
XFIT(1)=0
YFIT(1)=.372
XFIT(2)=10
YFIT(2)=.421

(1/T(K)-MIN= -1 (1/T(K))-MAX= 11

LN(T*T/R)-MIN= .36 LN(T*T/R)-MAX= .44

1/C(PF)^2 VS. BIAS (V)

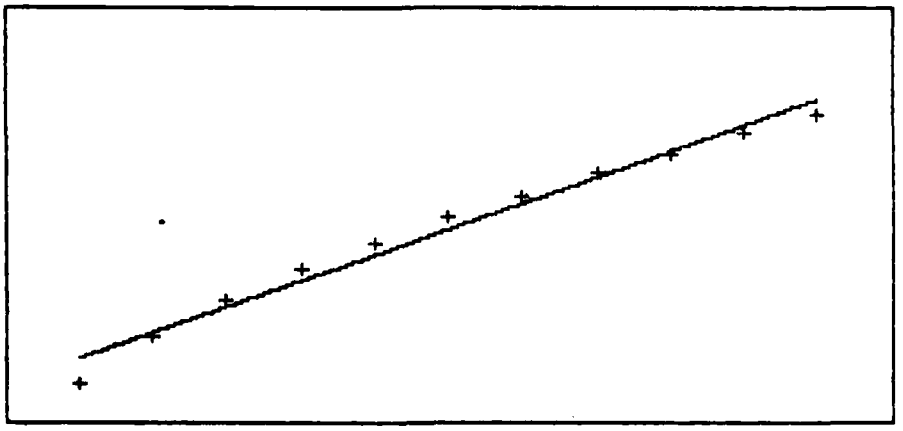

1/C*C VS. BIAS(V)

RUN DATE-21APR83
RUN DATA - INP PAD 11 22DEG C

INPUT DATA

V-BIAS	C(PF)	1/C*C
0	1.846	.29345
1	1.816	.30322
2	1.794	.3107
3	1.773	.31811
4	1.76	.32283
5	1.751	.32615
6	1.745	.3284
7	1.735	.3322
8	1.72	.33802
9	1.71	.34198
10	1.705	.34399

SLOPE=4.75842212E-03
INTERCEPT=.29976217
XFIT(1)=0
YFIT(1)=.299
XFIT(2)=10
YFIT(2)=.347

(1/T(K)-MIN= -1 (1/T(K))-MAX= 11

LN(T*T/R)-MIN= .29 LN(T*T/R)-MAX= .35

1/C(PF)^2 VS. BIAS (V)

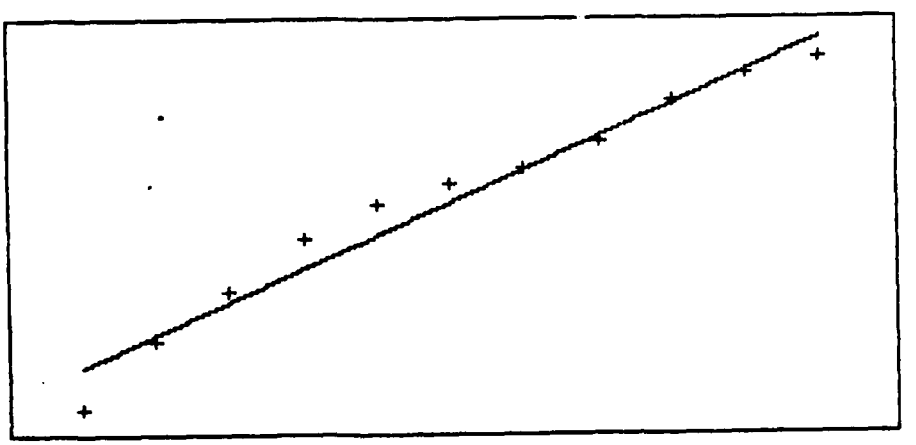

I-V-T Characteristics

Section V-3

As temperature varies, the resistance values change drastically. They also change enormously with a light pulse. The light excitation is harder to explain in terms of modeling in comparison to electical excitation. In a light pulse the C_o value for the p+-metal junction would most certainly change. Optically it is tough to find a theoretical equation as to how the width is effected by a light pulse. One can speak in general terms, but to claim that the width shrinks to 7/12 of its quiescent width under the optical pulse considers the simple one capacitive model of excitation. This is certainly not even a good approximation.

Some important data that might help the situation further is the I vs T curve that is carried out at a specific voltage. Figure V-5.1 and V-5.2 are those curves for a forward bias of +5V and a reverse bias of -8V respectively. Because of the interaction that is involved in the sweeping of temperatures , I plotted lnI vs 1/T in an Arrhenius fashion for R=Roexp(-E/kt). These plots are shown in FigV-6.1 and V-6.2. The excitation energy was recorded as .08ev for forward and .25ev for the reverse. It should be noted that these plots are merely attempts to observe some data for I vs T; therefore, taking those energy values too seriously would be a mistake.

Not much work was done on optically pulsed I-V curves, because of time limitations but the folowing is a general summary

Fig V-5.1

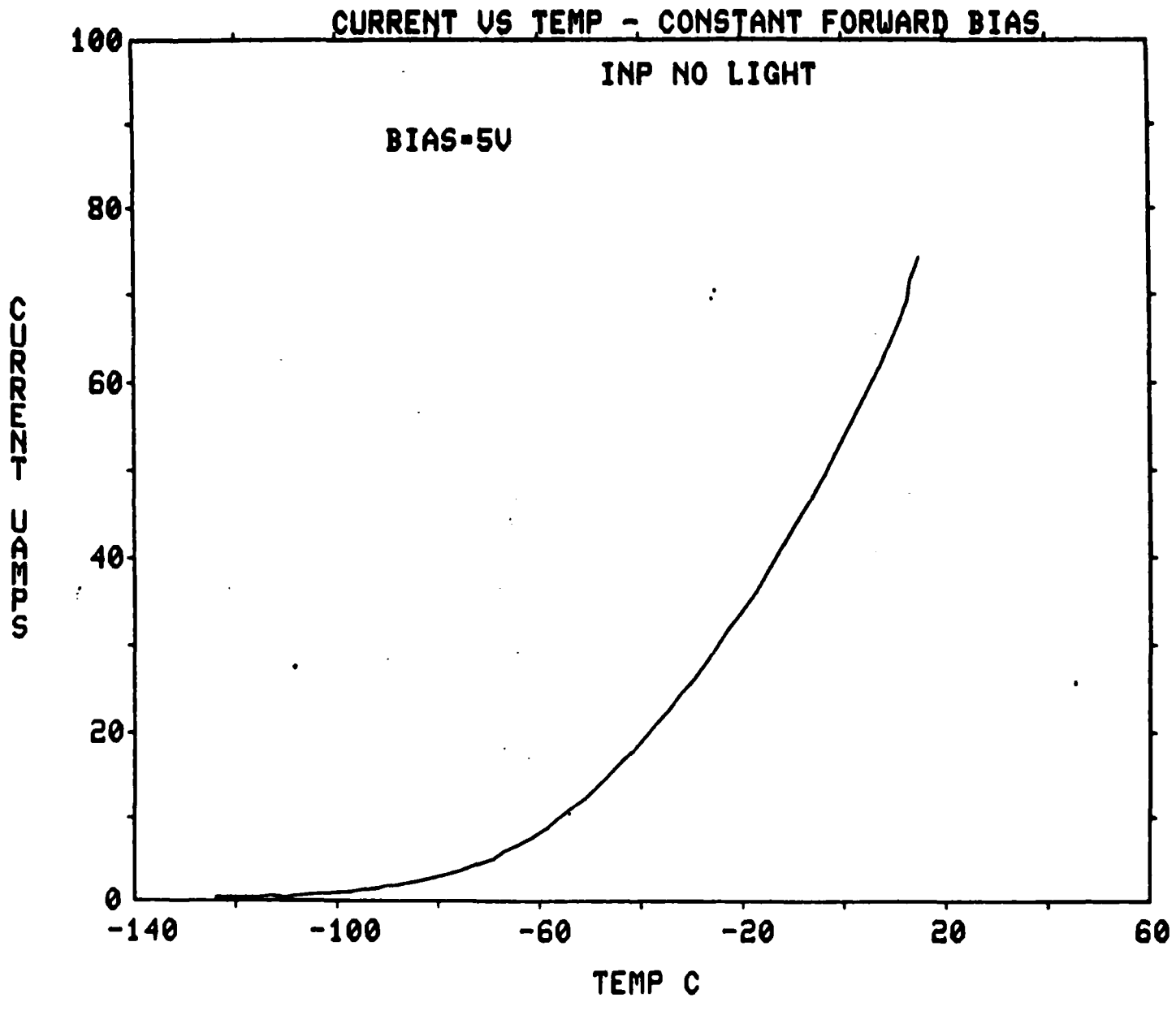
CURRENT VS TEMP - CONSTANT FORWARD BIAS
INP NO LIGHT
BIAS=5V
100
80
60
40
20
0
CURRENT UAMPS
-140
-100
-60
-20
20
60
TEMP C

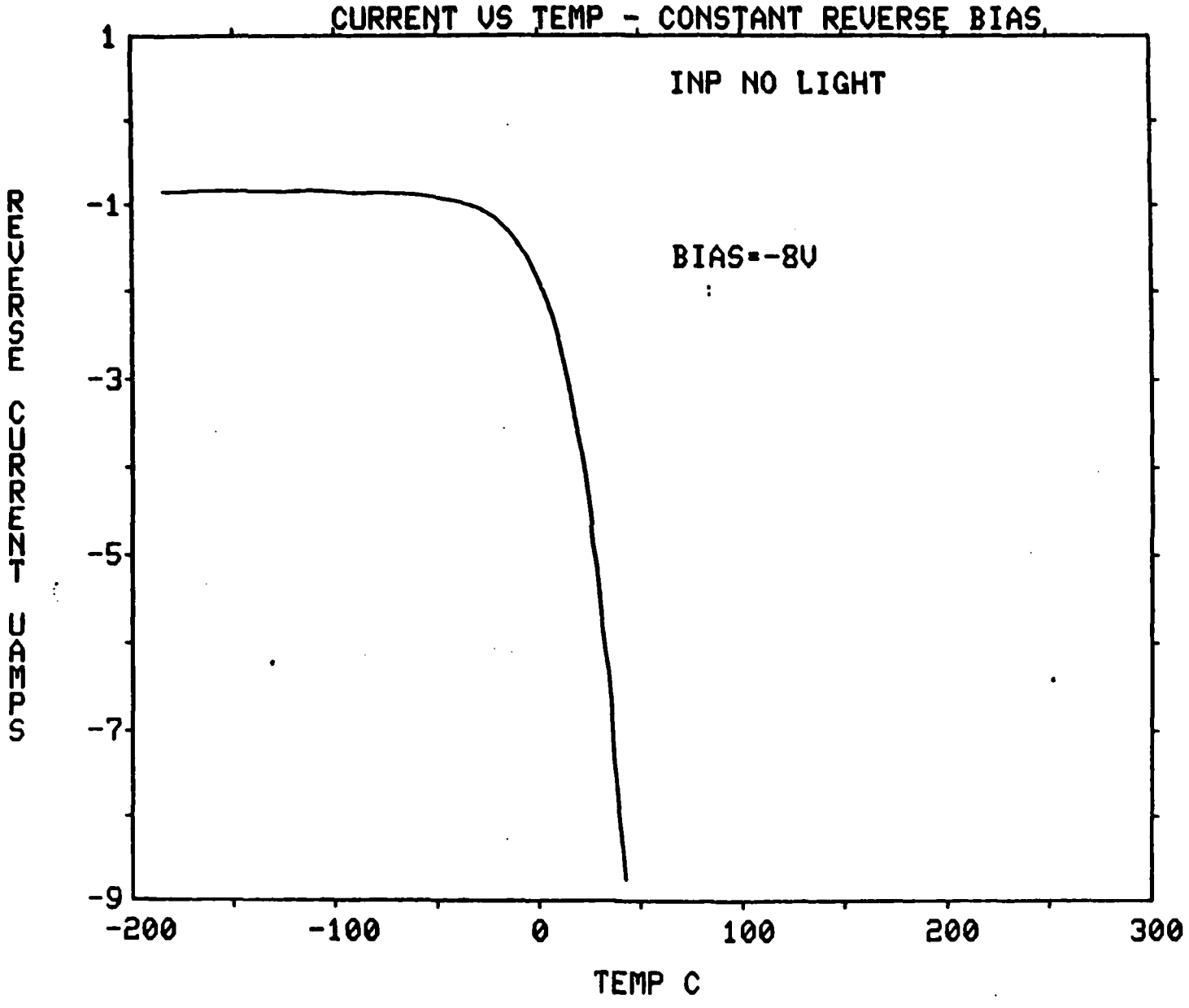
CURRENT VS TEMP - CONSTANT REVERSE BIAS
INP NO LIGHT
BIAS=-8V
REVERSE CURRENT UAMPS
1
-1
-3
-5
-7
-9
-200
-100
0
100
200
300
TEMP C

Fig V-6.1

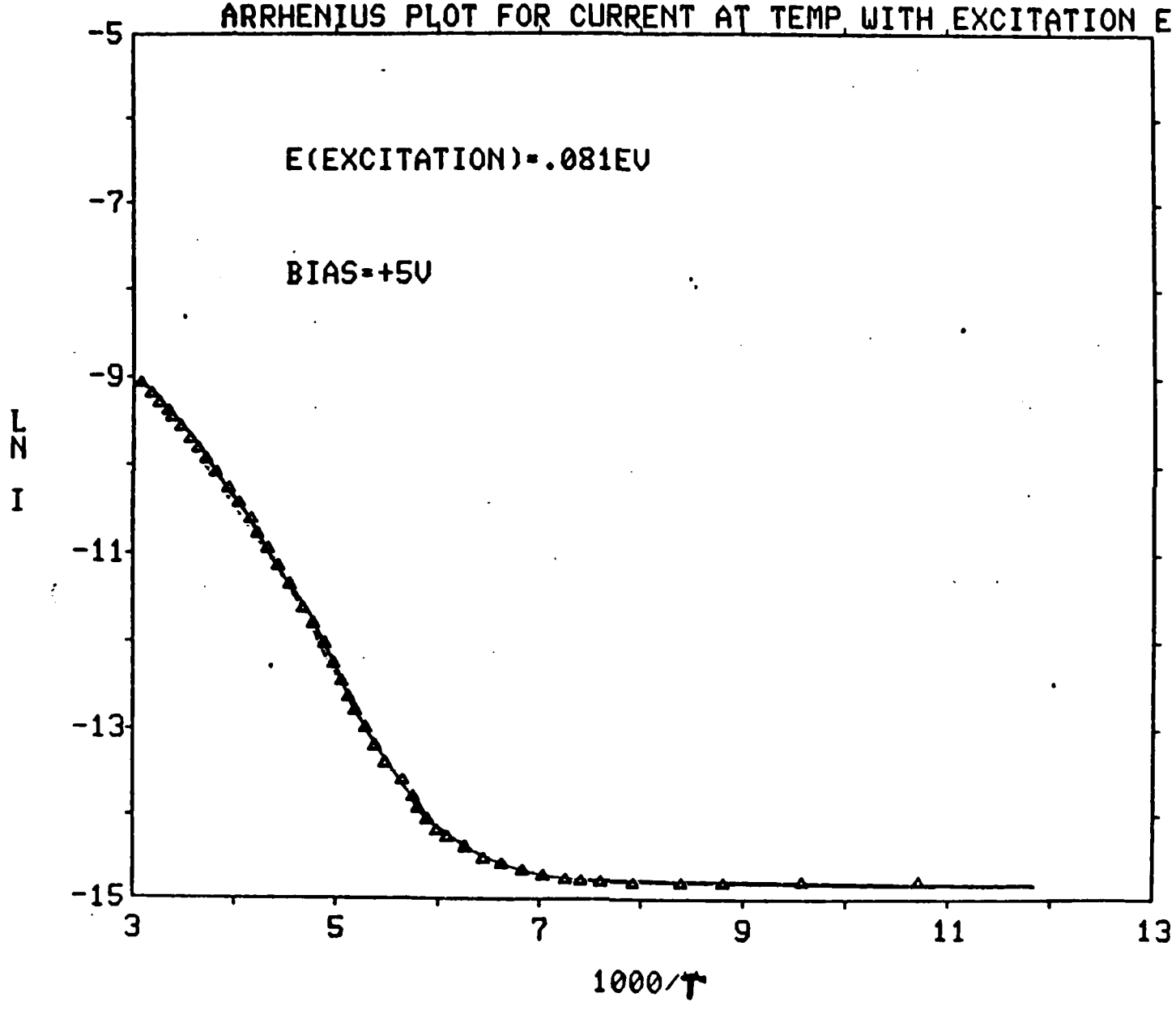
ARRHENIUS PLOT FOR CURRENT AT TEMP WITH EXCITATION E
E(EXCITATION)=.081EV
BIAS=+5V
LN I
-5
-7
-9
-11
-13
-15
3
5
7
9
11
13
1000/T

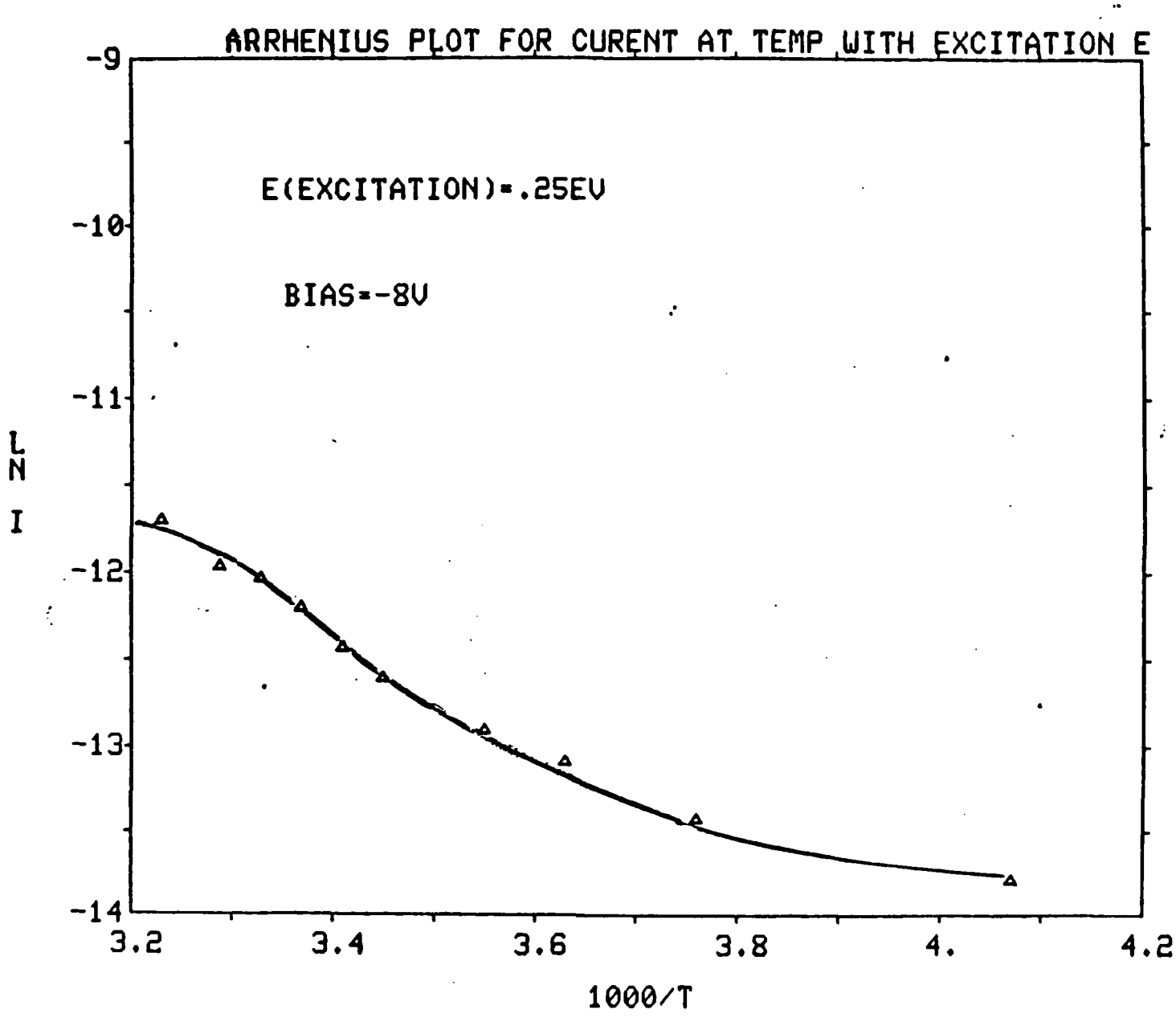
ARRHENIUS PLOT FOR CURENT AT TEMP WITH EXCITATION E
E(EXCITATION)=.25EV
BIAS=-8V
LN I
-9
-10
-11
-12
-13
-14
3.2
3.4
3.6
3.8
4.
4.2
1000/T

in the three temperature regions (remember that the LED spectrum changes with temperature):

1. At high temperatures the light does little to effect a change in the I-V plots.

2. At moderate temperatures(-40 to 10 C), the forward resistance increases slightly and the reverse impedance decreases slightly.

3. At low temperatures (-120 C down), the diode looks like a resistor when no light is present. Its impedance is very high at about 10Mohms. With the light on, the diode behaves ideally with R(forward)=30Kohms and R(reverse) =600Kohms.

Fe Transition Models

Section V-4

The importance of studying the Fe doped samples has been discussed earlier, but it must be emphasized the models put forth here and by other groups today are by no means unique or totally unambiguous. These models help explain why one state is seen, if it is seen at all; while some are allowed in certain regions and other aren't. If certain Fe+ levels do indeed exist, then they could appear as trapping states in the semiconductor using optical or electrical excitation. First, I would like to give some background on the doping of Fe and then I can discuss the most recent theories and transition models in the world to date. After that I will put forth my own model similar in nature to others. Finally , but most importantly, I will offer one possible explanation of the peaks observed experimentally in terms of the Fe transition model and the capacitance model developed in the last section. The importance of the capacitance model here is obvious. Because the two junctions are probably in transition, majority traps supposedly seen on the n-side as an electron trap could well be a majority trap in the p+ region of that junction and vice versa. This ambiguity could complicate analysis of the results, but it is certain factors that are unique to a trap that lead me to believe that certain traps are iron related even if the hole trap was a mistaken electron trap.

For the iron doping, iron is substitutional on an In site. Different experiments led to the Fe+2 and Fe+3 states being identified.

The most notable work was done by Fung et al. in 1975[9]. They postulated a model with three charge states, Fe+3, Fe+2 and Fe+1. He began identifying traps.

In n-type InP Fung proposed a stable Fe+1 state in the neutral n-type region. Theoretically, all the iron in a neutral site would be in its most negative state allowed which Fung thought to be Fe+1. Recently the Fung model has been seriously questioned by Eaves, Williams and and Cockayne[10] who suggest that Fe+2 is actually the stable neutral state and evidence most recently suggested by Tapster et al.[11] have suggested this is the case. The Tapster model suggests that Fe+2, Fe+2*(the excited state where lasing has occurred), Fe+3 and perhaps Fe+4 all exist in the energy gap.

The problem now is to locate energies that are associated with iron transitions through photocapacitance or DLTS techniques. Before an analysis of the transitions is done, one must first have some previous model to work from. FigureV-7 is one of the most recent models suggested by Eaves et al.. The figure suggests thermal emission of both holes and electron are possible. His conventions are handy and I will use them also. Transition lines up and to the left are electron emissions and up and to the right are hole emissions. Horizantally, the charge states of +4, +3 and +2 are present in the gap implicitly assuming that the +1 state is in the conduction band. One must

Fig V-7

Fe Transition Model From Eaves et al.

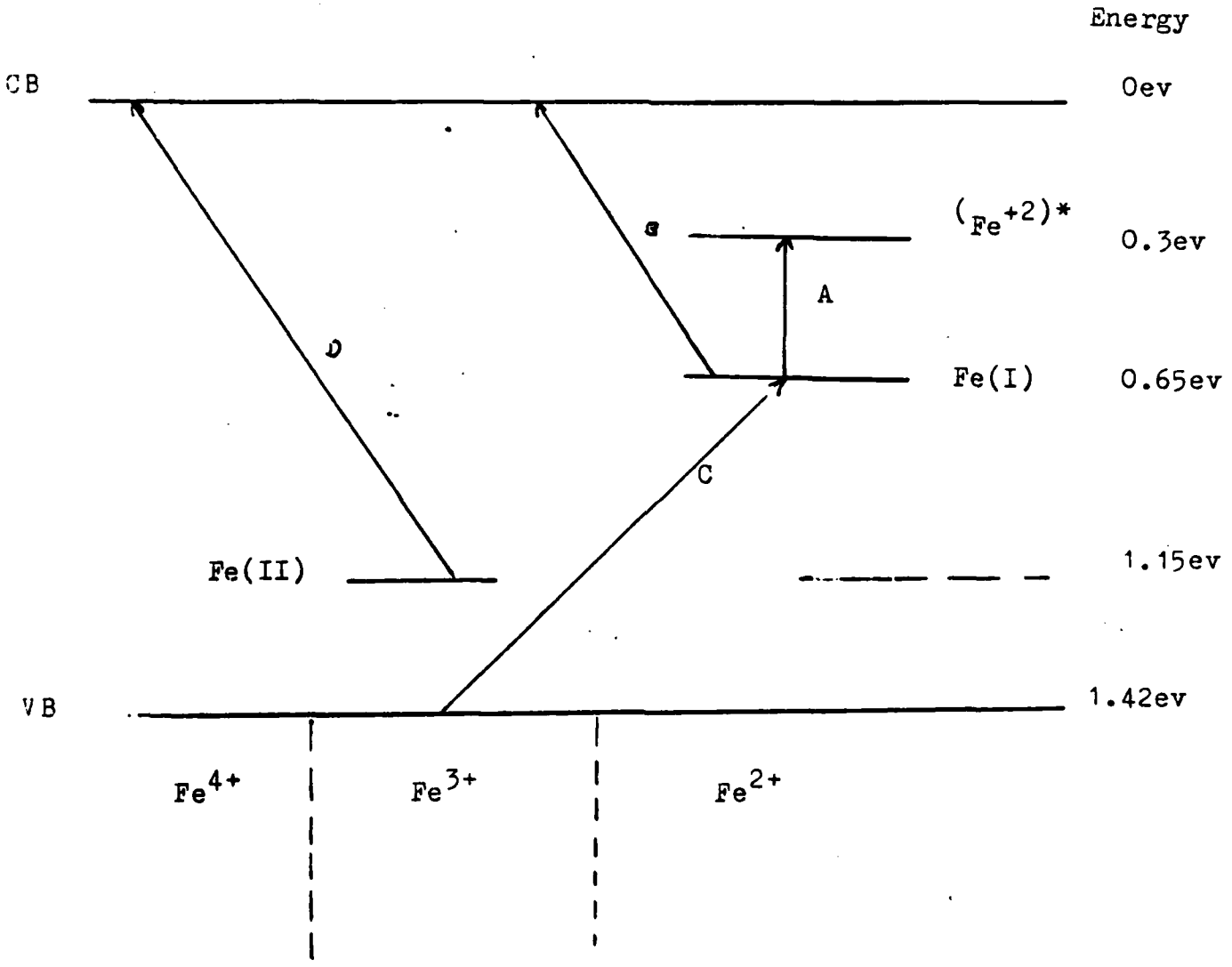

be careful in the literature to determine the energies that are stated. Up until now, the assumption has been made that the DLTS energy is the trap energy with respect to a band. This is not necessarily true if the capture cross section varies with temperature. Guillot, Bremond et al.[12]used a capture cross section that varied as, $\sigma n = \sigma n_{\infty} \exp(-E\sigma/kt)$. The measured DLTS peak would yield data that corresponded to Eta=Et+Eσ. Some of these activation energies have been found to be as low as 0ev and as high as .1ev. These tedious calculations have been done by Rhee et al.[13] by mapping the cross sections at different temperatures. Generally, the capture rates are too fast to be observed with accuracy.

Returning to FigV-7, one sees that electron emissions are simple enough. For example, Trap D has an electron thermally emitting to the conduction band creating Fe+4. The energy of that electron process is straightforward and is Ec-E(Fe+3)=electron emission +3 to +4 state. Hole emission is confusing . But the key to finding the right emission energy is to consider the actual process of electron capture to that trap. This makes it clear that a hole emission to a certain state has the energy that is related to valence band and the state that is receiving the electron(the final state) not the state that emitted the hole. For example, a hole emission from the state of Fe+3 yields the state Fe+2. The energy related to this transition is the final state's energy difference with the valence band: E(Fe+2)-Ev=hole transition from +3 to +2.

With a solid knowledge of the energy conventions and a known model, one can analyze in great depth the transitions zones that are present with and without light. Using that knowledge, a working model for this study can be done.

Figure V-8 represents a view of a band that is bending with the Fermi energy crossing through the states. It is merely an arbitrary selection so all possible transitions may be studied. Later in the band modeling for the Fe states the actual position is important. Two cases will studied: excitation of holes and electrons (by light injection etc.) and response after the excitation is gone.

Region A

1.electron emission impossible

2.a hole emission Fe+4 to Fe+3

2.b electron capture - Fe+4 to Fe+3

Region B Fe+3

1.a electron emission Fe+3 to Fe+4

1.b hole capture Fe+3 to Fe+4

2.a hole emission Fe+3 to Fe+2

2.b electron capture Fe+3 to Fe+2

Region C Fe+2

1.a electron emission Fe+2 to Fe+3

1.b hole capture Fe+2 to Fe+3

2. electron capture and hole emission impossible

Region D Fe+2*

1. consider Fe+2 to Fe+2* to Ec as possible

Now that the excitation has provided changes in state of Fe in the specific regions, one can now look at the return to

Fig V-8

Fe Regions in the Band

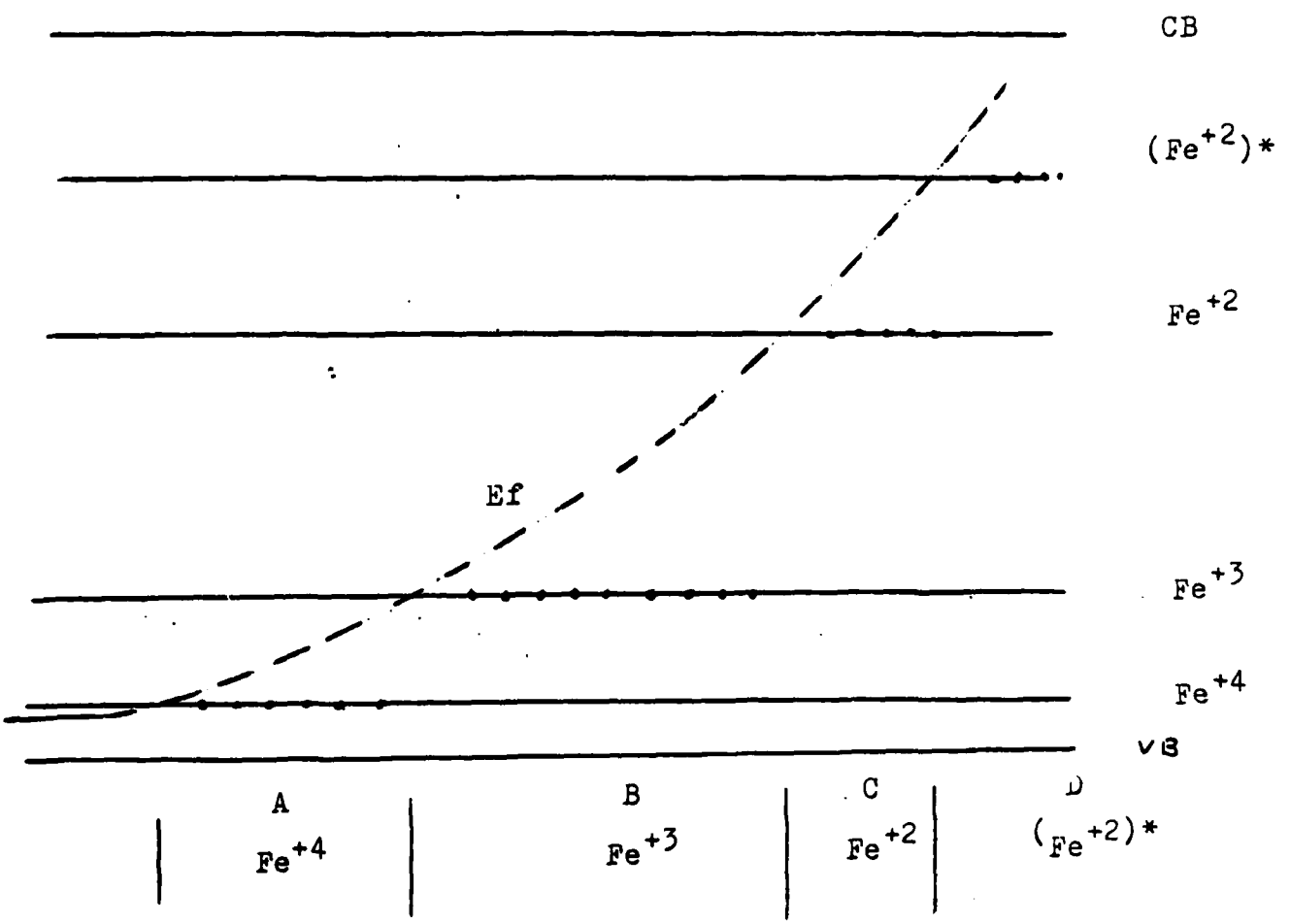

equilibrium in these regions. Again all possible transitions will be included(even the ones that are highly improbable).

Region A

1. no transition

2.a hole capture E=Fe+3-Ev

2.b electron emission E=Ec-Fe+3

Region B

1.a electron capture E=Ec-Fe+4

1.b hole emission E=Fe+3-Ev

2.a hole capture E=Fe+2-Ev

2.b electron emission E=Ec-Fe+2

Region C

1.a electron capture E=Ec-Fe+2

1.b hole emission E=Fe+2-Ev

Region D

All transitions going from +2 up to the conduction band can go through +2*.

With a full list of possible transitions one can narrow down the choices. In region A hole capture is usually impossible, but near the depletion p -side some holes may be allowed to slip across(it is unlikely). In The key region B, one must assume spontaneous thermal emission,therefore, B 1.a and B 2.a are not allowed. The other two transitions, hole emission and electron emission are possible. In region C for the same reasons as above the spontaneous capture of an electron from the depletion region

is rare. After this elimination, the following transitions are allowed:

Table V-1

Region	Meas. E	Transition
A-Fe+3	Fe+3-Ev	hole capture(Fe+4 ?)
B-Fe+3	Fe+3-Ev	hole emission
B-Fe+3	Ec-Fe+2	electron emission
C-Fe+3	Fe+2-Ev	hole emission
D-Fe+2*	Ec-Fe+2*	electron emission

The logged results in the table above are the transitions that are possible in the stable regions given. In the bulk, the n type InP has Fe+2 as the stable state, but in the depletion region, the above transitions are possible. The next step is to model a transition region using some of the known parameters. Even though the width decrease is not a positive fact due to the two junctions, it will help in the initial model to use a known number. The model is presented as FigV-9.1,2,3,4,5. The diagrams are self-explanatory in their heading. There are two conditions: quiescent reverse bias and excitation of holes and electrons. The different pictures represent different parts of the region. Some depict the band bending and some depict the Fe transition region. One point that is not addressed is how the Fermi level bends in the depletion region. Before I was able to slip out of the argument like other authors do, I made the voltage assumption that the position of a trap at the reverse bias is directly proportional to its position at the built in voltage(no bias present).

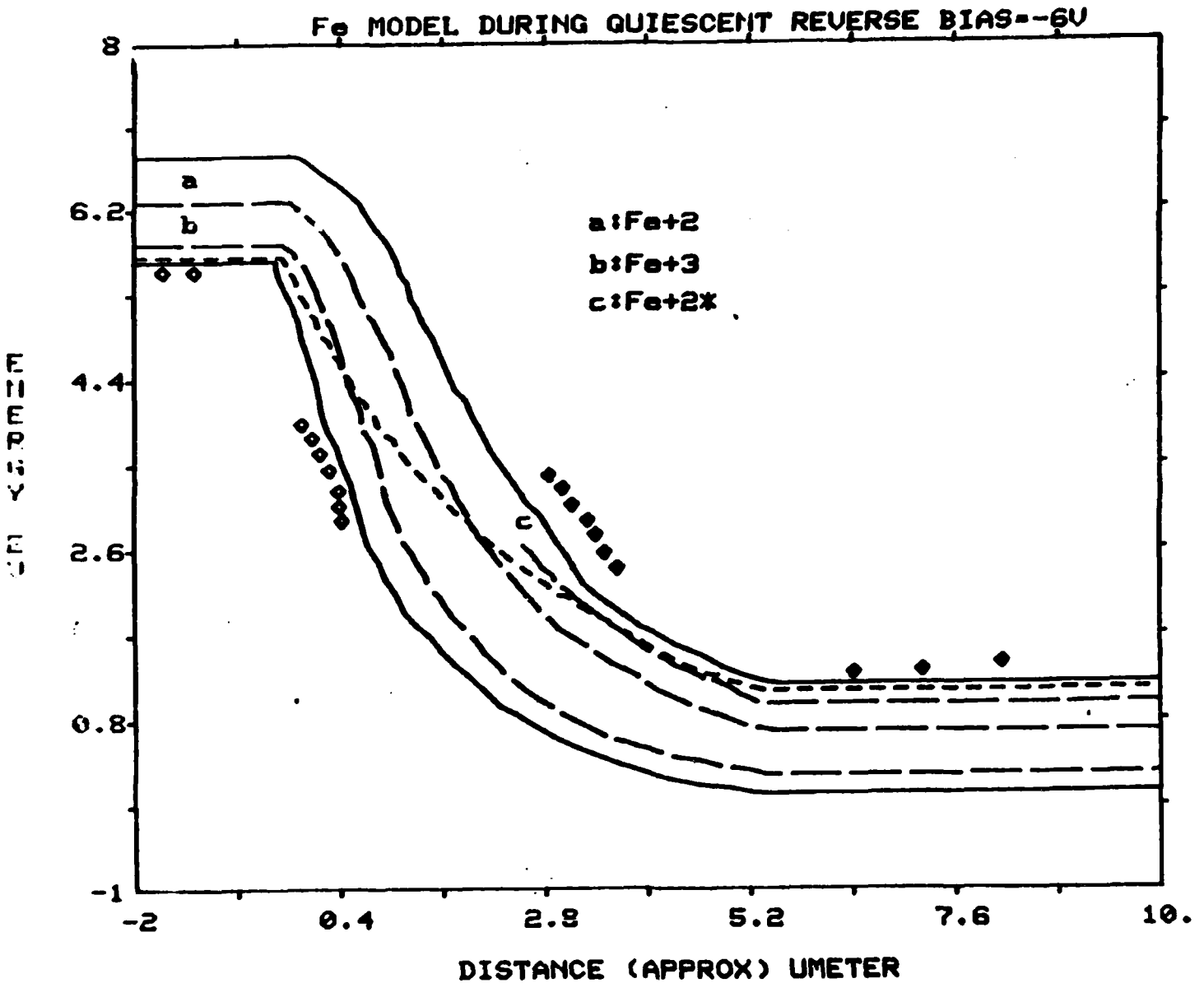
Fe MODEL DURING QUIESCENT REVERSE BIAS=-6V
8
6.2
4.4
2.6
0.8
-1
a
b
c
a:Fe+2
b:Fe+3
c:Fe+2*
-2
0.4
2.8
5.2
7.6
10.
DISTANCE (APPROX) UMETER

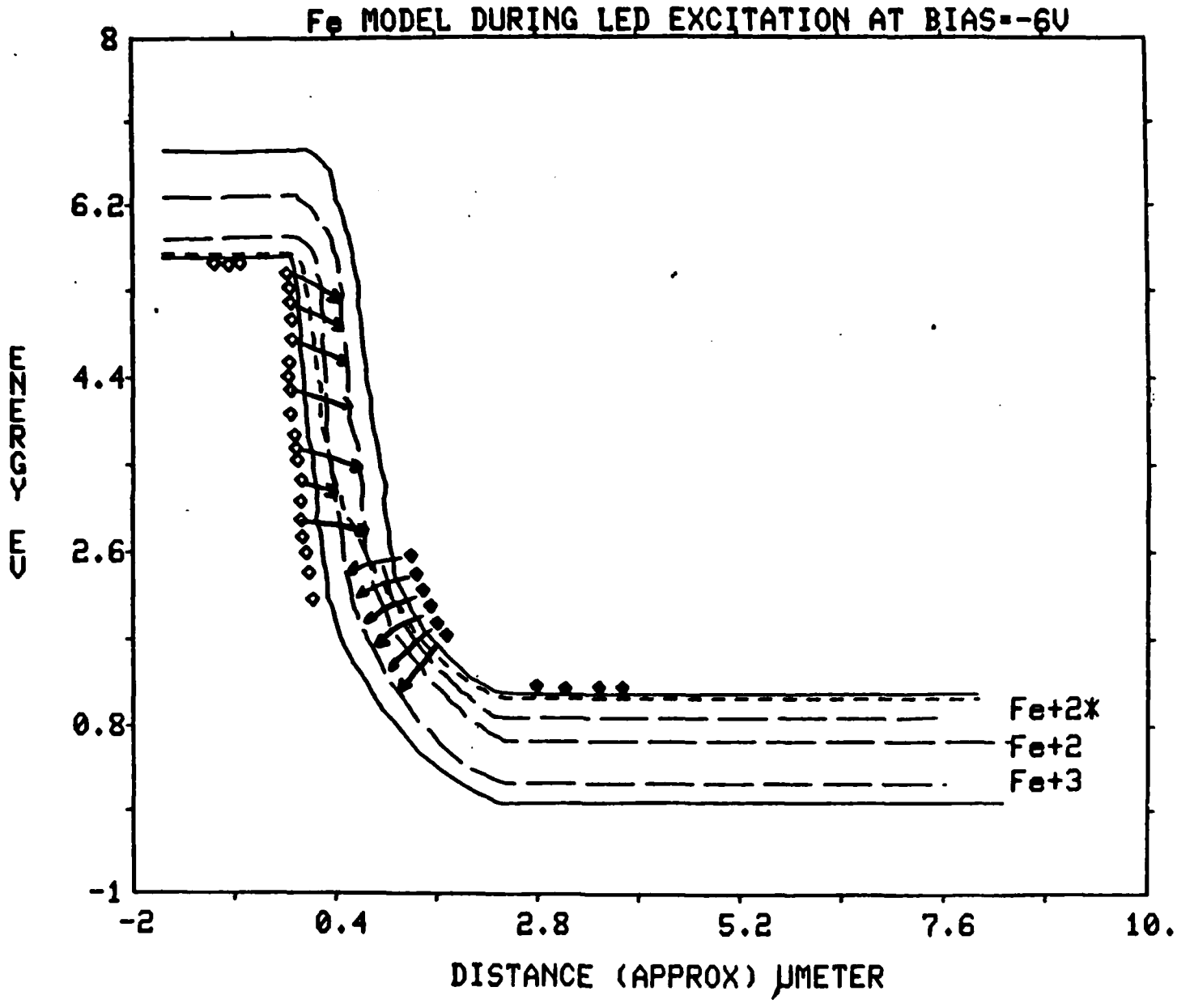
Fe MODEL DURING LED EXCITATION AT BIAS=-6V
8
6.2
4.4
2.6
0.8
-1
ENERGY eV
-2
0.4
2.8
5.2
7.6
10.
DISTANCE (APPROX) μMETER
Fe+2*
Fe+2
Fe+3

Fig V-9.3

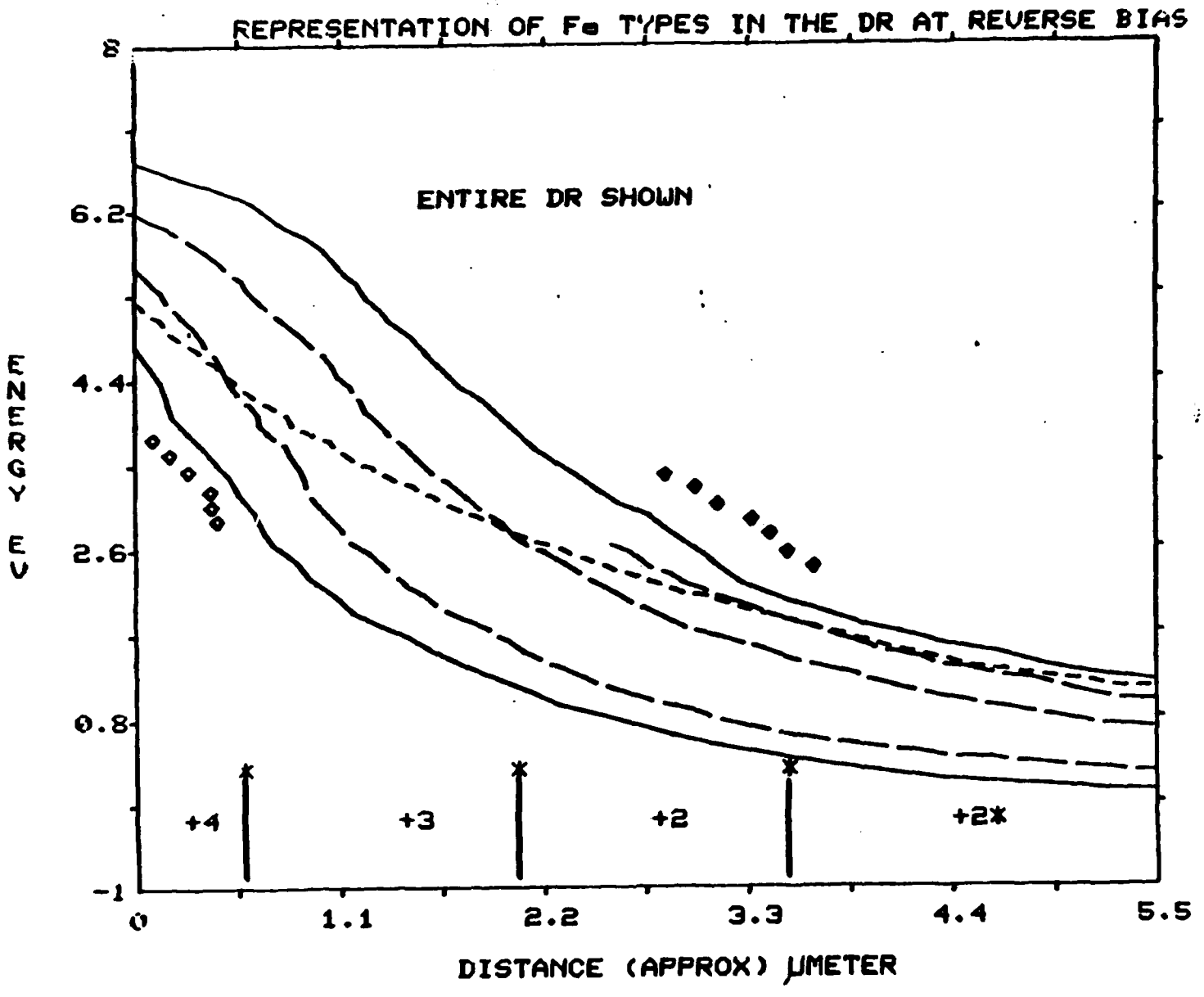
REPRESENTATION OF Fe TYPES IN THE DR AT REVERSE BIAS
ENTIRE DR SHOWN
ENERGY EV
8
6.2
4.4
2.6
0.8
-1
+4
+3
+2
+2*
0
1.1
2.2
3.3
4.4
5.5
DISTANCE (APPROX) μMETER

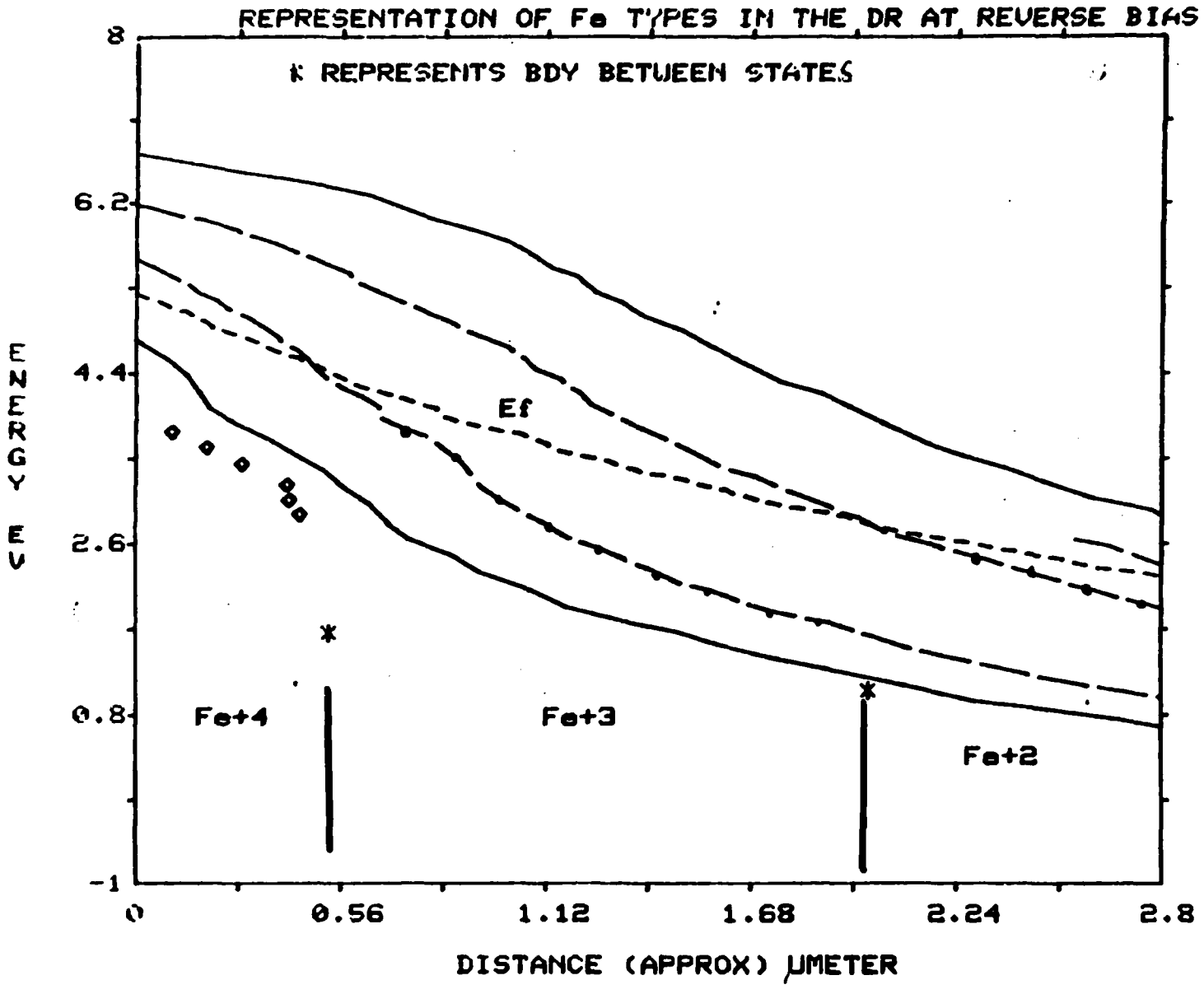
REPRESENTATION OF Fe TYPES IN THE DR AT REVERSE BIAS
K REPRESENTS BDY BETWEEN STATES
8
6.2
4.4
2.6
0.8
-1
ENERGY EV
Ef
Fe+4
Fe+3
Fe+2
0
0.56
1.12
1.68
2.24
2.8
DISTANCE (APPROX) UMETER

AD-A134 183 OPTICAL EXCITATION OF TRAPPING STATES IN FE DOPED INP (U) NAVAL ACADEMY ANNAPOLIS MD J GIESSNER 20 JUN 83 USNA-TSPR-124 2/2

UNCLASSIFIED F/G 20/12 NL

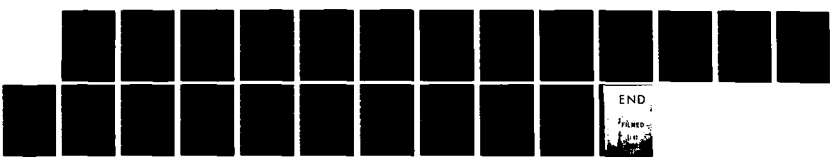

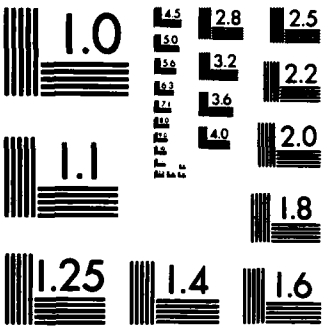

Fig V-9.5

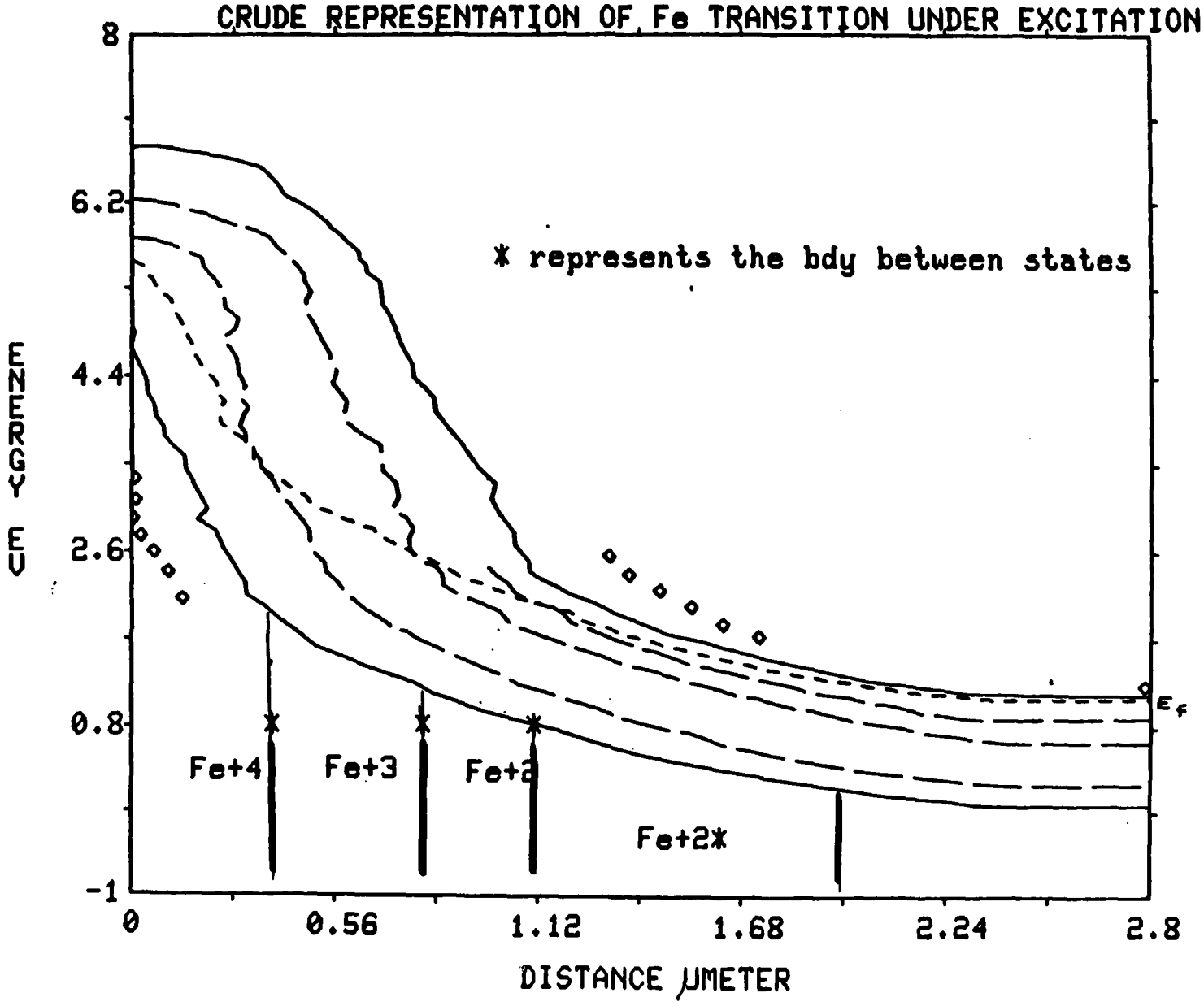
CRUDE REPRESENTATION OF Fe TRANSITION UNDER EXCITATION
* represents the bdy between states
ENERGY EV
8
6.2
4.4
2.6
0.8
-1
0
0.56
1.12
1.68
2.24
2.8
DISTANCE ΛMETER
Fe+4
Fe+3
Fe+2
Fe+2*
ϵ_f

With the model presented, I can compare my possible transitions to that of Eaves et al.[14]. My model is very similar to his except for some possible transitions involving the Fe+2* state (this is no surprise, however, this is one area of heavy debate today) and a possible Fe+4 to Fe+3 hole emission that is predicted as quite possible according to my model, but was not in Eaves' model. My model is given in Fig V-10. One comment in regard to the location of the Fe+4 energy level. In region A, it was noted that maybe a Fe+4-Ev could be seen near the depletion region edge; however, this is only a postulate.

There are many energies given for certain traps and they vary because, there is the capture cross section dependence on temperature and activation energy. 2. the band gap itself, varies with temperature and 3. basic experimental inaccuracies in determining the energy such that the error limits are broadened. Table V-2 shows the energy values for the allowed transitions at room temperature and absolute zero. In calulating the energies I assumed that the valence band moved up and not the conduction band moving down.

Table V-2 Current Energy Transitions

Temp	Region	State	State
	A	Fe+4-Ev	Fe+3-Ev
0K		?	.27ev
300K		?	.19ev

Fig V-10

Proposed Model

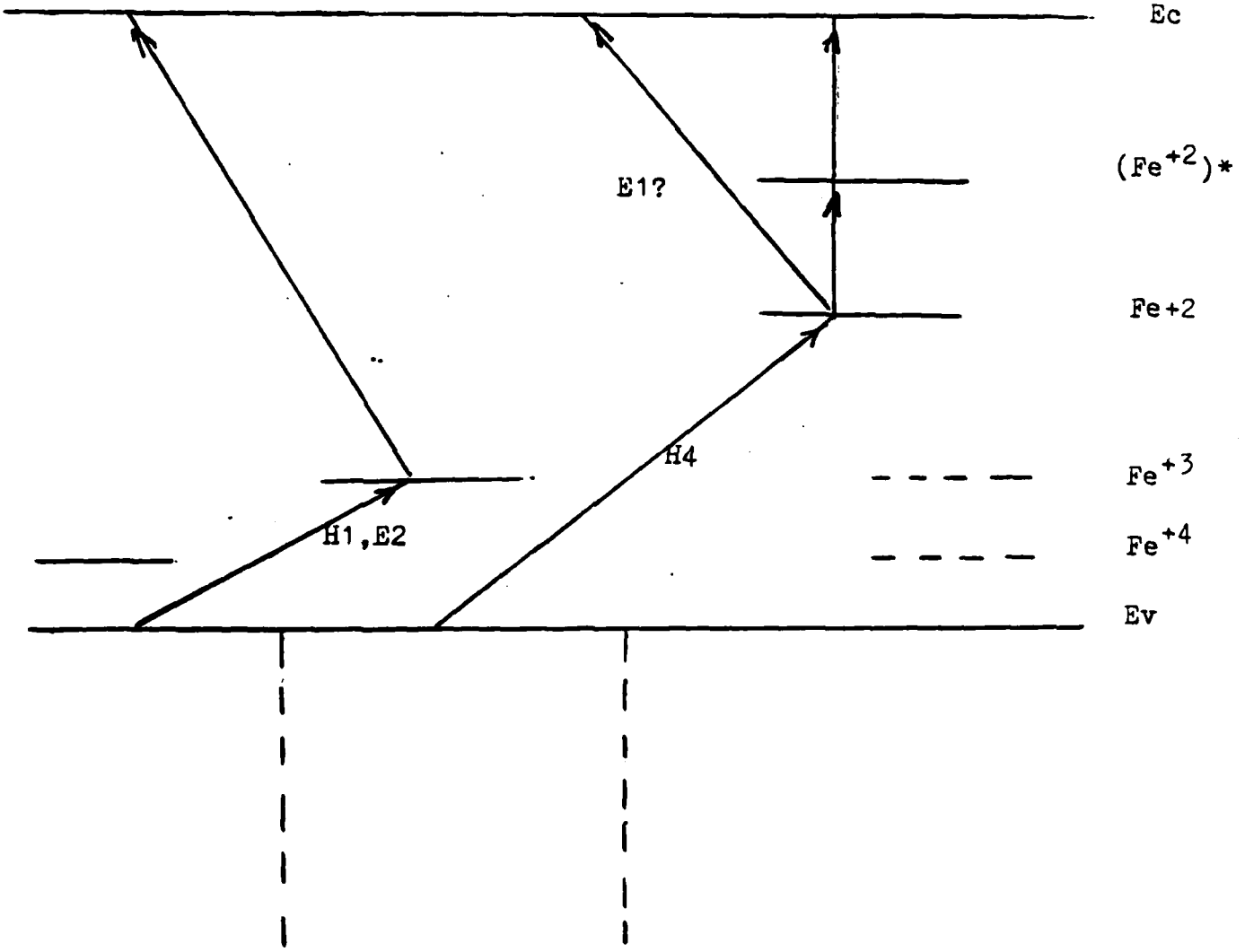

	B	Fe+3-Ev	Ec-Fe+2
0K		.27ev	.65ev
300K		.19ev	.65ev*

	C	Fe+2-Ev
0K		.77ev
300K		.69ev

	D	Ec-Fe+2*
0		.35ev
300		.35ev

* The assumption is that the VB moves with E_g

Model Application to the Data

Section V-5

The possibilty that the two optical traps at low temperatures are actually two hole traps with the majority trap E2 actually majority trap on the p+ side is a real possibility with this model. The energies compare with the literature E=.238(maj- hole trap)$_v$ for E2 and E=.24ev for H11. The coupling action may actually be a chacteristic of the two junction semiconductor. The above mentioned traps appear to be related to the Fe+4 to Fe+3 transition. All the coupling factors discussed seem to suggest that state. Much evidence comes from the high saturation PW needed in those traps which suggest a high trap concentration which is associated with the heavily doped iron.

The only other candidate for Fe transitions would be at that high temperature optical region, because of the high saturation levels. The peaks here (one of the group, consider H4, because of the non-exponential nature of H3C)are good candidates for what is termed the dominant hole emission in Fe. It is the Fe+3 to Fe+2 hole emission . This ends the optical search for Fe transitions with the possible exception that trap H12, part of the duo, is actually the Fe+4 transition. But there are not enough trap characteristics to make an educated guess.

The case for the optical pulsing is good, but the electrical case is not so good. The similar coupling as was previously stated may be due to the two depletion regions and not related to Iron transitions. But the energies are close to suggesting the minority trap H2 is actually an electron trap on the p+ side.

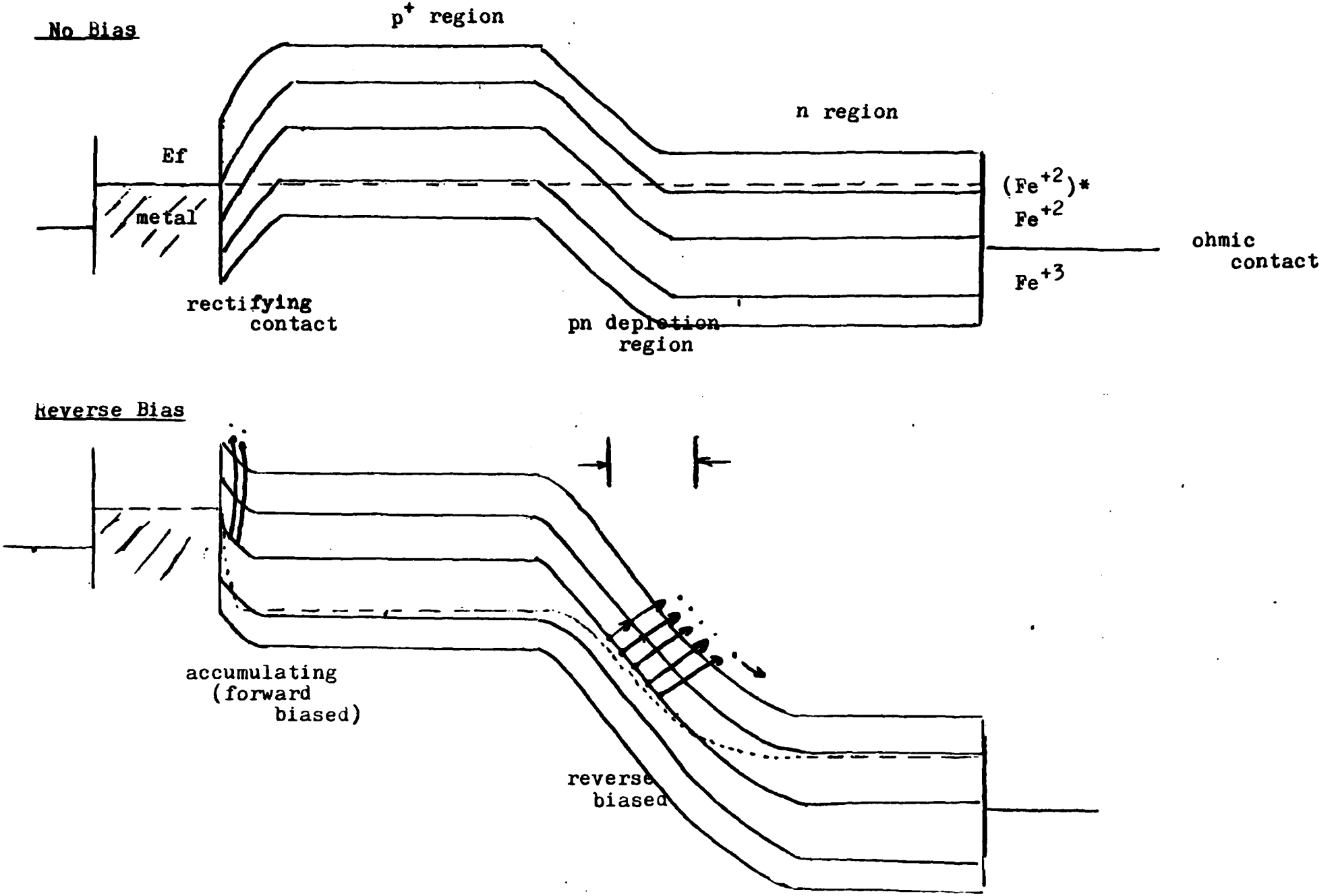
No Bias
p+ region
n region
Ef
metal
(Fe+2)*
Fe+2
Fe+3
ohmic contact
rectifying contact
pn depletion region
Reverse Bias
accumulating (forward biased)
reverse biased

Fig V-11

One can argue that although the energy for E1 is low,it is due to that pulling of H2 and E1. But this argument is not a strong one and suggesting that the two traps are the electron emission Fe+2 to Fe+3 traps is just that , a suggestion. See Fig V-11 for a two-junction band diagram

Table V-3 is a list of the experimental energies and their possible transition mechanisms in Fe.

Table V-3 Fe Transitions from Experimental Data

Trap	Junction/Type	Transition	Region	Energy
H11	n/hole-min	Fe+4 to Fe+3	B-1	.24ev
H2	p/elec-min	Fe+2 to Fe+3	B-2	.69ev
E1	n/elec-maj	Fe+2 to Fe+3	B-2	.5ev
E2	p/hole-maj	Fe+4 to Fe+3	B-1	.238ev
H4	n/hole-min	Fe+3 to Fe+2	C-1,3	.807ev
H12	n/hole-min	Fe+3 to Fe+4	A1	.15ev?

Other traps analyzed can be due to defects and impurities of the semiconductor. Checking the most recent literature Table V-4 was constructed with some of the prominent peaks in InP defects noted. To these peaks, I associated traps that have similar cross sections and energies.

Table V-4 This Defect Data in Comparison to Most Recent Work

Recent Data				Data For This Work			
Trap	Authors	Eev	σ cm^2	Trap	Eev	σ cm^2	Note
E3	McAfee et al	.49	E-20	E1	.499	2E-15	1
H2	McAfee et al	.64	-	H3B1	.602	6E-15	
SK2	McAfee et al	.55	-	E1	.499	2E-15	
C	Wada et al	.47	1.3E-14	E1	.499	2E-15	2
L-2	Yuba et al	.31	2.1E-14	H3A	.316	3.1E-15	
LA-1	Yuba	.81	1.5E-11	H3C	.794	3.1E-11	3
-	Rhee et al	.68	4.7E-15	H2	.691	2.4E-14	4
S5	Lim,Sagnes	.410	1E-16	H3B2	.388	1E-16	
SB	Lim, Sagnes	.33	H3A	.32	3.1E-15		

Notes

1.Peak is also seen by White et al,Guha et al

2.Seen in bulk of n type InP

3.Very Large cross sections do compare nicely

4.Rhee claims this is E4(.59ev) in bulk by MacAfee

Authors cited in [15-24]

Conclusion

The InP sample that was studied was modeled in many ways. It was modeled with regard to its junction characteristics. It was modeled with regard to iron transitions in the depletion region. After the modeling, experimental data was used to show the self-consistency of the model and also, to help explain theoretical problems. Although there are no all-encompassing models to explain all the results that were obtained, the simple and not so simple models that were developed are good, working models that were used effectively.

References

1.D.V. Lange,"Capacitance Transient Spectroscopy," Ann Review of Material Science, (1977), pp377-400.

2.D.V. Lange and Bleicher,"Shottky -Barrier Capacitance Measurements for Deep Level Impurity Determination," Solid State Electronics, 16,1973, pp. 375-300.

3.Stephen L. Spehn, "Deep Level Transient Spectroscopy as An Experimental Technique," Diss. U.S. NAval Academy 1980, pp 24-27.

4.Ibid.

5.Harvey S. Hopkins,"Characterization of Trapping States in Semiconductors, Diss. U.S. NAval Academy 1981, pp1-20

6. Pamplin, B.,"Table of Properties of Semiconductors," NDG.

7. Sze,S., Physics of Semiconductor Devices,2nd ed ,Wiley INC,NY,1979.

8. D.V. Lange "Capacitance",pp380-390.

9. Fung,S,Nicholas,Stradling,1979, J. Phys. C, Solid State Physics, 12,5145-55.

10. L. Eaves, A.W. Smith, P.J. Williams, B.Cockayne, W. Macewan,"Energy Levels for Fe in InP," submitted to J. Phys. C, published 1981.

11. Tapster, P. R., Skolnick,M.S., Humpreys, R.G.,Dean,P.J Cockyane,B and Macewan,W.T,"Optical and Capacitance Spectroscopy of InP:Fe," accepted for publication, J. Phys. C.,1982.

12. Bremond, G., Nouailhat A.,and Guillot, G.,"Fe Deep Level Optical Spectroscopy in InP," Solid State Comm.,41(6),1982, pp477-481.

13. Rhee,J.K and Bhattacharya, P.K, "Photoinduced Current Transient Spectroscopy of Semi-insulating InP:Fe and Cr," J. Appl. Phys., 53(6),pp 4247-4250.

14 Eaves, et al..

15 Bishop, S.G., Klein, Henry, and McCombe,1980, Semi-insulating III-V materials, Nottingham,ED G.J. Rees, Published Shiva, 161-6.

16 Look, D.C., 1979, Phy Rev. B,20,4160-66.

17 Choudhury, A.N. and P.N. Robson,"Hole Traps in n-InP by DLTS and Transient Capacitance Techniques," Electronic Letters, 15(26 April 79), pp 247-279.

18 White, A.M., Grant, A.J. and Day,B,"Deep Traps in Ideal n-InP Schottky Diodes," Electronic Letters, 1978,14, pp 409-411.

19 Chiao,S.H. and Antypass, G.A,"Photocapacitance Effects of Deep Traps in n-type InP," J. Appl. Phys., 49(1), Jan 1978, pp 466-468.

20 McAfee, S.R., Capasso,F.,Lange, D.V.Hutchinson, A. and Bonner,A.W., "A Study of Deep Levels in Bulk n-InP by Transient Spectroscopy," J. Appl. Phys., 52(10), Oct 1981, pp6158-6164

21 Sibille, A. and Mircea, A.,"Metastable Electron-hole Pair Self-trapping at a Deep Center in InP," Phy. Rev. Let, 47(2), 13 July 1981, pp142-144.

22 Lim, H.,Sagnes,G., Bastide,G. and Rouzeyre,M.,"Deep Level Optical SpectroscopyStudy in n-type InP," J. Appl Phys., 53(4), April 1982, pp3317-3320.

23 Wada, O., Majerfield,A. and Choudhury, A.,"Interaction of Deep-Level Traps with Lowest and Upper Conduction Minima in InP," J. Appl. Phys., 51(1), Jan 1980, pp423-432.

24 Yuba, Judai, Gamo and NAmaba,"OTCS Study of Defect States in Fe Doped InP Induced by Ion Irradiation and Thermal Annealing," Presented 12th International Conference on Defect States, Sep 1982, Amsterdam.

Appendix

a Characteristics of LED

1. non-coherent light 880nm.
2. Forward Voltage(20mA):1.75V
3. Reverse Voltage 3.0V
4. Forward Current 60mA
5. Reverse Current 10uA
6. Power Diss (25 C) 1mW
7. Dispersion - half power - angle: 24°

b,c Energy Plots and Capacitance Data

RUN DATE-24JAN83
RUN DATA - INP P+/N FE ELEC PULSE MIN TRAP

INPUT DATA

TEMP(C)	EMISSION RATE(1/SEC)
21	7.187
30	13.769
37.5	26.1202
41	47.432
49	86.868

T(K)	1000 / T(K)	LN(T*T/R)
294	3.401	9.394
303	3.3	8.805
310.5	3.22	8.213
314	3.184	7.639
322	3.105	7.084

ENERGY= .6907 EV
PREFACTOR A= 50662550
XFIT(1)=3.401E-03
YFIT(1)=9.499
XFIT(2)=3.105E-03
YFIT(2)=7.13

(1/T(K)-MIN= 3E-03 (1/T(K))-MAX= 3.5E-03

LN(T*T/R)-MIN= 7 LN(T*T/R)-MAX= 9.5

LN(T*T/R) VS. 1000/T(K)

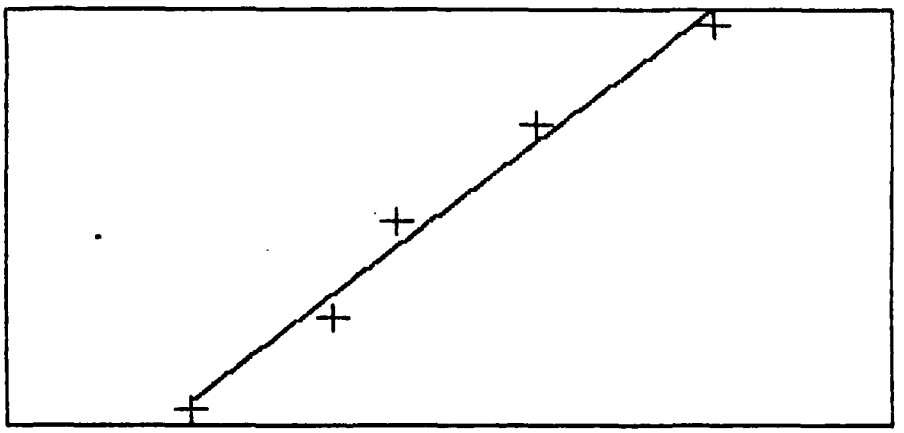

RUN DATE-14 MARCH OP PULSE LED MIN TRAP 3B2
RUN DATA - INP FE IN BULK HIGHFPW=100MICRO-LOWER PW=10MICRO

INPUT DATA

TEMP(C)	EMISSION RATE(1/SEC)
-58	7.267
-52	14.063
-45.3	28.165
-38	55.85
-32	103.3
-26	197

T(K)	1000 / T(K)	LN(T*T/R)
215	4.651	8.757
221	4.524	8.152
227.7	4.391	7.517
235	4.255	6.896
241	4.149	6.331
247	4.048	5.735

ENERGY= .4265 EV
PREFACTOR A= 1490307
XFIT(1)=4.651E-03
YFIT(1)=8.786
XFIT(2)=4.048E-03
YFIT(2)=5.806

(1/T(K)-MIN= 3.8E-03 (1/T(K))-MAX= 4.8E-03

LN(T*T/R)-MIN= 5.6 LN(T*T/R)-MAX= 9

LN(T*T/R) VS. 1000/T(K)

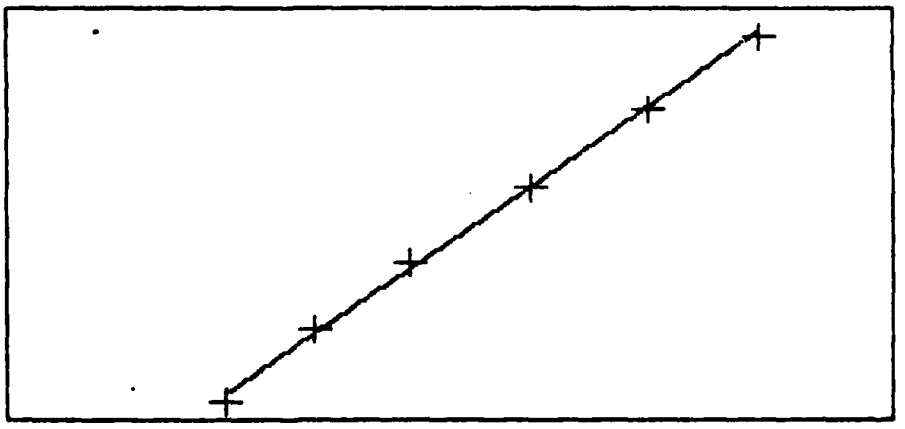

RUN DATE-24JAN83
RUN DATA - INP P+/N FE EL ELEC PULSE MAJ TRAP NO GATE

INPUT DATA

TEMP(C)	EMISSION RATE(1/SEC)
-26.3	3.898
-18.5	7.596
-10.5	14.651
-4.5	27.6
12.5	116.508
20.5	220

T(K)	1000 / T(K)	LN(T*T/R)
246.7	4.053	9.655
254.5	3.929	9.05
262.5	3.809	8.455
268.5	3.724	7.867
285.5	3.502	6.55
293.5	3.407	5.97

ENERGY= .4985 EV
PREFACTOR A= 873996
XFIT(1)=4.053E-03
YFIT(1)=9.75
XFIT(2)=3.407E-03
YFIT(2)=6.014

(1/T(K)-MIN= 3.3E-03 (1/T(K))-MAX= 4.1E-03

LN(T*T/R)-MIN= 5.5 LN(T*T/R)-MAX= 10

LN(T*T/R) VS. 1000/T(K)

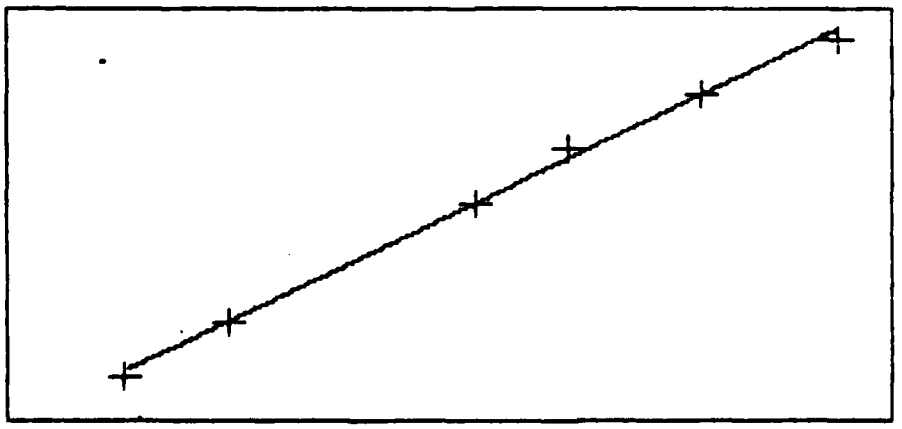

1/C*C VS. BIAS(V)

RUN DATE-THEORET MODEL INP FE IN BULK
RUN DATA - RL=2M CO=1PF CXO=55.8PF

INPUT DATA

V-BIAS	C(PF)	1/C*C
0	1.04995	.90711
1	1.04186	.92125
2	1.03574	.93217
3	1.03063	.94144
4	1.02617	.94964
5	1.02218	.95707
6	1.01853	.96394
7	1.01516	.97035
8	1.01201	.9764
9	1.00905	.98214
10	1.00625	.98761

SLOPE=7.73500573E-03
INTERCEPT=.914886743
XFIT(1)=0
YFIT(1)=.914
XFIT(2)=10
YFIT(2)=.992

(1/T(K)-MIN= -1 (1/T(K))-MAX= 11

LN(T*T/R)-MIN= .9 LN(T*T/R)-MAX= 1.05

1/C(PF)^2 VS. BIAS (V)

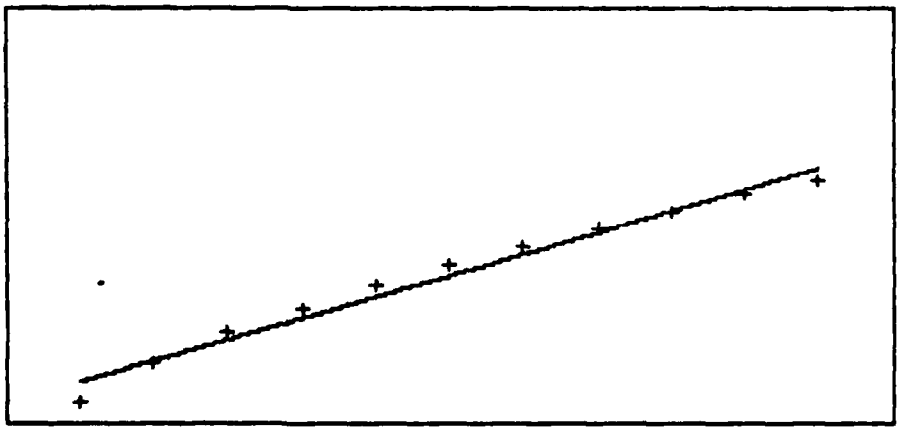

1/C*C VS. BIAS(V)

RUN DATE-15MAR83
RUN DATA - INP PAD 11 -11 DEG C

INPUT DATA

V-BIAS	C(PF)	1/C*C
0	1.408	.50442
.5	1.403	.50802
1	1.4	.5102
1.5	1.398	.51166
2	1.396	.51313
2.5	1.394	.5146
3	1.392	.51608
4	1.387	.51981
5	1.378	.52662
6	1.368	.53435
7	1.364	.53749
8	1.361	.53986
9	1.358	.54225
10	1.353	.54626

SLOPE=4.29529685E-03
INTERCEPT=.504945094
XFIT(1)=0
YFIT(1)=.504
XFIT(2)=10
YFIT(2)=.547

(1/T(K)-MIN= -1 (1/T(K))-MAX= 11

LN(T*T/R)-MIN= .5 LN(T*T/R)-MAX= .55

1/C(PF)^2 VS. BIAS (V)

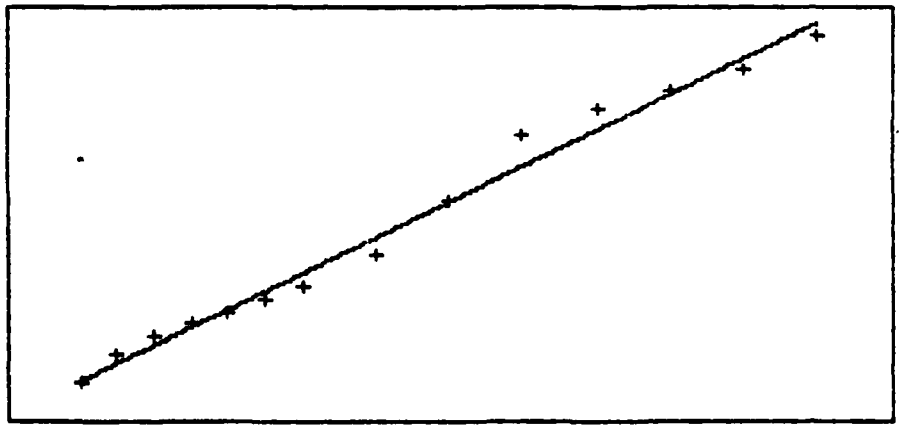

1/C*C VS. BIAS(V)

RUN DATE-3/15/83
RUN DATA - INP PAD 11 -65DEG C

INPUT DATA

V-BIAS	C(PF)	1/C*C
0	1.315	.57829
.5	1.311	.58182
1	1.311	.58182
1.5	1.31	.58271
2	1.31	.58271
2.5	1.309	.5836
3	1.309	.5836
4	1.307	.58539
5	1.306	.58629
6	1.305	.58719
7	1.304	.58809
8	1.303	.58899
9	1.302	.58989
10	1.301	.5908

SLOPE=1.07290365E-03
INTERCEPT=.580530611
XFIT(1)=0
YFIT(1)=.58
XFIT(2)=10
YFIT(2)=.591

(1/T(K)-MIN= -1 (1/T(K))-MAX= 11

LN(T*T/R)-MIN= .57 LN(T*T/R)-MAX= .6

1/C(PF)^2 VS. BIAS (V)

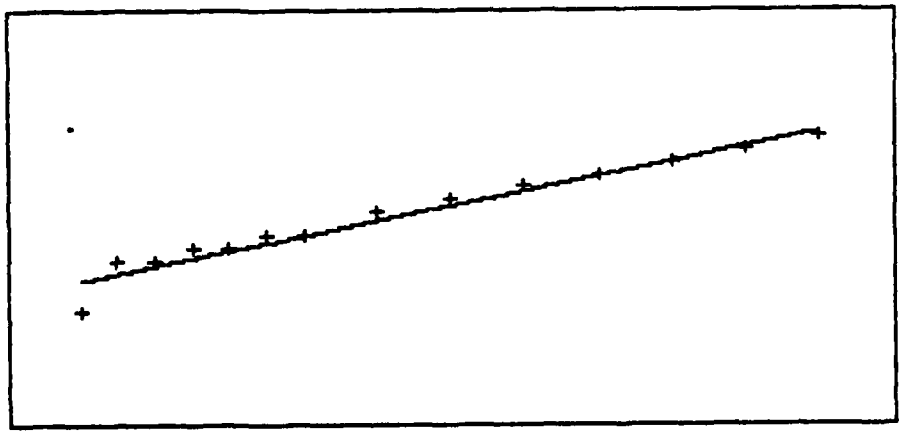

1/C*C VS. BIAS(V)

RUN DATE-3/15/83
RUN DATA - INP PAD 11 -75DEG C

INPUT DATA

V-BIAS	C(PF)	1/C*C
0	1.312	.58094
.25	1.31	.58271
.5	1.308	.58449
.75	1.307	.58539
1	1.306	.58629
1.5	1.305	.58719
2	1.304	.58809
2.5	1.303	.58899
3	1.302	.58989
4	1.301	.5908
5	1.299	.59262
6	1.298	.59354
7	1.297	.59445
8	1.295	.59629
9	1.294	.59721
10	1.293	.59814

SLOPE=1.53301054E-03
INTERCEPT=.584022156
XFIT(1)=0
YFIT(1)=.584
XFIT(2)=10
YFIT(2)=.599

(1/T(K)-MIN= -1 (1/T(K))-MAX= 11

LN(T*T/R)-MIN= .58 LN(T*T/R)-MAX= .6

1/C(PF)^2 VS. BIAS (V)

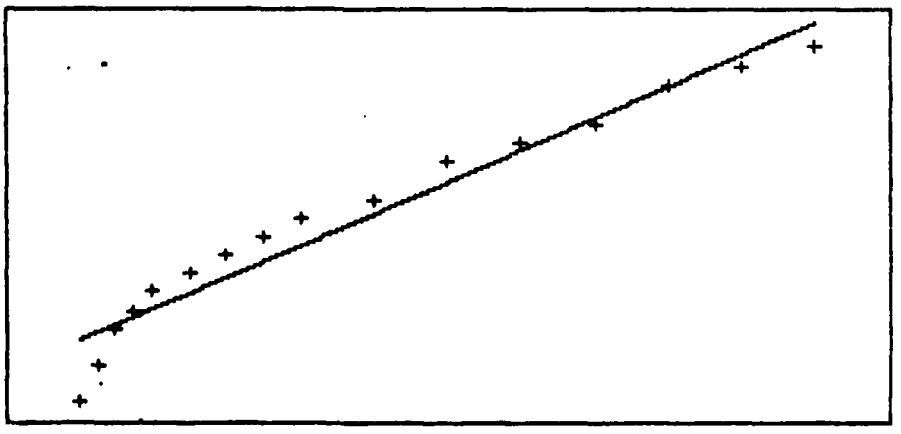

UNCLASSIFIED

SECURITY CLASSIFICATION OF THIS PAGE (When Data Entered)

REPORT DOCUMENTATION PAGE		READ INSTRUCTIONS BEFORE COMPLETING FORM
1. REPORT NUMBER U.S.N.A. - TSPR: 124 (1983)	2. GOVT ACCESSION NO. A134183	3. RECIPIENT'S CATALOG NUMBER
4. TITLE (and Subtitle) OPTICAL EXCITATION OF TRAPPING STATES IN Fe DOPED InP.		5. TYPE OF REPORT & PERIOD COVERED Final: 1982/1983 6. PERFORMING ORG. REPORT NUMBER
7. AUTHOR(s) Giessner, Jack		8. CONTRACT OR GRANT NUMBER(s)
9. PERFORMING ORGANIZATION NAME AND ADDRESS United States Naval Academy, Annapolis.		10. PROGRAM ELEMENT, PROJECT, TASK AREA & WORK UNIT NUMBERS
11. CONTROLLING OFFICE NAME AND ADDRESS United States Naval Academy, Annapolis.		12. REPORT DATE 20 June 1983 13. NUMBER OF PAGES 115
14. MONITORING AGENCY NAME & ADDRESS(if different from Controlling Office)		15. SECURITY CLASS. (of this report) UNCLASSIFIED 15a. DECLASSIFICATION/DOWNGRADING SCHEDULE

16. DISTRIBUTION STATEMENT (of this Report)

This document has been approved for public release; its distribution is UNLIMITED.

17. DISTRIBUTION STATEMENT (of the abstract entered in Block 20, if different from Report)

This document has been approved for public release; its distribution is UNLIMITED.

18. SUPPLEMENTARY NOTES

Accepted by the U. S. Trident Scholar Committee.

19. KEY WORDS (Continue on reverse side if necessary and identify by block number)

Semiconductors

20. ABSTRACT (Continue on reverse side if necessary and identify by block number)

The knowledge that defect states affect the performance and speed of semiconductors is well known. Defect and trapping states are categorized according to their sex (hole or electron trap), energy in the gap and capture cross sections. The deep Level Transient Spectroscopy (DLTS) technique that is useful for electrical pulsing, becomes increasingly profitable using optical pulsing. The optical pulsing was accomplished using a simple, but efficient, infrared light emitting diode (LED). The LED had the fortunate property (OVER)

DD FORM 1 JAN 73 1473 EDITION OF 1 NOV 68 IS OBSOLETE

S/N 0102-LF-014-6601

UNCLASSIFIED

SECURITY CLASSIFICATION OF THIS PAGE (When Data Entered)

that with decreasing temperature, the average energy output of the LED stayed about equal to the bandgap for the III-V semiconductor InP. Because of these fortuitous findings, I concentrated on Fe-doped InP using LED excitation. These particular samples are being studied by Naval Research Labs (NRL) in connection with lasing that results from Fe transitions. I set up models for both the p+n junction and Fe transitions to help explain experimental results obtained. A coupled state that could be related to Fe+3 to Fe+2 hole emission was found to have an energy of .24ev on the n-side of the p+n junction, and an energy of .24 ev on the p+ side of the metal-p+ rectifying junction(a result proposed in the capacitance-junction model). Another energy related to the Fe+2 to Fe+3 electron emission was found in agreement with the model (E=.807ev). Trap states related to defects inherent in the growth of InP were also found. Many of the states seen by authors recently could be explained by the energy data in these experiments.

END

FILMED

11-83

DTIC